



**UNIVERSITA' DEGLI STUDI DI UDINE**

**CORSO DI DOTTORATO DI RICERCA IN  
SCIENZE E TECNOLOGIE CLINICHE  
CICLO XXVI**

**TESI DI DOTTORATO DI RICERCA**

**THE EMILIN1- $\alpha$ 4/ $\alpha$ 9 INTEGRIN INTERACTION  
IS CRUCIAL IN LYMPHATIC VESSEL  
FORMATION AND MAINTENANCE**

**Ph.D. student: Dr. Lisa Del Bel Belluz**

**Supervisor: Prof. A. Colombatti**

**Co-supervisor: Dr. P. Spessotto**

*A. Colombatti*  
*P. Spessotto*  
*Lisa Del Bel Belluz*

**ANNO ACCADEMICO 2013/2014**



**UNIVERSITA' DEGLI STUDI DI UDINE**

**CORSO DI DOTTORATO DI RICERCA IN  
SCIENZE E TECNOLOGIE CLINICHE  
CICLO XXVI**

**TESI DI DOTTORATO DI RICERCA**

**THE EMILIN1- $\alpha$ 4/ $\alpha$ 9 INTEGRIN INTERACTION  
IS CRUCIAL IN LYMPHATIC VESSEL  
FORMATION AND MAINTENANCE**

**Ph.D. student: Dr. Lisa Del Bel Belluz**

**Supervisor: Prof. A. Colombatti**

**Co-supervisor: Dr. P. Spessotto**

**ANNO ACCADEMICO 2013/2014**

# TABLE OF CONTENTS

<b>SUMMARY</b> .....	<b>1</b>
<b>ABBREVIATIONS</b> .....	<b>3</b>
<b>INTRODUCTION</b> .....	<b>5</b>
1. THE EMILIN PROTEIN FAMILY.....	6
1.1 EMILIN1 structure.....	7
1.2 EMILIN1 localization and functions.....	8
2. EMILIN1 AND LYMPHATIC SYSTEM.....	11
2.1 Lymphatic vessels.....	11
2.2 Lymphatic vessel development.....	13
2.3 ECM regulates lymphatic valve development.....	17
2.4 A new abnormal lymphatic phenotype in EMILIN1 deficient mice.....	19
<b>AIM OF THE STUDY</b> .....	<b>23</b>
<b>MATERIAL AND METHODS</b> .....	<b>25</b>
1. Antibodies and reagents.....	26
2. Mouse procedures and cell cultures.....	26
3. Whole mount staining.....	27
4. Electron microscopy.....	27
5. Cell adhesion assay.....	27
6. Migration assays.....	28
6.1 Wound healing assay.....	28
6.2 Transwell chamber migration/haptotaxis assay.....	28
6.3 Transmigration assays.....	28
7. EMILIN1 silencing.....	28
8. Lymphangiography.....	29
9. Computer-assisted morphometric analyses.....	29
10. Histological and immunofluorescence analysis.....	29
11. RNA extraction and RT-PCR.....	30
12. Statistical analysis.....	30

<b>RESULTS</b> .....	<b>31</b>
1. EMILIN1 AND LYMPHATIC COLLECTING VESSELS.....	32
1.1 EMILIN1 is expressed in developing and in mature lymphatic valves...	32
1.2 EMILIN1 deficiency leads to abnormal lymphatic valve phenotype.....	35
1.3 EMILIN1 deficiency impairs functionality of lymphatic valves.....	41
1.4 Phenotype differences are associated to different mouse strains.....	47
1.5 EMILIN1 co-localizes with $\alpha 9$ integrin in the valve leaflets.....	51
1.6 EMILIN1 contributes to valve formation, maintenance and function more than FN-EIIIA.....	55
1.7 EMILIN1- $\alpha 9\beta 1$ integrin interaction regulates LEC proliferation and migration.....	60
2 EMILIN1 DEFICIENCY PROMOTES CELL PROLIFERATION IN THE SKIN	66
3 EMILIN1 AND SKIN CARCINOGENESIS.....	69
3.1 <i>Emilin1</i> <sup>-/-</sup> mice were more susceptible to chemically induced skin carcinogenesis.....	69
3.2 In <i>Emilin1</i> <sup>-/-</sup> mice lymphangiogenesis and metastatization increase.....	70
<b>DISCUSSION</b> .....	<b>73</b>
<b>REFERENCES</b> .....	<b>79</b>
<b>APPENDIX</b> .....	<b>90</b>

# **SUMMARY**

Lymphatic system is the second circulatory system and it is crucial for the maintenance of tissue interstitial fluid balance and it plays important roles in human diseases, including lymphedema, chronic inflammation and cancer metastasis. Lymphatic vasculature is divided essentially in two types of vessels: capillaries and collectors. Lymphatic capillaries allow absorption of fluid from interstitium whereas lymphatic collectors transport the lymph to lymph nodes and in the end in the blood circulation. A previous work demonstrated that EMILIN1, an extracellular matrix glycoprotein associated with elastic fibers, has a crucial role in the proper formation of lymphatic capillaries. *Emilin1*<sup>-/-</sup> mouse is the first abnormal lymphatic phenotype associated with an extracellular matrix component deficiency: enlargement of lymphatic vessels in several tissues and reduction of anchoring filaments. This morphological alterations cause impair of lymph uptake, increase of leakage and the development of a mild lymphedema condition. Moreover, through the engagement with by  $\alpha 4\beta 1$  integrin, EMILIN1 exerts a regulatory role in cell proliferation: in *Emilin1*<sup>-/-</sup> background there is an increase of proliferative rate.

In this study we focus our interest on the role of EMILIN1 in the lymphatic vessel formation process. Our results show that EMILIN1, expressed in embryonic, postnatal and adult mouse valve structures, regulates lymphatic valve formation, maturation and maintenance. *Emilin1*<sup>-/-</sup> mice exhibit an immature vessel and valve leaflet structures, which affect also their functionality. We demonstrate that also in the lymphatic contest EMILIN1 is able to regulate cell proliferation. Moreover this extracellular matrix protein influences also the migratory ability of the endothelial lymphatic cells. The regulatory ability of EMILIN1 in the lymphatic is mediated by  $\alpha 9\beta 1$  integrin engagement. EMILIN1 influences the lymphangiogenesis process not only in the physiological but also in the pathological environment: it exerts a protective role in tumor growth, in tumor lymphangiogenesis as well as in metastatic spread to lymph nodes.

Our data demonstrate for the first time a fundamental role for EMILIN1- $\alpha 9\beta 1$  integrin interaction in lymphatic vasculature, especially in lymphatic valve formation and maintenance. Moreover our data underline the importance of this extracellular matrix component in displaying a regulatory function in proliferation and acting as a “guiding” molecule in migration of lymphatic endothelial cells.

# **ABBREVIATIONS**

**Ang2** = Angiopoietin 2

**COL** = Collagenous domain

**ECM** = Extracellular Matrix

**EMI** = EMI domain

**EphB2** = Ephrin B2

**FN** = Fibronectin

**gC1q** = globular C1q-like domain

**HMVEC-dLyNeo** = Human Microvascular Endothelial Cells Dermal Lymphatic-Neonatal

**HMVEC-LLy** = Human Microvascular Endothelial Cells Lung Lymphatic

**LAEC** = Mouse Lymphangioma Endothelial Cell

**LEC** = Endothelial Lymphatic Cell

**LN** = Lymph Nodes

**LYVE-1** = Lymphatic Vessel Hyaluronan Receptor-1

**Nrp2** = Neuropilin2

**SMA** = Smooth Muscle Actin

**SMC** = Smooth Muscle Cell

**TEM** = Transmission Electron Microscopy

**TGF $\beta$**  = Transforming Growth Factor  $\beta$

**VEGF-A** = Vascular Endothelial Growth Factor A

**VEGF-C** = Vascular Endothelial Growth Factor C

**VEGF-D** = Vascular Endothelial Growth Factor D

**VEGFR-2** = Vascular Endothelial Growth Factor Receptor 2

**VEGFR-3** = Vascular Endothelial Growth Factor Receptor 3

**WMS** = Whole Mount Staining

# **INTRODUCTION**

## 1. THE EMILIN PROTEIN FAMILY

The EMILIN family belongs to the EDEN (EMI Domain Endowed) gene superfamily (Fig. 1) (Braghetta et al., 2004). This superfamily comprises seven genes, which can be grouped into three families on the basis of the major protein domains. The first is the EMILIN/Multimerin family, characterized by the N-terminal EMI domain (Doliana et al., 2000), a central part formed by coiled-coil structures, and a region homologous to the gC1q domain at C-terminal. The family includes EMILIN1 (Colombatti et al., 1985; Bressan et al., 1993; Doliana et al., 1999), EMILIN2 (Doliana et al., 2001), Multimerin1 (MMRN1; Hayward, 1997), and Multimerin2 (MMRN2; Sanz-Moncasi et al., 1994; Christian et al., 2001). The second family comprises only one gene, EMILIN-truncated (EMILIN-T), with a structure similar to the first larger family, but lacking the C-terminal globular domain of C1q (gC1q). Finally, the third family is formed by two genes, Emu1 and Emu2, which have a structure completely different from the others members, except for the presence of EMI domain (Leimester et al., 2002).

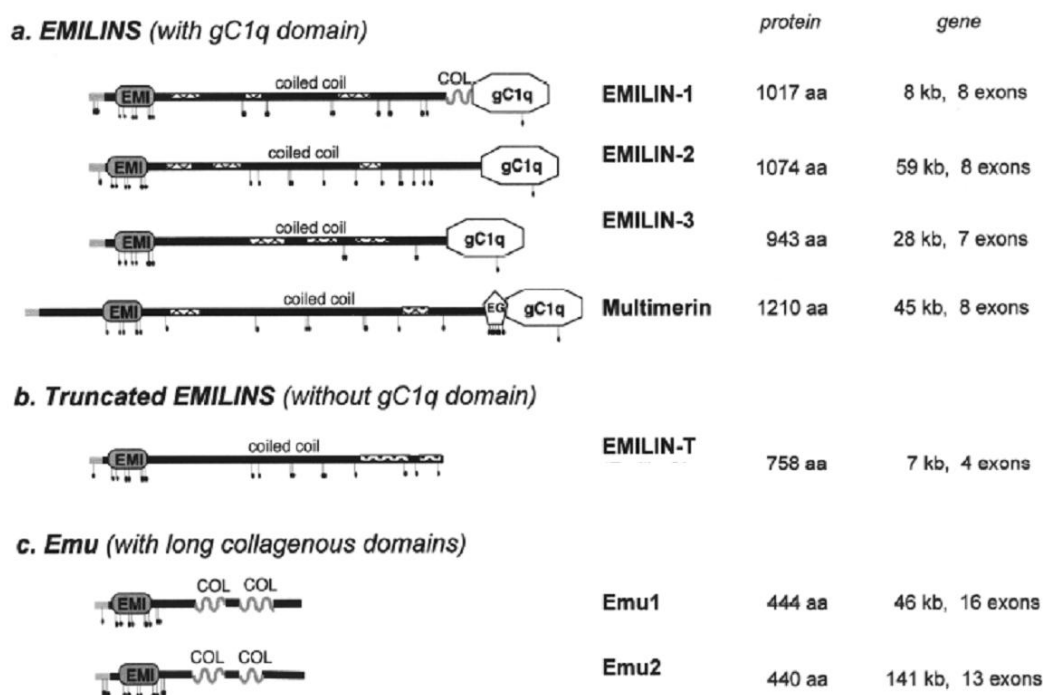


**Figure 1. The EDEN gene superfamily.** This superfamily is further subdivided into three families, which differ for domain composition. Grey box, signal peptide; EMI, EMI domain; hatched box, region with high probability of coiled coil conformation; COL, collagenous domain; gC1q, globular C1q-like domain; EG, region with partial similarity with EGF domain. Vertical bars mark the position of cysteines; (from Braghetta et al., 2004).

## 1.1 EMILIN1 structure

EMILIN1 is an extracellular matrix (ECM) glycoprotein that is associated to elastic fibers and it is involved in the interaction between the cell surface of elastin forming cells and the surrounding environment. It is a 115 kDa glycoprotein purified for the first time from the heterogeneous fraction of a newborn chick aorta (Bressan 1983, Colombatti 1985). Later it was named EMILIN (Elastin Microfibril Interface Located proteIN) for its peculiar fine distribution between the surface of amorphous elastin and microfibrils (Bressan et al., 1993).

The EMILIN1 gene is contained in 2p23.2-23.3 region and it is constituted by 8 exons and 7 introns. The amino-terminus domain is characterized by extracellular localization sequence followed by the EMI domain, a sequence of approximately 80 amino acids that includes seven conserved cysteine residues. The central part of the molecule is formed by a region, of approximately 700 amino acids, with high probability for coiled-coil structures presenting heptad repeats. This is followed by a 91-long residue sequence, containing two sequences corresponding to structures referred to as the “leucine zippers”. The finding of leucine zippers is rather unusual especially for an ECM protein as there are very few precedents in the literature reporting the presence of this type of regular spacing of leucines outside the nuclear compartments (Colombatti et al., 2000). This region is followed by the COIL domain, an interrupted collagenous stalk of 17 GXY triplets. At the end of the C-terminal there is the gC1q domain, a region homologous to the globular domain of the complement. It is formed by 151 amino acids mainly hydrophobics. The gC1q domain is particularly important for the protein polymerization and the interaction with cellular adhesion molecules (Mongiat et al., 2000). Unlike other gC1q domains, that one of EMILIN1 presents an insertion of nine residues, which disrupts the strand organization and forms a highly dynamic protruding loop. In this loop, the residue E933 is the site of interaction with  $\alpha 4\beta 1$  and  $\alpha 9\beta 1$  integrins (Verdone et al., 2008 and 2009, Danussi et al., 2008 and 2011).

## 1.2 EMILIN1 localization and functions

EMILIN1 is strongly expressed in the large blood vessel wall and in the connective tissue of a wide array of organs as skin, lung, cornea, kidney, intestine and lymph nodes (LNs) (Colombatti et al., 1985). Recently, it was demonstrated its expression in the abluminal side of lymphatic vessels in several mouse tissues (Danussi et al., 2008).

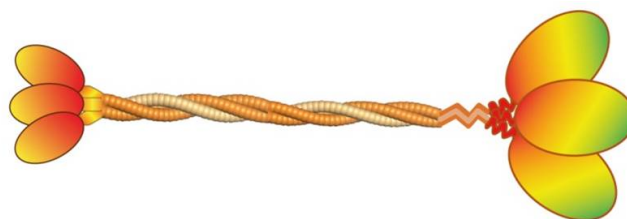
EMILIN1 is implicated in multiple functions as summarized in Figure 2. It is involved in elastogenesis and in the maintenance of blood vascular cell morphology since it is intimately associated with elastic fibers and microfibrils in blood vessels (Colombatti et al., 1985, 2000). The interaction between EMILIN1, elastin and fibulin-5 stabilizes the elastic fibers (Zanetti et al., 2004). EMILIN1, via the EMI domain, regulates pro-TGF $\beta$  maturation, preventing cleavage of LAP by furin convertase, and so it regulates blood pressure homeostasis (Zacchigna et al., 2006). Indeed in *Emilin1*<sup>-/-</sup> mice the increased levels of TGF $\beta$  induce an increase of vascular cell proliferation, a narrow blood vessels, increases peripheral resistance and consequently elevates systemic blood pressure. EMILIN1 has even a key role in promoting extravillous trophoblast migration and/or invasion into maternal decidual, contributing to the vascular remodelling during the first trimester of pregnancy (Spessotto et al., 2006).

Many EMILIN1 functions are regulated by the ligand-receptor interaction by the gC1q domain (reviewed in Pivetta et al., 2013). This domain contains the site of interaction with  $\alpha$ 4 $\beta$ 1 and  $\alpha$ 9 $\beta$ 1 integrins (Verdone et al., 2008, Danussi et al., 2008 and 2011). The two molecules have several common ECM ligands, such as fibronectin (FN), osteopontin, thrombospondin1, over EMILIN1 (Hoye et al., 2012).

$\alpha$ 4 $\beta$ 1 integrin is expressed on the surface of several cell type of the hematopoietic lineage in which drives proliferation, survival and migration (Rose et al., 2007). This integrin supports cell adhesion and spreading, promotes lamellipodia formation (Pinco et al., 2002), and not stress fibers and focal adhesion (Iida et al., 1995), likely promoting cell motility.

$\alpha$ 9 $\beta$ 1 integrin is expressed in various cell types and it plays a role in cell adhesion, migration, lung development and wound healing (Hoye et al., 2012). It is determinant during lymphatic structure formation, especially for intraluminal valve:  $\alpha$ 9 null mice die perinatally of massive chylothorax and display sever defect in the lymphatic valve (Huang et al., 2000, Bazigou et al., 2009). Bazigou (2009) demonstrated that  $\alpha$ 9 $\beta$ 1 integrin and embryonic isoform of fibronectin FN-EIIIA, interaction regulates FN fibril assembly, which is essential for the formation of ECM

core of valve leaflets. Moreover, both  $\alpha 4$  and  $\alpha 9$  integrins are involved in tumor progression. In fact they promote cell dissemination:  $\alpha 4$  inducing lymphangiogenesis (Garmy-Susini et al., 2010) and  $\alpha 9$  inducing cell invasion and epithelial-mesenchymal transition (Allen et al., 2011).



Domains	Biological function
EMI 	Blood hypertension, pro-TGF $\beta$ processing (Zacchigna et al., 2006)
Coiled-coil Region 	Homotrimerization (Colombatti et al., 2000, Mongiat et al., 2000, Verdone et al., 2008)
Collagenic region 	Homotrimerization
gC1q 	Homotrimerization Cell adhesion (Spessotto et al., 2003) and migration (Spessotto et al., 2006) $\alpha 4\beta 1/\alpha 9\beta 1$ integrin mediated Cell proliferation homeostasis (Danussi et al., 2011)
	Homotrimerization Elastogenesis and vascular cell morphology maintenance (Zanetti et al., 2004) Antitumorigenic (Danussi et al., 2012) Lymphangiogenesis (Danussi et al., 2008, Danussi and Del Bel Belluz et al., 2013)

**Figure 2. EMILIN1 structure and functions.** Schematic list of EMILIN1 biological properties in association with the respective involved domain. The regulation of elastogenesis and lymphangiogenesis has not been pinpointed to a specific domain although it is tempting to assume that gC1q plays an important role; (modified from Pivetta et al., 2013).

EMILIN1 displays strong adhesive, migratory and proliferative properties for different cell types from keratinocytes and fibroblast to tumor cells as SW982 (Doliana et al., 1999, Spessotto et al., 2003 and 2006, Danussi et al., 2011 and 2013). The first ligand involved in the regulatory role of EMILIN1 to be identified is  $\alpha4\beta1$  integrin. The interaction of  $\alpha4\beta1$  integrin and gC1q domain of EMILIN1 provides very strong adhesion and migration (Spessotto et al., 2003 and 2006). Cells attached to EMILIN1, via  $\alpha4\beta1$  integrin, loss stress fiber and focal adhesion stimulating the migratory process. The second receptor identified as EMILIN1 ligand is  $\alpha9\beta1$  integrin which positively influence the promigratory activity of EMILIN1 (Danussi et al., 2011). It was associate to the migratory “pathway” of EMILIN1 studying the skin district. Another important aspect of this ligand/receptor engagement is related to proliferation. Evidences demonstrated that the EMILIN1- $\alpha4/\alpha9$  integrins engagement regulate the proliferative homeostasis in the skin compartment. Usually integrin engagement induces a positive regulation of cell growth (Streuli et al., 2009), but in this case, ECM component-integrin binding leads to a reduction of cell proliferative rate. A possible explanation of their binding specificity and activity could be that  $\alpha4$  and  $\alpha9$  integrin are highly homologous; indeed they share 39% amino acid identity (Palmer et al., 1993).

EMILIN1 has a crucial role in maintenance of structural and functional integrity of lymphatic vessels depending on the interaction with  $\alpha4$  or  $\alpha9$  integrins. This property is the principal topic discussed in this thesis and we’re going to introduce this subject in the last section of the introduction (*2.4 A new abnormal lymphatic phenotype in *Emilin1* deficient mice*).

## **2. EMILIN1 AND LYMPHATIC SYSTEM**

### **2.1 Lymphatic vessels**

Lymphatic and blood vascular systems have distinct structural characteristics that reflect their specific and complementary functions. The lymphatic vasculature represents a second circulatory system and maintains tissue fluid homeostasis; it plays a major role in the absorption of dietary fat and in immune response, transporting lymphocytes and antigen-presenting cells to regional LNs; finally, it provides routes for tumor metastasis (Cueni et al., 2006 and 2008). The lymphatic vasculature consists of a complex network of capillaries and collecting vessels (Fig. 3). The lymphatic capillaries are blind-end vessels composed only by a single layer of overlapping endothelial cells (LECs), which are uniquely adapted for the uptake of protein-rich lymph from tissue interstitium. LECs in capillaries exhibit button-like junctions anchored to filaments in the ECM, that exert the necessary tension to keep the junctions opened and allow fluid entry (Gerli et al., 1990). Abnormalities of anchoring filaments may reduce adsorption from the interstitium, the propulsion of lymph and promote pathological conditions, such as lymphedema or diseases related to impaired immune responses (De Cock et al., 2006; Gerli et al., 1990; Danussi et al., 2008). The collecting lymphatic vessels are surrounded by a basement membrane and smooth muscle/mural cells, which are less organized than in blood vessels (Maby-El Hajjomi and Petrova 2008). In collecting vessels LECs have zipper-like junctions and contribute to the development of luminal valves (Baluk et al., 2007), often present at vessels branch points, those prevent lymph backflow (Bazigou et al., 2009). Intraluminal valves are composed of an ECM core covered by a LECs layer (Fig. 4) and allow to identify the function units of collectors, the lymphangion (Fig. 3). The perivascular ECM plays an integral role in lymphatic vessel function; indeed the fluid equilibrium is controlled by the cooperation of both lymphatic function and the ECM. The elasticity and hydration of a tissue is determined by the composition and organization of the ECM. Extensive and chronic degradation of the ECM eventually renders lymphatic vessels not responsive to the changes in the interstitium and therefore causes dysfunction (Negrini et al., 1996; Pelosi et al., 2007). All these structural features allow efficient fluid uptake of protein-rich lymph from tissue interstitium by capillaries and transport of lymph back to the blood vascular system by collecting vessels (reviewed by Makinen et al., 2007, Tammela et al., 2010).

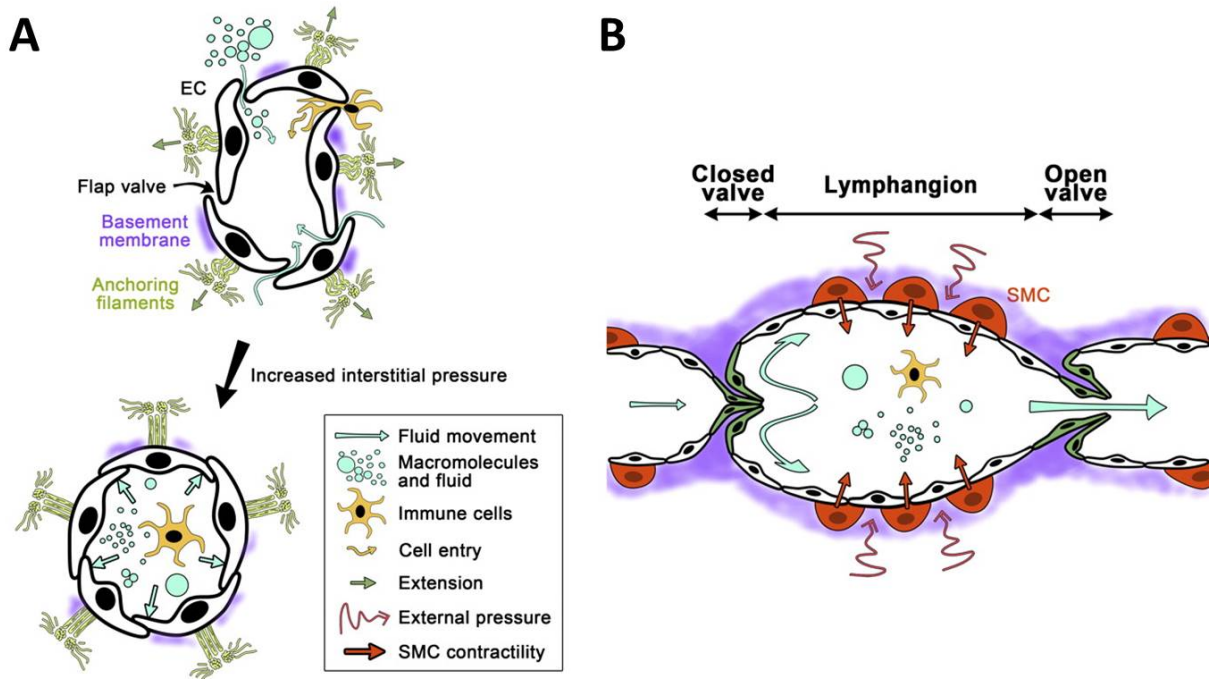


**Figure 3. Schematic representation of the structure and function of lymphatic vessels.** (A) Lymphatic capillaries usually have an irregular lumen and consist of a single layer of overlapping LECs without basement membrane coverage. LECs are connected to the surrounding ECM by anchoring filaments. When interstitial pressure (black arrow) increases, these filaments exert tension LECs and are thought to pull open the gaps between lymphatic endothelial cells so that fluid and cells enter the vessels for recirculation. (B) Mechanism of lymph propulsion in collecting vessels. Coordinated opening and closure of lymphatic valves is important for efficient lymph transport. SMCs covering each lymphangion. EC, endothelial cell; (from Shulte-Merker *et al.*, 2011).

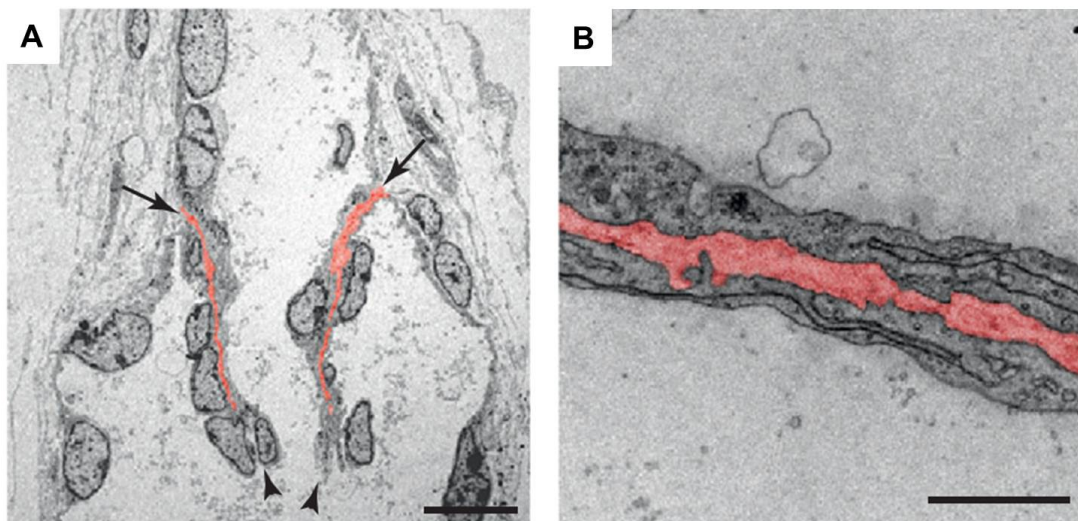


**Figure 4. ECM core in the valve leaflet.** (A and B) Transmission electron micrographs of wild-type valves in mesenteric lymphatic vessels of P6 mice. Arrows in (A) point to the matrix core (red) anchored into the vessel walls, arrowheads mark the free edges of the valve leaflets. (B) shows a valve leaflet with a connective tissue core (red). Scale bars: 10mm in (A), 1mm in (B); (from Bazigou *et al.*, 2009).

## 2.2 Lymphatic vessel development

In mice, lymphatic system formation (Fig. 5) begins around E9/E9.5 when a few endothelial cells in the anterior cardinal vein start expressing the lymphatic vessel hyaluronan receptor-1 (LYVE-1) (Jackson, 2004), followed by polarized expression of the transcription factor prospero-related homeobox 1 (Prox-1) (Wigle et al., 1999, 2002, Hong et al., 2002, Petrova et al., 2002). Prox-1 is a determinant factor critical to lymphatic differentiation and its overexpression in human blood vascular endothelial cells suppresses many blood vascular-specific genes and upregulates LECs-specific transcripts (Hong et al., 2002, Petrova et al., 2002). At E12.5 buds from anterior cardinal vein becomes evident and so the lymphatic vessels sprouting takes place. Several molecules sustain the lymphangiogenetic events such as vascular endothelial growth factor receptor 3 (VEGFR-3), VEGF-C/D (Karkkainen et al., 2000 and 2004, Baldwin et al., 2005), Neuropilin2 (Nrp2) (Yuan et al., 2002) and secondary lymphoid chemokine (SLC). Full-length VEGF-C and VEGF-D have the highest binding affinity for VEGFR-3 and their proteolytically processed forms interact and activate another member of the vascular endothelial growth factor receptor family, VEGFR-2 (Joukou et al., 1996 and 1997). They are involved in lymphangiogenetic stimuli also in adulthood.

Other important lymphatic factors are: desmoplakin and  $\beta$ -chemokine, involved in later embryogenesis and maturation (Ebata et al., 2001); transmembrane growth factor Ephrin B2 (EphB2) involved in postnatal remodeling of lymph vasculature and valves (Makinen et al., 2005); podoplanin crucial for the correct vessel formation and functionality (Schacht et al., 2003); Angiopoietin 2 (Ang2) involved in remodeling and maturation (Gale et al., 2002, Saharinen et al., 2005). Two molecules expressed only in the hematopoietic cells lead to the separation of blood-lymphatic vasculature: tyrosine kinase Syk and adaptor protein SLP76 (Abtahian, et al., 2003). Lymphatic-venous anastomoses occur in different sites of circulatory system: thoracic duct connects to the left subclavian and the internal jugular veins, other anastomoses are in the renal, hepatic and adrenal veins, in the LNs and in other peripheral locations (Aalami, et al., 2000, Jeltsch et al., 2003). Moreover lymphatic-venous anastomoses are frequently observed in lymphoedema, chylous ascites and chylothorax, where they are an adaptive response to lymphatic hypertension (Alitalo et al., 2005).

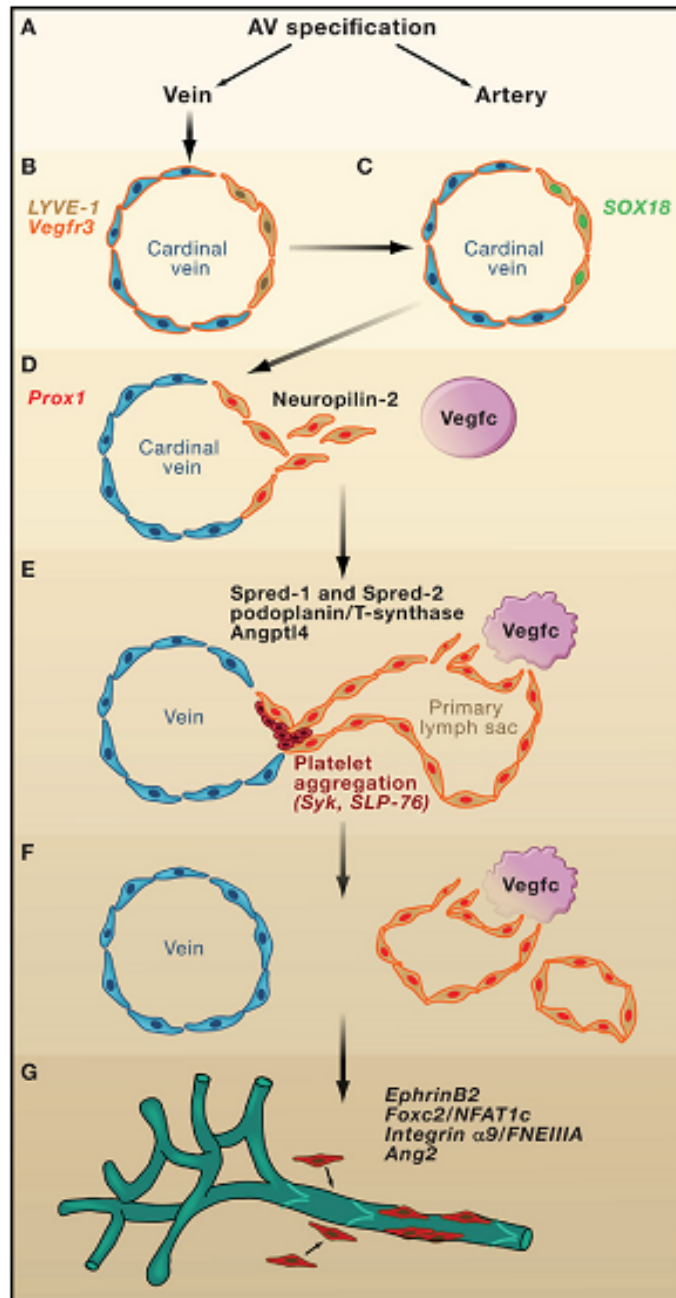


**Figure 5. Development of the mammalian lymphatic vasculature.** (A) After differentiation from angioblasts, endothelial cells undergo arterialvenous (AV) specification. (B) Embryonic veins express high levels of VEGFR-3, whereas a subpopulation of endothelial cells in the large central veins upregulate LYVE-1. (C) The transcription factor SOX18 is induced in the LYVE-1-positive LECs precursors. (D) SOX18 induces Prox1 expression, the first marker for LEC determination. At this time, VEGFR-3 expression is downregulated in the blood vessels, but it remains high in the LEC precursors, which also begin to express neuropilin-2, rendering them more responsive to VEGF-C signals arising from the lateral mesenchyme. These signals are required for sprouting of the LECs, which form lymph sacs lateral to the central veins. (E) The LECs begin to express podoplanin, which activates the Syk tyrosine kinase in platelets. This leads to platelet aggregation, which blocks lymphatic-venous connections and helps to separate the blood and lymphatic vascular systems. (F) Further centrifugal growth of the lymphatic vessel network ensues, driven by VEGF-C/VEGFR-3 and possibly Ccbe1 signals. (G) The final steps of lymphatic vascular development involve differentiation to lymphatic capillaries and collecting lymphatic vessels. The latter forms intraluminal valves, recruit SMCs, develops continuous interendothelial junctions, and produces a basement membrane. (from Tammela and Alitalo, 2010)

Lymphatic valves originate around E16.5 by specification of valve forming cells. These cells express high levels of the transcription factors Prox-1 and Foxc2 (Norrmen et al., 2009). Prox-1 is required for the establishment of LEC identity (Wigle et al., 1999), and Foxc2 for the specification capillaries vs collecting and so for the onset of lymphatic valve formation (Norrmen et al., 2009) and their positioning within the collecting vessels. Following specification, valve cells delaminate from the vessel wall, extend and migrate into the lumen and mature into heart-shaped leaflets capable of preventing lymph backflow. The crucial role of Foxc2 in the valve formation is demonstrated in a KO model, where its absence leads to loss of luminal valves, acquisition of basement membrane and smooth muscle cells (SMC) coverage by capillaries and so an abnormal lymph flow (Petrova et al., 2004). Moreover, Foxc2 shows high expression levels even in the adult valves. Downstream of Prox1 and Foxc2 and as a response to oscillatory shear stress, connexin 37 and calcineurin/NFAT system regulates the formation of a ring-like valve area, valve-territory delimitation, and postnatal valve maintenance (Kanady et al., 2011, Sabine et al., 2012).

Abnormal phenotype occurs when these factor are mutated or they expression are altered (Table 1). In all cases the deficiency of their expression leads to embryonic or perinatal lethality while genetic mutations of some factors induce pathological conditions. In these regards not only mouse models are useful to study lymphangiogenic process, but also Zebrafish and Xenopusembryos, as small vertebrate models, represent a good opportunity for identification of novel regulators of lymphatic vascular development and detailed analysis using in vivo imaging approaches (Ny et al., 2005; Yaniv et al., 2006; Maby-El Hajjami and Petrova, 2008). These models are very versatile, in fact it is possible to induce mutations in genes extremely important during lymphangiogenesis. In this way it could to improve the knowledge about the role of these genes and which kind of disease could originated by their altered expression.

The deletion of Prox1, the transcription factor crucial for lymphatic differentiation, leads to a complete absence of the lymphatic vasculature; endothelial cells bud from the cardinal vein but fail to express lymphatic endothelial markers and do not migrate (Wigle et al., 2002). *Prox-1*<sup>-/-</sup> mice die perinatally in most genetic backgrounds except in the outbred NMRI background, in which they develop chylous ascites and adultonset obesity (Harvey et al., 2005). VEGF-C homozygous deletion leads to the complete absence of the lymphatic vasculature in mouse embryos because the endothelial cells in the cardinal veins fail to migrate and to form primary lymph sacs. Its heterozygous deletion displays severe lymphatic hypoplasia (Karkkainen et al.,

2004). On the contrary the deletion of VEGF-D doesn't affect development of the lymphatic vasculature, although exogenous VEGF-D protein rescues the impaired vessel sprouting in *Vegf-C*<sup>-/-</sup> embryos (Karkkainen et al., 2004, Baldwin et al., 2005). More severe is the VEGFR-3 deletion: it induce defects in blood-vessel remodelling and embryonic death at mid-gestation (Dumont et al., 1998). Heterozygous missense point mutations in VEGFR-3, which lead to tyrosine kinase inactivation, have been found in patients with Milroy disease. The mutation leads to hypoplasia of cutaneous lymphatic vessels and lymphedema (Karkkainen et al. 2000). Chy mice have a similar mutation and develop lymphedema. In *Nrp2* knockout mice, the lymphatic capillaries are absent or severely reduced until postnatal stages, whereas larger lymphatic vessels develop normally (Yuan et al. 2002). Mutated form of EphB2, lacking the C-terminal site for binding PDZ-domain-containing proteins, leads to a normal blood vasculature but display a not correct postnatal remodelling of the lymphatic vasculature. The collecting lymphatic vessels appear hyperplastic, without luminal valve and remodelling of the primary lymphatic capillary doesn't occur (Makinen et al., 2005). Podoplanin KO mice die perinatal and display lymphedema and abnormal lymphatic function and patterning, perhaps due to impaired migration of LECs (Schacht et al., 2003). Ang-2 deficiency leads to vessel hypoplasia which is rescue by administration of Ang1 (Gale et al., 2002). Mice with mutations in Syk and SLP76 have arterio-venous shunts and abnormal lymphatic-venous communications (Abtahin et al., 2003). Heterozygous loss-of-function mutations of FOXC2 instead induce lymphoedema-distichiasis, another autosomal dominant disease, likely due to defective vessel patterning and abnormal lymphatic valves (Ferrell, 2002 and reviewed by Petrova et al., 2004, Alitalo et al., 2005).

Gene	Function	Lymphatic phenotype	Other defects	Lethality
<i>Angpt2</i> , gene targeted <sup>43</sup>	Growth factor, ligand of Tie-2	Hypoplasia, chyloous ascites <sup>(-/-)</sup>	Eye hyaloid vasculature fails to regress <sup>43</sup> , abnormal inflammatory response (H. Augustin, personal communication)	<sup>-/-</sup> : perinatal or normal
<i>Efnb2</i> , PDZ-binding mutant <sup>38</sup>	Ligand of EphB receptors	Retrograde lymph flow, chylothorax, ectopic mural cells, absent valves ( $\Delta V/\Delta V$ )	Lung development defects (R. Klein, personal communication)	<sup>-/-</sup> : perinatal <sup>+/-</sup> : normal
<i>Foxc2</i> , gene targeted	Transcription factor	Abnormal lymphatic patterning, presence of mural cells, absent valves <sup>(-/-347)</sup> ; lymphatic vessel and lymph node hyperplasia <sup>(+/-389)</sup>	Aortic arch malformations, heart septal defects, abnormal kidney and urethra development	<sup>-/-</sup> : E12.5-perinatal <sup>+/-</sup> : normal
<i>Itga9</i> , gene targeted <sup>23</sup>	Adhesion receptor	Lymphoedema, chylothorax <sup>(-/-)</sup>	Not reported	<sup>-/-</sup> : perinatal <sup>+/-</sup> : normal
<i>Elk3</i> (Net), gene targeted <sup>90</sup>	Transcription factor Mutant form lacks DNA-binding domain	Lymphangiectasis, chylothorax <sup>(-/-)</sup>	Impaired wound and tumour angiogenesis <sup>+/-</sup>	<sup>-/-</sup> : perinatal <sup>+/-</sup> : normal
<i>Nrp2</i> , gene targeted <sup>10</sup>	Receptor for VEGF165, VEGF145, PlGF, VEGF-C and class 3 semaphorins	Transient hypoplasia of lymphatic capillaries <sup>(-/-)</sup>	Defects in neural fasciculation and guidance	<sup>-/-</sup> : perinatal <sup>+/-</sup> : normal
Podoplanin ( <i>Gp38</i> ), gene targeted <sup>51</sup>	Membrane glycoprotein	Lymphangiectasis, abnormal lymph transport, lymphoedema <sup>(-/-)</sup>	Respiratory failure due to abnormal lung development	<sup>-/-</sup> : perinatal <sup>+/-</sup> : normal
<i>Pik3r1</i> , gene targeted <sup>91</sup>	Regulatory subunits of class I <sub>A</sub> PI(3)K	Chyloous ascites <sup>(-/-)</sup>	Liver necrosis, enlarged skeletal muscle fibres, brown fat depositions, calcification of heart tissue	<sup>-/-</sup> : perinatal (129Sv × C57Bl6) or 30% survival (outbred) <sup>+/-</sup> : normal
<i>Prox1</i> , gene targeted or endothelial specific deletion <sup>29,33</sup>	Transcription factor	No lymphatic vessels <sup>(-/-)</sup> Chyloous ascites, adult onset obesity <sup>(+/-)</sup>	Abnormal eye, liver and pancreas development	<sup>+/-</sup> : perinatal in most backgrounds <sup>-/-</sup> : E14.5
<i>Lcp2</i> (SLP-76) and <i>Syk</i> , gene targeted <sup>41</sup>	Tyrosine kinase (Syk); adaptor protein (SLP-76)	Failure of separation of blood and lymphatic vasculature, chyloous ascites <sup>(-/-)</sup>	Failure of T-cell development and fetal haemorrhage (Slp76) Block of B-cell development and fetal haemorrhage (Syk)	<i>Lcp2</i> <sup>-/-</sup> : perinatal <i>Lcp2</i> <sup>+/-</sup> : normal <i>Syk</i> <sup>-/-</sup> : perinatal <i>Syk</i> <sup>+/-</sup> : normal
<i>Sox18</i> (ragged) <sup>92</sup>	Transcription factor Spontaneous missense mutations	Edema and chyloous ascites <sup>(-/-)</sup>	Lack of vibrissae and coat hairs, generalized oedema and cyanosis due to cardiovascular defects	<sup>-/-</sup> : perinatal <sup>+/-</sup> : normal
Trisomy 16 (Ts16) <sup>93</sup>	Many	Nuchal oedema, abnormal size and structure of jugular lymph sacs from E14	Multiple cardiac or craniofacial development defects	E16–E20
<i>Vegfc</i> , gene targeted <sup>16</sup>	Growth factor, ligand of VEGFR-3	No lymphatic vessels <sup>(-/-)</sup> hypoplasia, chyloous ascites <sup>(+/-)</sup>	Not reported	<sup>-/-</sup> : E17–E19 <sup>+/-</sup> : perinatal or normal
<i>Vegfr3</i> ( <i>Chy</i> , ethylnitrosourea-induced mutation) <sup>9</sup>	Receptor tyrosine kinase, kinase-inactivating mutation I1053F	Hypoplasia, chyloous ascites <sup>(+/-)</sup>	Failure of remodelling of primitive blood vascular plexus <sup>(-/-)</sup>	<sup>-/-</sup> : E10 <sup>+/-</sup> : perinatal or normal

**Table 1. Genes that mediate lymphatic vasculature formation and patterning; (from Alitalo et al., 2005).**

## 2.3 ECM regulates lymphatic valve development

Ultrastructural analyses demonstrate a close physical association between ECM and LECs in the valve leaflets (Navas et al., 1991). Valve development is accompanied by deposition of ECM constituents such as laminin  $\alpha 5$  and collagen IV and increased expression of their ligands on the cell membrane such as integrin  $\alpha 9$  (Norrmen et al., 2009, Bazigou et al., 2009) suggesting that ECM provides structural integrity during valve morphogenesis and it might control LEC functions.

The knowledges about the molecular mechanisms by which ECM regulates LECs behaviour are poor. The first ECM components expressed in the lymphatic environment are laminin  $\alpha 5$  and collagen IV around E10.5–11.0 (Wigle et al., 2002, Oliver, 2004). Another ECM molecule

expressed since the early stages of lymphatic formation is EMILIN1, a component of anchoring filaments in lymphatic capillaries (Danussi et al., 2008) and it is essential to sustain the proper formation and functionality of the lymphatic vessel (Danussi et al., 2008, 2013 and this thesis). Also the FN-EIIIA is involved in the formation of the lymphatic valves (Bazigou et al., 2009) regulating FN fibril assembly, which is essential for the formation of ECM core of valve leaflets. Therefore the ECM component role during lymphangiogenesis depends on the presence of particular ligand, such as integrin, on the surface of the cells. A decisive molecule is  $\alpha 9\beta 1$  integrin. The  $\beta 1$  integrin activation by VEGF-C and VEGF-D but also extracellular matrix proteins as collagen and FN, enhance tyrosine phosphorylation of VEGFR-3 (Wang et al., 2001). Furthermore VEGF-C is able to interact with Nrp2 and  $\alpha 9$  integrin. Nrp2 is cointernalized with VEGFR-3 in lymphatic endothelial cells upon stimulation with VEGF-C or VEGF-D, suggesting that Nrp2 modulates VEGFR-3 signaling (Karpanen et al., 2006).  $\alpha 9\beta 1$  integrin binding activates ERK1/2 and Paxillin in cultured endothelial cells, suggesting that integrin activation is involved in LEC migration (Vlahakis et al., 2005). Integrins, interacting with ECM ligands, contribute to VEGFC/D/VEGFR3 signaling. We in this thesis demonstrate that also EMILIN1 can engage  $\alpha 9\beta 1$  integrin and that this binding is crucial for the proper formation of lymphatic vessel and intraluminal valve leaflet. Also another glycoprotein associated to ECM, usually implicated in the development of the nervous system, is involved in lymphangiogenesis: Reelin. It is widely expressed in the lymphatic vasculature during development and in adult tissues. Reelin influence the maturation of collecting vessel and regulate the deposition of the collectors coverage (Lutter et al., 2012).

Also ECM protein deficiency leads to abnormal lymphatic vessels developing. EMILIN1 deficiency doesn't cause mice die, but leads to altered capillaries and collecting vessels structure and functionality (Danussi et al., 2008, 2013 and this thesis). Dysplastic intraluminal valves are presented also in FN-EIIIA null mice (Bazigou et al., 2009). Reelin deficient mice had normal lymphatic capillaries but exhibited specific dermal collecting vessel defects, characterized by reduced SMC coverage and high expression of lymphatic capillary marker LYVE-1 (Lutter et al., 2012). Moreover, the absence of the connection between LECs and ECM compartment in  $\alpha 9^{-/-}$  *integrin* mice leads to chylothorax during the early postnatal period and so their death (Huang et al., 2000) and the formation of abnormal lymphatic valve leaflets, with a disorganized FN in the matrix core, short cusps and retrograde lymphatic flow (Bazigou et al., 2009).

## 2.4 A new abnormal lymphatic phenotype in EMILIN1 deficient mice

A previous study on the role of EMILIN1 in lymphatic system performed in our laboratory, demonstrated the first abnormal lymphatic phenotype associated to an ECM molecule deficiency (Danussi et al., 2008).

A microarray analysis showed that LECs express abundant EMILIN1 mRNA (Podgrabinska et al., 2002). The study reported that EMILIN1 is also expressed in mouse skin, intestine, lung and lymph node tissues in association with lymphatic vessels and it colocalizes with the LEC-specific marker LYVE-1. Moreover, it is clearly expressed within the abluminal surfaces of LECs and EMILIN1-positive fibers radiating from LECs to the surrounding perivascular area are frequently detected (Fig. 6).

*Emilin1*<sup>-/-</sup> mice display hyperplasia and enlargement of dermal, as well as intestine lymphatic vessels. These vessels frequently present a tortuous and irregular pattern. An immunofluorescence performed to assess the growth and the patterning of lymphatic vasculature, demonstrated that the lymphatic vessels are more abundant and dilated in *Emilin1*<sup>-/-</sup> mice compared to those of WT mice in the skin as well as in the intestine (Fig. 7). In addition, *Emilin1*<sup>-/-</sup> mouse lymph nodes also show a significant increase of lymphatic, but not in blood vessel density.

Therefore to evaluate the influence of EMILIN1 in lymphatic vessel growth *in vivo*, a model of neolymphangiogenesis was investigated by inducing the formation of hyperplastic lymphatic vessels. Lymphangioma plaques were more numerous and larger in *Emilin1*<sup>-/-</sup> mice and lymphatic but not blood vessel density was significantly increased in *Emilin1*<sup>-/-</sup> mouse lymphangiomas compared with those of their WT littermates. This phenotype was partially due to an altered proliferation process as demonstrated by *in vitro* assay. An *in vitro* tubulogenesis assay showed that *Emilin1*<sup>-/-</sup> mouse lymphangioma endothelial cells (LAECs), isolated from lymphangiomas, induced in WT and KO mice, produce tube-like structures poorly organized compared to those of WT cells.

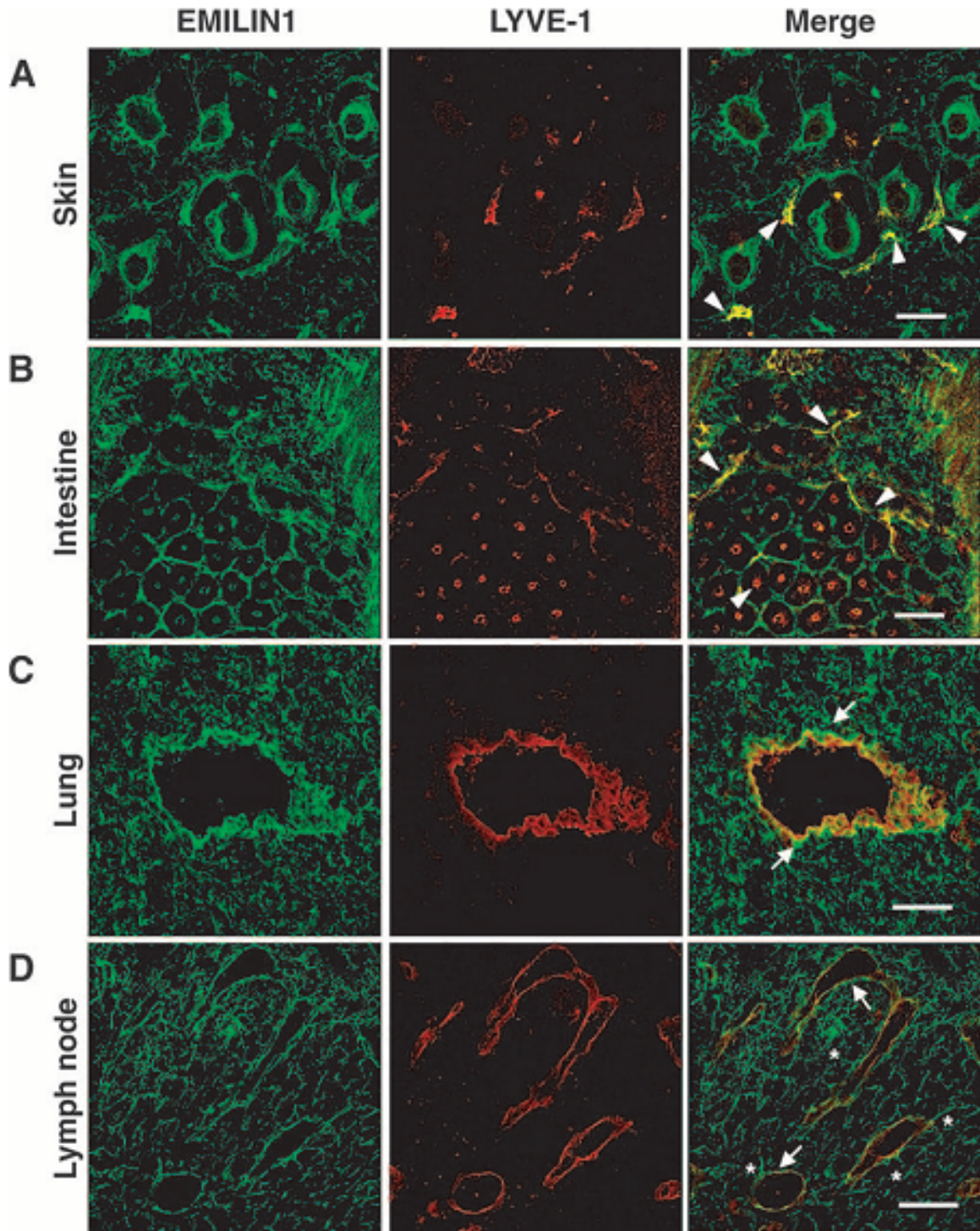


**Figure 6. EMILIN1 is expressed in association with lymphatic vessels.** (A to D) Cryostat sections of normal mouse tissues doubly stained with anti-EMILIN1 (green) and anti-LYVE-1 (red) antibodies. In all mouse tissues and organs examined, EMILIN1 was uniformly distributed in the stroma. (A) In the skin, EMILIN1 staining colocalizes with LYVE-1-positive lymphatic vessels surrounding hair follicles (arrowheads). (B) In the small intestine, EMILIN1 colocalizes with LYVE-1-positive lacteals and submucosal lymphatic vessels (arrowheads). (C and D) At higher magnification, in the lung and lymph nodes, it is more evident that EMILIN1 is distributed at the abluminal surface of LECs (arrows). In the lymph node, EMILIN1-positive fibers connecting LECs to the surrounding ECM are evident (asterisks); (from Danussi *et al.*, 2008).

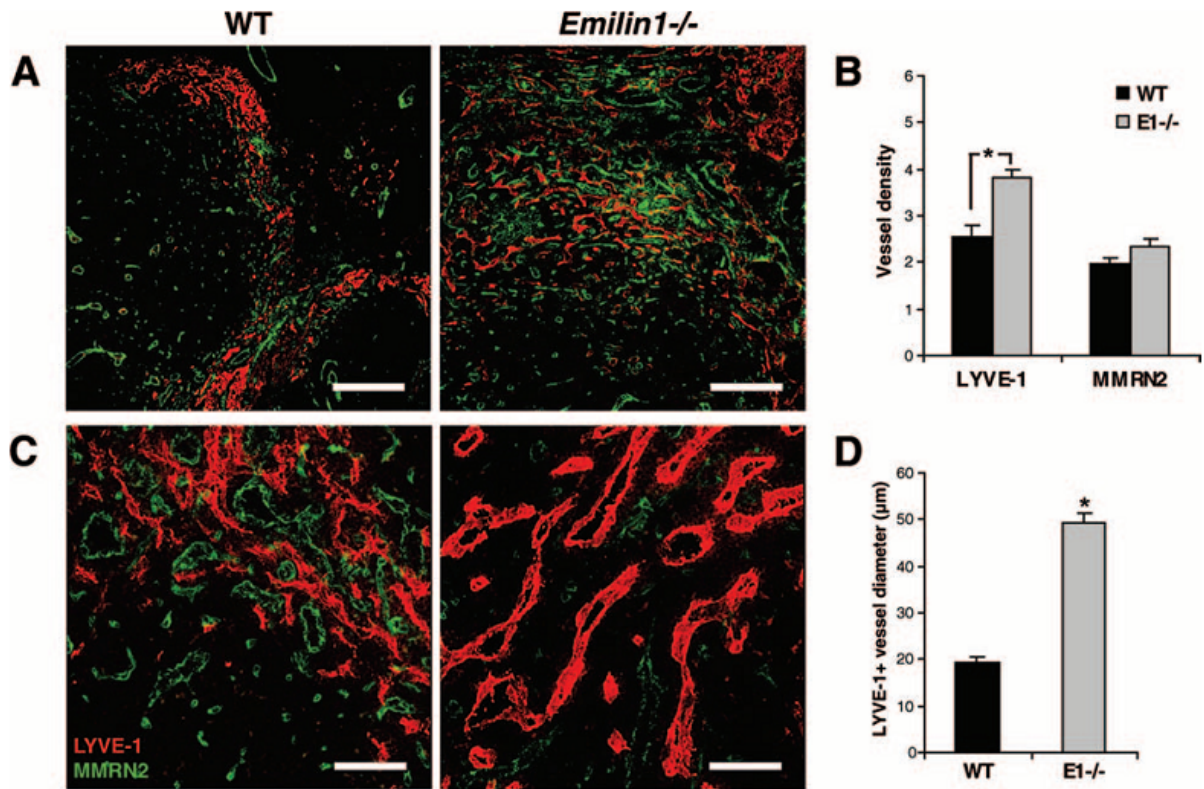


**Figure 7. Hyperplasia and enlarged lymphatic vessels in lymph nodes of *Emilin1* deficient mice.** (A) Representative immunofluorescence images of mouse inguinal lymph node cryostat sections stained for LYVE-1 (red) and MMRN2 (green). Scale bars, 300µm. (B) ImageJ software analysis revealed that the relative area occupied by lymphatic vessels in lymph nodes of *Emilin1*<sup>-/-</sup> (E1<sup>-/-</sup>; n=9) mice was significantly higher (mean standard error [SE]; \*,  $P < 2 \times 10^{-6}$ ) than in those of their WT littermates (n=9). (C) Higher-magnification images show dilated LYVE-1-positive vessels (right). Scale bars, 75µm. (D) The mean value  $\pm$ SE of the diameters (ImageJ software analysis) of lymphatic vessels is reported. \*,  $P < 2 \times 10^{-7}$ ; (from Danussi et al., 2008).

The structural lymphatic vessel abnormalities of *Emilin1*<sup>-/-</sup> mice as hyperplasia, enlargement of lymphatic vessels, reduction of anchoring filaments numbers and abnormal overlapping intercellular junction, are functionally relevant. EMILIN1 deficiency, in fact, induces inefficient lymph drainage and lymph leakage both under normal conditions and in response to an inflammatory agent. In accord with these lymphatic vessel defects, the absence of EMILIN1 induces mild lymphedema observed in *Emilin1*<sup>-/-</sup> mice in the swelling of the paws (Fig. 8).

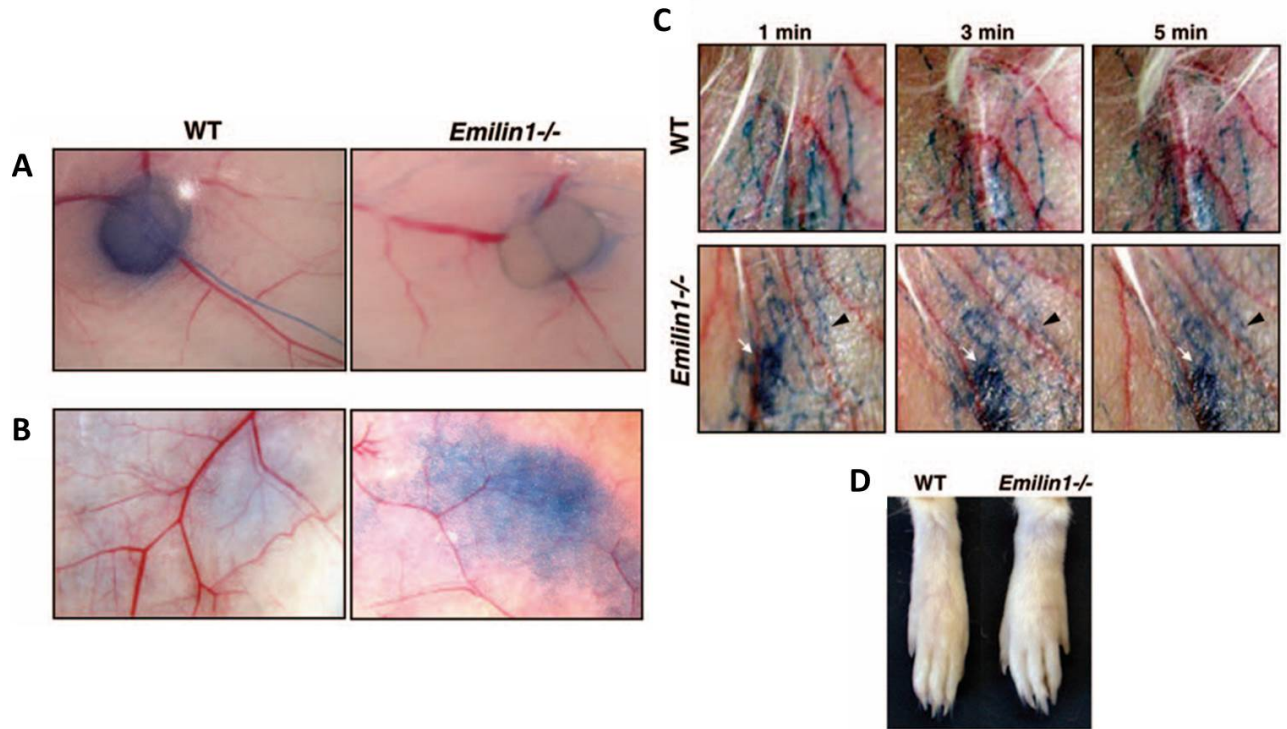


**Figure 8. Impaired lymphatic function in *Emilin1* deficient mice.** (A) Evans blue dye accumulation in inguinal lymph nodes. The dye is barely detectable in *Emilin1*<sup>-/-</sup> mice (right), whereas the inguinal lymph node is easily visualized in WT mice. (B) Lymph leakage. Spots of Evans blue extravasation in mustard oil-treated mouse skin. (C) Lymphatic vessels in the rims of the ears of WT and *Emilin1*<sup>-/-</sup> mice. The arrows indicate the major leakage areas in *Emilin1*<sup>-/-</sup> mouse ears. (D) Peripheral edema in the hind limbs of WT and *Emilin1*<sup>-/-</sup> mice (from Danussi et al., 2008).

# **AIM OF THE STUDY**

## **AIM OF THE STUDY**

EMILIN1 is expressed in lymphatic system and it has a crucial role for the proper formation of lymphatic capillaries. *Emilin1*<sup>-/-</sup> mouse is the first abnormal lymphatic phenotype associated with an ECM molecule deficiency, displaying enlargement of lymphatic vessels in several tissues and the reduction of anchoring filaments. The morphological abnormalities lead to inefficient lymph drainage, increase of lymph leakage and a mild lymphedema. EMILIN1 binds to  $\alpha4\beta1$  and  $\alpha9\beta1$  integrins in a very specific way, through its functional domain gC1q, and exerts an important role in the control of cell proliferation and migration in several districts.

The overall aim of this thesis is to extend the study of the role of EMILIN1 in the lymphatic system. The goal is to answer to the following questions:

- Since EMILIN1 leads to a proper formation and functionality of the lymphatic capillaries, is it also involved in the structure and function of the collecting lymphatic vessels and their intraluminal valves?
- Does EMILIN1 have a regulatory role in the mechanisms that control the proper setting of lymphatic endothelial cells in the formation and maintenance of lymphatic valves?
- How the engagement between EMILIN1 and  $\alpha4/\alpha9$  integrins is important in these processes?
- Is EMILIN1 involved in metastatic spread through lymphatics?

# **MATERIAL AND METHODS**

1. **Antibodies and reagents.** Rat monoclonal anti-mouse EMILIN1 and mouse anti-human gC1q antibodies were produced in our laboratories as previously described (Danussi et al., 2008, Spessotto et al., 2003); rabbit polyclonal anti-mouse LYVE-1 and anti-Prox-1 (Abcam); mouse monoclonal anti-integrin  $\alpha 9\beta 1$  (clone Y9A2) and anti-integrin  $\alpha 4$  (clone P1H4; Chemicon), goat polyclonal anti-mouse integrin  $\alpha 9$  (R&D Systems Inc.); Cy-3-conjugated mouse antibody against  $\alpha$ -smooth muscle actin (Sigma); rat anti-mouse PECAM-1 (CD31, BD Biosciences Europe) antibodies were used. The rabbit polyclonal anti Ki67 proliferation marker was purchased from Abcam. Human recombinant EMILIN1 was obtained as previously described (Spessotto et al., 2006). The C-terminal domain of EMILIN1 (gC1q) and the recombinant mutant (E933A) of the integrin binding sequence of gC1q were produced as previously described (Spessotto et al., 2003, Verdone et al., 2008). For the production of recombinant ED-A domain (EIIIA) the 273-bp cDNA sequence coding for the complete amino acid sequence of the mouse EIIIA domain, from residue 1721 to residue 1811 (NCBI NP\_034361.1) was generated by RT/PCR using as template mouse embryo total RNA transcribed with AMV (Promega), amplified with Phusion taq DNA polymerase (NEB), and the following specific primers : (a) 5' CCGGATCCAACATTGATCGCCCTAAA 3' including the underlined BamHI restriction site, and (b) 5' GGGGTACCTTAGGCTGTGGACTGGATTCCAATC 3' including the underlined KpnI restriction site. PCR product was isolated, digested with BamHI and KpnI restriction enzymes, (Promega) ligated in pQE-30 expression vector with a 5' 6x His tag (QIAGEN), and then transformed in M15 Escherichia coli bacterial strain. A clone carrying the cloned sequence was amplified and the 6x His NH<sub>2</sub>-tagged rEIIIA extract from bacterial pellet by sonication was purified using a Ni-NTA resin column (QIAGEN) according to the manufacturer. The eluted recombinant fragment was then dialyzed against PBS and concentration and purity verified by Comassie blue staining after SDS-page on a 4-20% precast polyacrilamide gel (Bio-Rad Laboratories).

2. **Mouse procedures and cell cultures.** Procedures involving animals and their care were conducted according to the institutional guidelines in compliance with national laws (Legislative decree no. 116/92). *Emilin1*<sup>-/-</sup> mice (CD1 and C57Bl/6 strains) and *Fn-EIIIA*<sup>-/-</sup> mice were generated as previously described (Zanetti et al., 2004, Muro et al., 2003). Human Microvascular Endothelial Cells Dermal Lymphatic-Neonatal (HMVEC-dLyNeo), Human Microvascular Endothelial Cells Lung Lymphatic (HMVEC-LLy) and the media optimized for their growth

were purchased from Lonza. Mouse lymphangioma endothelial cells (LAEC) were isolated following the procedure previously described (Danussi et al., 2008). The cells were cultured on 1% porcine skin gelatin (Sigma)-coated plates in EGM-2 MV medium (Cambrex Bio Science) and immortalized by means of SV40 infection (Danussi et al., 2012). PC3 (prostate), MDA-MB-231 (breast), and SKOV-3 (ovarian) carcinoma cells were from American Type Culture Collection and each were cultured in RPMI medium supplemented with 10% fetal calf serum. All human cell lines were authenticated by BMR Genomics srl Padova, Italia, on December 2011 according to the Cell ID System (Promega) protocol using Genemapper ID Ver 3.2.1 to identify DNA short tandem repeat profiles.

3. **Whole mount staining.** Mice were anesthetized with 0.4 g Avertin (Sigma)/kg of body weight, and sacrificed. Tissue specimens of interest were extracted and fixed in 4% PFA for 18 hours at 4°C. Then the blocking solution (PBS, 0.3% Triton X-100 and 5% serum) was added for 8 hours at 4°C, followed by primary antibody incubation for 18 hours at 4°C. After 5 washes with PBS 0.3% Triton X-100, the secondary antibody Alexa Fluor® or HRP conjugated was added and incubated for 18 hours at 4°C. Images were acquired with a Leica TCSSP2 confocal system (Leica Microsystems), using LCS Software, equipped with HC PL Fluotar 10x/0.30 NA, HCX PL Apo 40x/1.25-0.75 NA oil and HCX PL Apo 63x/1.40-0.60 NA oil objectives or captured with a Leica ICC50 camera connected with a Leica DM750 microscope equipped with N Plan objective 5x/-0.12 NA, HI-Plan objective 10x/0.25 NA and objective 20x, all from Leica.

4. **Electron microscopy.** Mesenteries were dissected from P21 mice, fixed with 2.5% glutaraldehyde in 0.1 M sodium cacodylate buffer (pH 7.4) for 3 hours, washed in 0.1 M sodium cacodylate buffer overnight, and fixed with 1% osmium tetroxide in 0.1 M sodium cacodylate buffer as previously described (Zanetti et al., 2004). All samples were dehydrated with ethanol and embedded in Epon E812. Serial semithin cross sections of collecting lymphatic vessels were stained with toluidine blue. Ultrathin sections were obtained from several blocks, stained with lead citrate and uranyl acetate, and observed in a Philips EM 400 transmission electron microscope operated at 100 kV.

5. **Cell adhesion assay.** The quantitative cell adhesion CAFCA assay was performed as previously described (Spessotto et al., 2009). CAFCA miniplates were coated with ECM protein. Cells were labeled with the vital fluorochrome calcein AM (Molecular Probes) for 15 minutes at

37°C and then aliquoted into the bottom CAFCA miniplates, which were centrifuged to synchronize the adhesion of the cells with the ligand. The miniplates were then incubated for 20 minutes at 37°C and subsequently mounted together with a similar CAFCA miniplate to create communicating chambers for subsequent reverse centrifugation. The relative number of cells which bound or not the ligand was estimated by top/bottom fluorescence detection in a computer interfaced GeniusPlus microplate reader (Tecan).

6. **Migration assays.** (6.1) *Wound healing assay.* Cells were allowed to grow to confluence in 12-well tissue culture plates. A 200- $\mu$ L tip was used to introduce a scratch in the monolayer. The wells were imaged and recorded at 10 $\times$  magnification with a Leica AF6000 fluorescence microscope system (Leica Microsystem) for 20 hours postscratch at 15 min intervals. (6.2) *Transwell chamber migration/haptotaxis assay.* Cellular migration was assessed by FATIMA assay as previously described with some slight modifications (Spessotto et al., 2009). The underside of the insert membranes was coated with 10  $\mu$ g/ml gC1q or EIIIA recombinant fragments. Cells were fluorescently tagged with Fast DiI (Molecular Probes), and added to the upper side of the inserts. After 8 hours, the membranes were cut off, mounted for analysis under a fluorescence microscope (Leica TCS SP2). The cells on the underside of the filter (transmigrated cells) were counted. (6.3) *Transmigration assays.* Tumor cell intravasation and extravasation throughout LAEC monolayers was conducted growing 2 X 10<sup>4</sup> WT and *Emilin1*<sup>-/-</sup> LAECs on the under- or upper-side of 1% gelatin-coated FluoroBlok inserts (8 mm poresize, BD Falcon). LAECs were allowed to grow in 24-well plates until confluence and then the inserts were added to each well to obtain separate chambers. DiI-labeled (Molecular Probes) tumor cells (1 X 10<sup>5</sup> cells) were added into the apical chamber. Migration was monitored at different time intervals by independent fluorescence detection from the top and bottom side of the membrane using GENios Plus reader (Tecan Italia)

7. **EMILIN1 silencing.** For production of lentiviral vectors, 293FT cells were transfected with pLP1, pLP2, pVSVG and scrambled pLKO or pLKO shRNA EMILIN1#33 lentiviral transfer vectors (Mission shRNA bacterial glycerol stock Sigma-Aldrich). The lentiviral vector yield was determined by measuring the amount of p24 Gag protein using a HIV-1 p24 Antigen ELISA Kit (PerkinElmer) according to manufacturer's instructions. 2.8 x 10<sup>4</sup> wild type LAEC cells were seeded in 6-well dishes 1 day before transduction. Cells were exposed for 24 hours to

lentivirus vector preparations with MOI ranging from 5 to 15, supplemented with polybrene. Transduced cells were grown in selective medium containing puromycin for 5 days.

8. **Lymphangiography.** Mice were anesthetized with Ketamine/Xilazine combination (100mg/Kg and 10mg/Kg respectively). 2  $\mu$ l of 5 mg/ml FITC-dextran (Mw ~2000 kDa; Invitrogen) was subcutaneously injected into the tail of anaesthetized mice (P21 or 6-week old) with a Hamilton syringe. At different time intervals, mice were sacrificed and draining lymph nodes and collectors were imaged using a stereomicroscope Leica M205 FA and Leica DFC310 FX digital camera (Leica Microsystems). LNs were excised, fixed with PFA 4% for 1 hour and fluorescent signals were detected in a computer interfaced GeniusPlus microplate reader (Tecan).

9. **Computer-assisted morphometric analyses.** To quantitatively evaluate valve density samples were analyzed using a Leica TCS SP2 confocal system detecting simultaneous positivity for Prox1 and  $\alpha$ -SMA. The series obtained were then processed with Volocity 3D Image Analysis Software (PerkinElmer). On the optical acquired images, computer-assisted morphometric analyses were performed using the ImageJ software (<http://rsb.info.nih.gov>).

10. **Histological and immunofluorescence analysis.** Mouse dorsal skin specimens were excised and processed, embedded in optimal cutting temperature compound (Kalttek), snap frozen, and stored at -80°C. Cryostat sections of 7  $\mu$ m were air dried at room temperature and kept at -80°C wrapped in aluminum foil. For histological analysis, sections were stained with hematoxylin/eosin (H/E). For immunofluorescence staining, the sections were equilibrated at room temperature, hydrated with PBS/1%Triton X-100 for 15 min, and fixed with PBS 4% PFA for 15 min. Then, they were permeabilized (with PBS, 1% BSA, 0.1% Triton X-100, and 2% FCS) for 5 min and saturated with the blocking buffer (PBS, 1% BSA, and 2% FCS) for 30 min. The primary antibodies were then incubated at room temperature for 1h followed by three 5 min washes in PBS, and the secondary antibody incubation was performed for 1h. Multiple staining was performed using a combination of different secondary antibodies conjugated with Alexa Fluor 488 and 568 (Invitrogen). Nuclei were visualized with TO-PRO (Invitrogen). Images were acquired with a true confocal scanner system (SP2; Leica) equipped with an HC PL Fluotar 10 $\times$ /0.30 NA and HCX PL Apo 40 $\times$ /1.25–0.75 NA and HCX PL Apo 63 $\times$ /1.40–0.60 NA oil objectives (Leica) using Leica confocal software.

11. **RNA extraction and RT-PCR.** Total cellular RNA was isolated from mouse lymph nodes using TRIZOL (Invitrogen) according to the manufacturer's protocol. RT reactions were conducted with 1mg of total RNA using AMV-Reverse Transcriptase (Promega Italia). RNA was reverse transcribed into the first-strand cDNA using random hexamer primers. The primers for mouse keratin 14 (KRT14) and 8 (KRT8) were: 5'-GGCCAACACTGAACTGGAGGTG-3' and 5'-CAGCTCCTCCTTGAGGCTCT-3' and 5'-AGGCTGAGCTTGGCAACATC-3' and 5'-GAGATCTGAGACTGCAACTCA-3', respectively. The size of the amplification products was 229 (KRT14) and 234 (KRT8) bp. The primers for mouse  $\beta$ -actin were: 5'-GGCATTGTGATGGACTCCG-3' and 5'-GCTGGAAGGTGGACAGTGA-3'. PCR reactions were conducted using Go Taq DNA Polymerase (Promega Italia). Amplification products were resolved on 1.2% agarose gels stained with ethidium bromide.

12. **Statistical analysis.** Statistical significance of the results was determined by using the two-tailed unpaired Student's  $t$  test to determine whether two datasets were significantly different. To compare more than two datasets, we additionally performed a one-way analysis of variance followed by Tukey's post-hoc test.  $\chi^2$  test was used in some analyses, as indicated. A value of  $P < 0.05$  was considered significant.

# **RESULTS**

## 1. EMILIN1 AND LYMPHATIC COLLECTING VESSELS

### 1.1 EMILIN1 is expressed in developing and in mature lymphatic valves.

It was demonstrated that EMILIN1 is expressed along the lymphatic capillaries and that its deficiency led, in a murine model, to lymphatic vasculature defects associated with inefficient lymph drainage, increase of lymph leakage and to a mild lymphedema as pathological condition (Danussi et al., 2008). Starting from the defects of lymphatic capillaries seen previously, in this study we investigated if EMILIN1 was also involved in the formation, maturation and maintenance of lymphatic collecting vessels and their intraluminal valves.

Using Whole Mount Staining (WMS) technique we analyzed the EMILIN1 expression from early stages of lymphatic vessel formation till their maintenance in adulthood. The WMS technique allows morphological analyses on intact lymphatic vessels in a right and “real“ conformation. We observed that EMILIN1 was expressed along the vessels since the early stages of lymphatic vasculature development (Fig. 9 A). Indeed, at E16.5 stage of embryonic mouse development, the primary lymph plexus is already formed, the creation of a lymphatic network has begun and the commitment and specification of LECs are visible through the labeling of the specific lymphatic marker Prox-1 (Wigle and Oliver, 1999). At this stage, EMILIN1 was expressed along both lymphatic and blood vessels: it was possible to see very clearly clusters of Prox1 positive cells in lymphatic vessels. These clusters, positive also for EMILIN1 staining, represented the buds of lymphatic valves. At E18.5 the EMILIN1 staining became more specific for lymphatic structures and in particular it was concentrated in areas of valve origin. In fact, a more evident staining for EMILIN1 was localized in lymphatic vessel constrictions, where buds of valves as indicated by arrows in Figure 9 B. The staining of EMILIN1 became increasingly specific for lymphatics in new born (P0) and adult mice (P21) (Fig. 9 C and 10). A strictly association between EMILIN1 and LECs (Prox-1 positive cells) was particularly detected in the free edge of the intraluminal lymphatic valves. In the Figure 9 C the *x* and *y* projections showed a clear association between EMILIN1 and Prox-1 staining, providing an evident expression of this ECM glycoprotein very close to LECs.

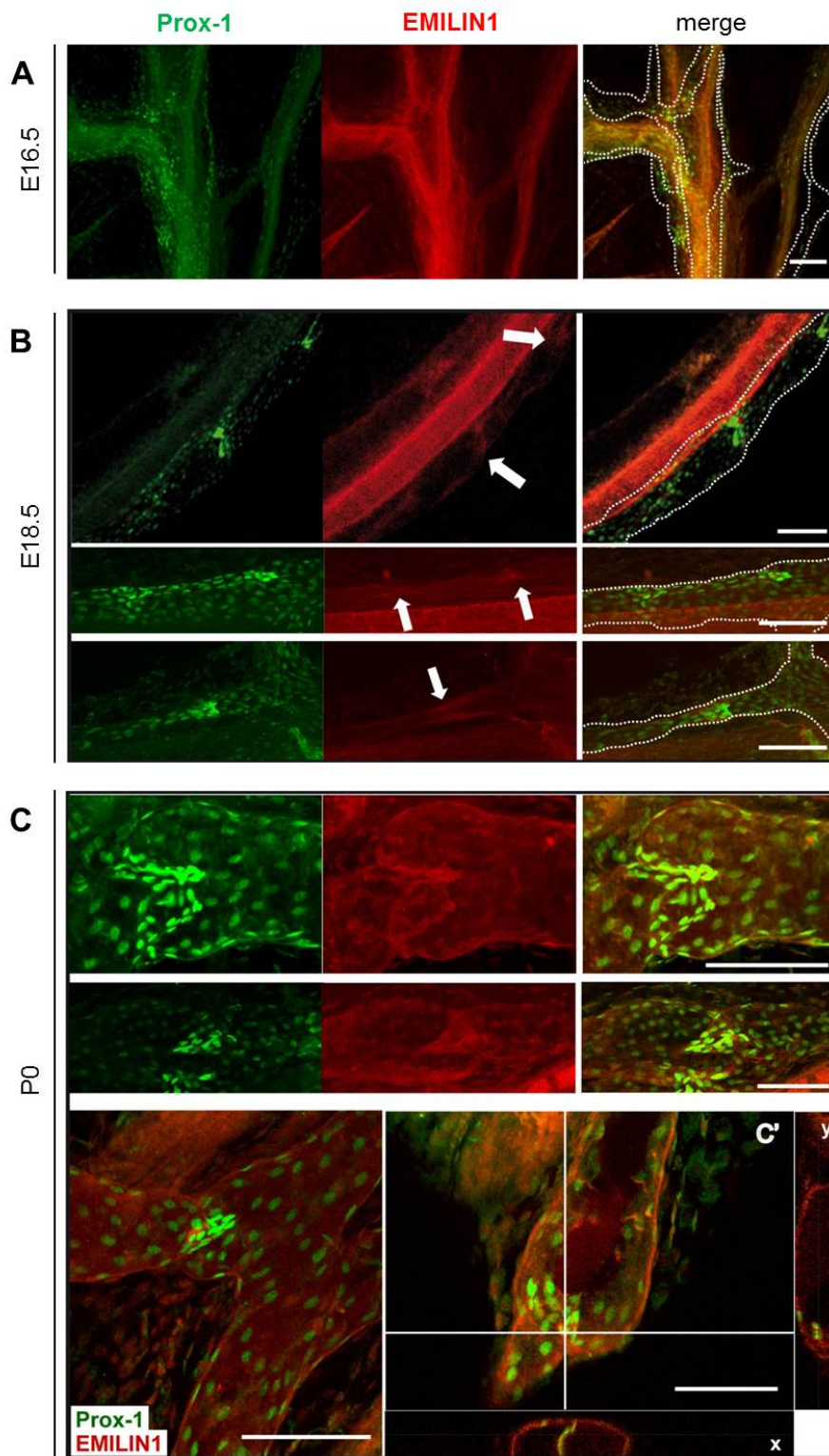


**Figure 9. EMILIN1 expression during lymphatic valves formation.** Immunofluorescence staining of lymphatic vessels of embryonic (A and B) and newborn mesentery (C) with antibodies against Prox1 (green) and EMILIN1 (red). The dotted line outlines the lymphatic vessels. The arrows in panel B indicate more evident EMILIN1 staining associated with endothelial cells expressing high levels of Prox1. Z-section of mesenteric lymphatic vessels and the corresponding x and y projection in panel C showing a clear association between EMILIN1 and Prox1 staining (C'). Scale bars, 100µm; (modified from Danussi et al., 2013).

A clear association between EMILIN1 and LECs was evident also in mature valves (Fig. 10). At P21, similarly at P0 stage but more pronounced, the entire valve matrix core was positive for EMILIN1 with the staining concentrated on the free edges of the valve leaflet as indicated by arrows in Figure 10.

All these data allowed us to conclude that EMILIN1 was expressed along lymphatic collecting vessels and in particular in the free edge of their intraluminal valves. This ECM glycoprotein constituted the core of the valve structure. During the late stages of embryonic development, EMILIN1, as well as the endothelial marker Prox-1, was upregulated just in specific sites, corresponding to constrictions along the collecting vessels. According to these evidences, we could suggest that EMILIN1 not only sustained the lymphatic valve and vessel formation, but it was able, modulating its expression, “to indicate” along the vessels the right localization where the valves will be formed.

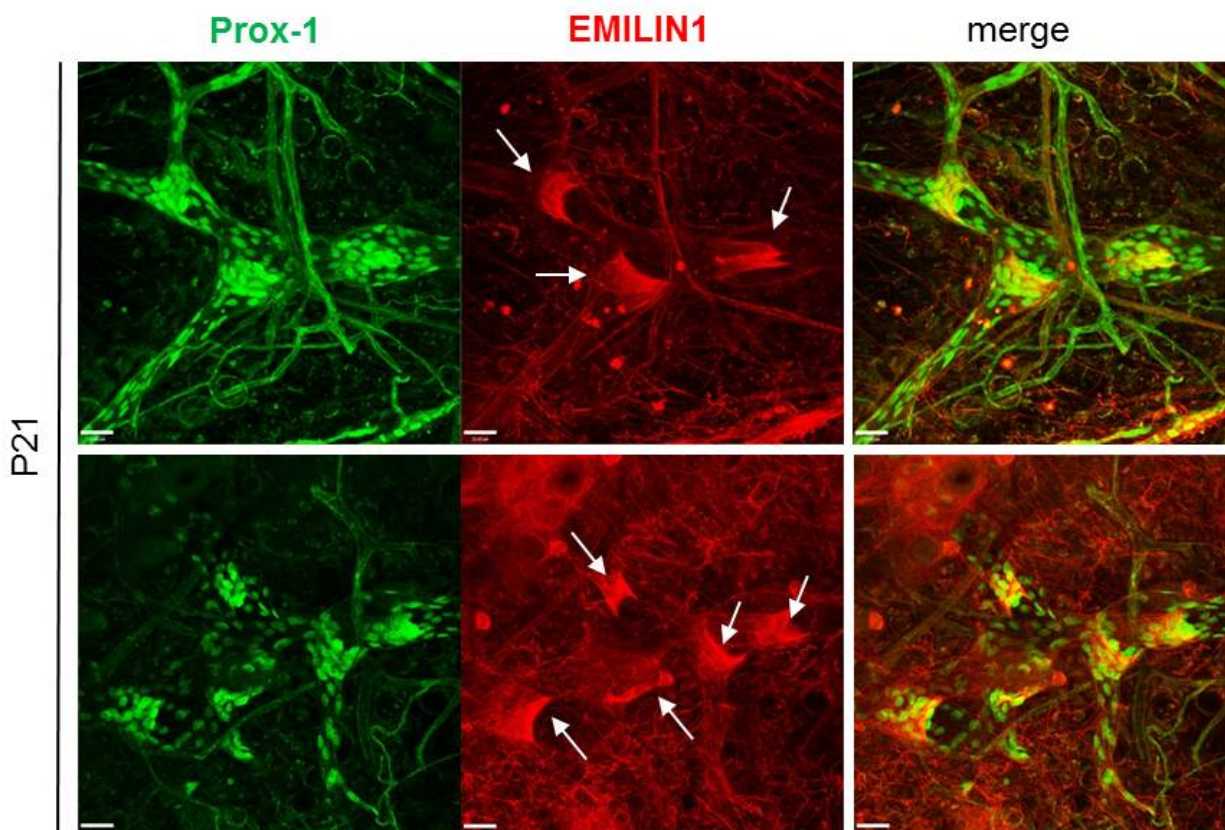


**Figure 10. EMILIN1 expression in mature lymphatic valves.** Immunofluorescence staining of lymphatic vessels of adult ear skin with antibodies against Prox1 (green) and EMILIN1 (red). Arrows indicate free edges of the leaflet fibers positive for EMILIN1 staining. Scale bars, 32 $\mu$ m; (modified from Danussi et al., 2013).

## 1.2 EMILIN1 deficiency leads to abnormal lymphatic valve phenotype.

Usually a well-formed lymphatic valve, that has completed its maturation process, presents a characteristic V-shape. When we analyzed mesenteries of WT mice with PECAM-1 staining using WMS technique, we observed that the vessels of E16.5 mice displayed a lot of buds indicating that valve formation was going on (Fig. 11 A). At E18.5 it was possible to appreciate some well-formed valves. On the contrary, at the same stages, in *Emilin1*<sup>-/-</sup> mice the valves appeared as horizontal ring-shape constrictions. This situation was detected also in neonatal stages and even at P6, when the lymphatic system development was terminated. Moreover, *Emilin1*<sup>-/-</sup> collectors appeared rather throttled, more convoluted and twisted than in WT mice (Fig. 11). The different collector appearance between the two genotypes was detectable also when we analyzed the chyle-filled mesenteric collecting vessels (Fig. 11 B). At P6, when mice are still breastfed, the chyle is rich in milk. It is very easy to see lymphatic vessels with stereomicroscopy since they appear white. With this kind of morphological observation the different characteristics of the WT and KO collectors were very evident: WT vessels were compact and had a higher number of mature intraluminal valves, whereas KO vessels displayed a reduced number of valves, which were mainly immature. The quantitative analysis performed on P6 mesenteric lymphatic collectors staining with PECAM-1, revealed that in WT mice about 80% of the valves had a V-shape, on the contrary just the 30% of *Emilin1*<sup>-/-</sup> mice displayed mature valves (Fig.12 A). As reported in the previous paragraph, EMILIN1 could be considered as a “guide” indicating the right site where the valves will be formed. Moreover, it could have a role in defining the valve number along the vessels. In both early stages, P0 and P6, WT collectors had a higher number of valves than *Emilin1*<sup>-/-</sup> mice. In fact, the analysis performed on mesenteric collecting vessels, after Prox-1 and  $\alpha$ -SMA (smooth muscle actin) staining, demonstrated that the distance between valves was significantly higher in *Emilin1*<sup>-/-</sup> mice compared to WT littermate (Fig. 12 B and C). All these data suggest that the deposition of EMILIN1 is an important element for a well-defined valve leaflet formation and setting. This conclusion comes out also from the results obtained using different mouse strains: both in CD1 (Fig.12 B) and C57Bl/6 (Fig. 12 C) strains we detected the same anomalies about lymphatic valves, confirming the crucial structural role of EMILIN1 in the valve formation process. Another important evidence was that altered structure of the *Emilin1*<sup>-/-</sup> lymphatic valves persisted also in adulthood (Fig. 13). Indeed, we found a consistent number of ring-shape valves

even in *Emilin1*<sup>-/-</sup> adult mice (P21). The quantitative analysis evidenced a lower number of valves and among these a higher percentage of ring-shape valves than WT mice.

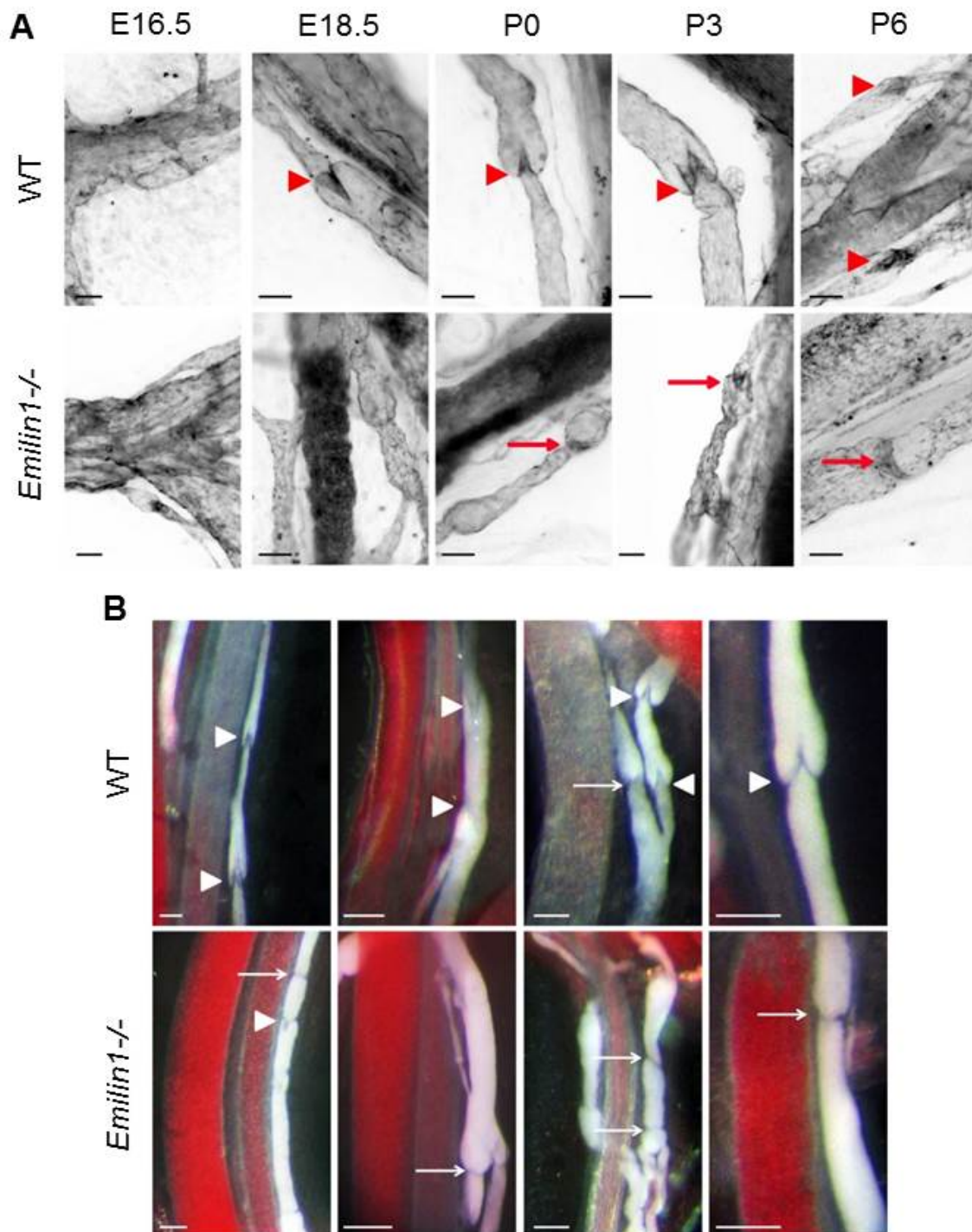


**Figure 11. Lymphatic valves alterations in embryonic, neonatal and young *Emilin1*<sup>-/-</sup> mice.** (A) PECAM-1 immunohistochemistry of WT and *Emilin1*<sup>-/-</sup> mesenteric vessels and luminal valves of embryonic (E16.5 and E18.5) and postnatal (P0, P3, and P6). Arrowheads highlight V-shape valves while arrows indicate abnormal valves. (B) Luminal valves in chyle-filled mesenteric P6 WT and *Emilin1*<sup>-/-</sup> mice. The arrowheads and arrows indicate normal (V-shaped) and abnormal (ring-shaped) valves, respectively. Scale bars, 50 $\mu$ m (A) and 100 $\mu$ m (B); (from Danussi *et al.*, 2013).

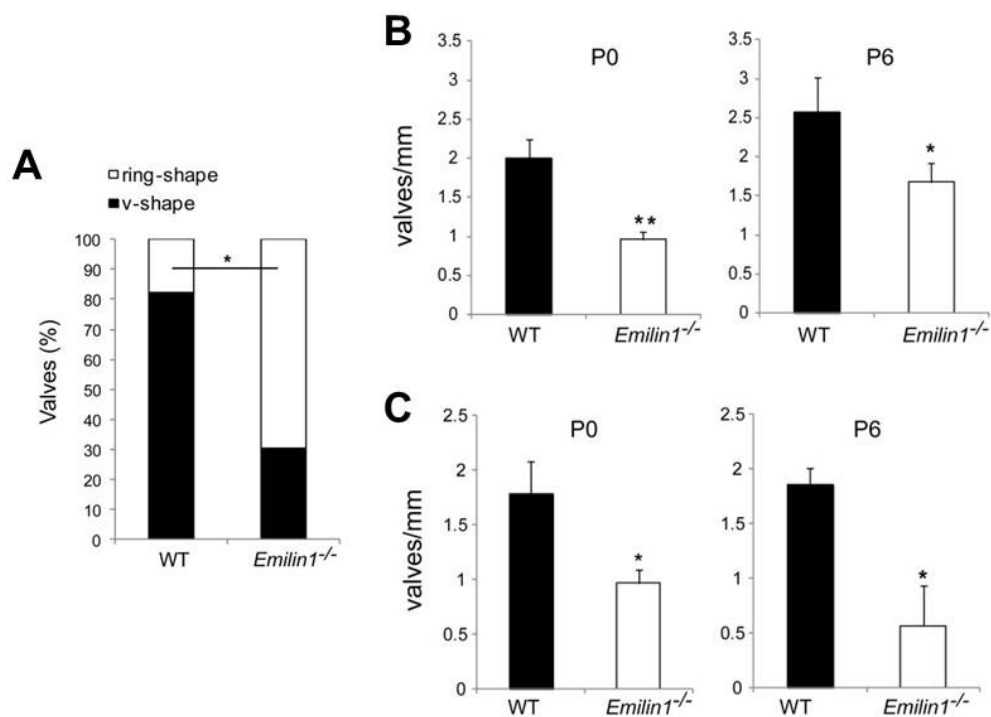


**Figure 12. Quantification of lymphatic valves alterations in neonatal and young *Emilin1*<sup>-/-</sup> mice.** (A) Morphological evaluation of valve shape in P6 WT and *Emilin1*<sup>-/-</sup> mesenteric lymphatic vessels. (n=3 animals per genotype; more than 100 valves were counted for each genotype). \*, P<0.05 ( $\chi^2$  test). (B) Quantification of the luminal valves in neonatal and postnatal WT and *Emilin1*<sup>-/-</sup> mesenteric lymphatic vessels of CD1 (P0 and P6) and C57BL/6 (P0 and P6) (C) mice (n=3 animals per genotype with 10 vessels each; \*, P<0.05; \*\*, P<0.01; unpaired Student's *t* test); (from Danussi et al., 2013).

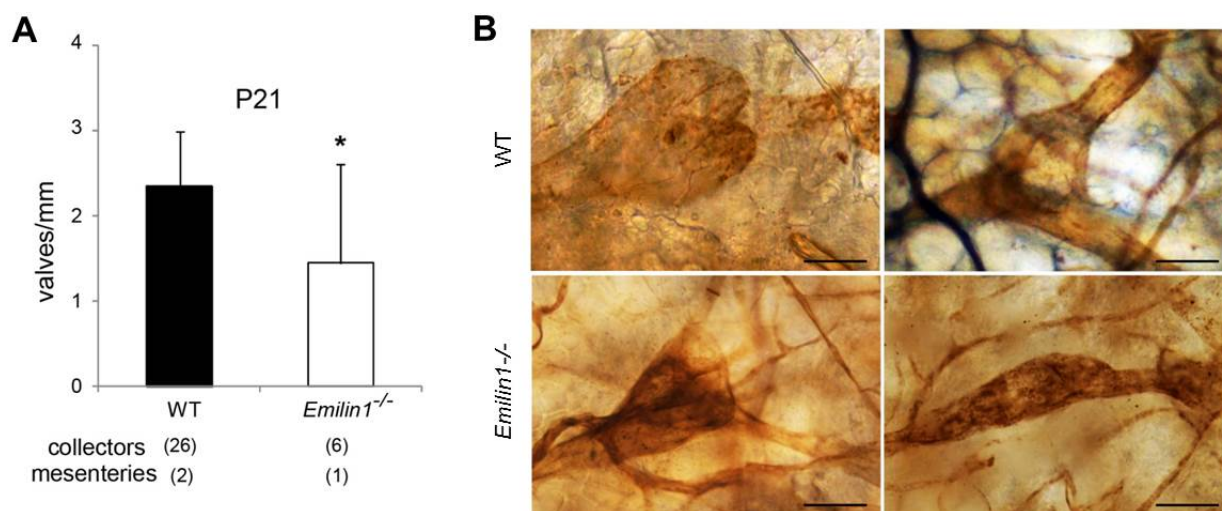


**Figure 13. Lymphatic valves alteration in *Emilin1*<sup>-/-</sup> mice.** (A) Quantification of the luminal valves along adult (P21) CD1 WT and *Emilin1*<sup>-/-</sup> mesenteric lymphatic vessels (n=3 animals per genotype with 10 vessels each; \*, P<0.01). (B) PECAM-1 staining of ear vessels in 6-month-old C57BL/6 mice. Scale bars, 50 $\mu$ m; (from Danussi et al., 2013).

To evaluate the presence of additional anomalies in *Emilin1*<sup>-/-</sup> mice we performed, in collaboration with dr. Sabatelli (Molecular Genetic Institute of Bologna), a transmission electron microscopy (TEM) analysis of P21 collecting vessels. *Emilin1*<sup>-/-</sup> vessels displayed thicker walls compared to WT littermates (Fig. 14). The valve leaflets were thicker, convoluted and folded. One explanation for the constriction of *Emilin1*<sup>-/-</sup> vessels and the presence of convoluted valves could be an increased number of cells in the vessel walls and in the valve leaflets. This increase could lead to a significant reduction of the lumen of the vessels and in particular in the valve areas in KO mice (Fig.15 B).

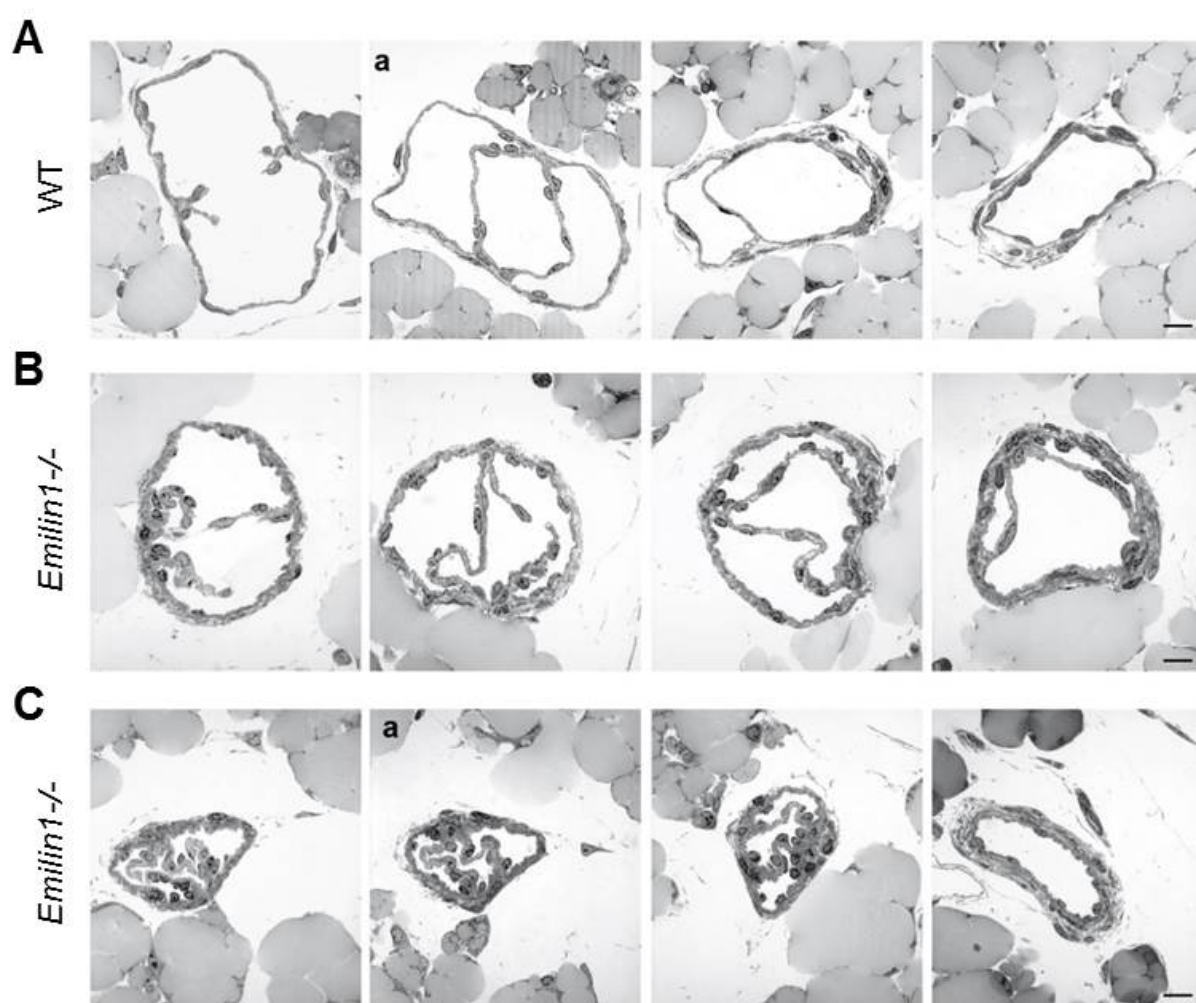


**Figure 14. Abnormal lymphatic structure in *Emilin1*<sup>-/-</sup> adult mice.** Serial semithin cross sections of P21 WT (A) and two representative *Emilin1*<sup>-/-</sup> (B and C) mesenteric valves. Note the increased thickness of the lymphatic wall in *Emilin1*<sup>-/-</sup> mice. The lumen of collecting vessels in the B and C panel appears contracted, with folded valve leaflets. The sections marked “a” in panels A and C were subjected to ultrastructural analysis (Fig.16). Scale bars, 25 $\mu$ m; (from Danussi et al., 2013).

A distinguish element of collecting lymphatic vessels when compared to the lymphatic capillaries is represented by the presence of a basement membrane and of a SMC coverage. In WMS sample, *Emilin1*<sup>-/-</sup> vessels displayed an increase of  $\alpha$ -SMA coverage (Fig. 15 A). This coverage increase was confirmed by semithin and ultrathin TEM sections (Fig. 16). By TEM analysis the increase of wall vessel thickness and of mural cell number in *Emilin1*<sup>-/-</sup> environment was very clear and evident if compared to the WT background. Very importantly, in Figure 17 it is possible to appreciate in KO vessels the presence of a basement membrane and the coverage of mural cells/pericytes with a myofibroblast-like phenotype. The principal characteristic of this type of cells was the presence of caveolae and cytoplasmatic filaments as indicated by the arrows and arrowheads, respectively (Fig. 17). Another curious and very interesting aspect derived by TEM analysis, was the presence of a LEC during the mitotic process in a KO section (Fig. 16, arrow). Since it is extremely rare to find mitotic LEC in this district, we could further support the hypothesis that in the *Emilin1*<sup>-/-</sup> environment the proliferation rate was higher and so the resulting increased number of cells was responsible for the thickness and folded valves.

Likely, just these mural cells with a myofibroblast-like phenotype could “sustain” LECs in KO vessels and guarantee a certain proliferative stimulus by a physical contact and by soluble factors (Danussi et al., 2011). In none of the TEM, WT samples analyzed mitotic cells were present.

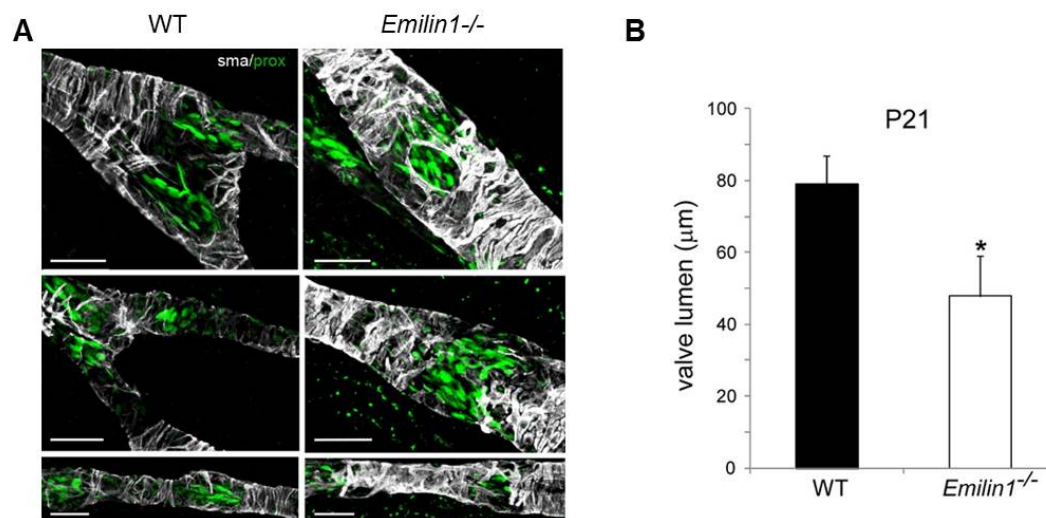


**Figure 15. *Emilin1*<sup>-/-</sup> collecting vessels coverage.** (A) WT and *Emilin1*<sup>-/-</sup> adult (P21) lymphatic mesenteric vessels stained for  $\alpha$ -SMA (gray) and Prox1 (green). (B) Lumen sizes of the valves in adult WT and *Emilin1*<sup>-/-</sup> mesenteric lymphatic vessels. Z-stack images were collected from whole-mount samples stained for  $\alpha$ -SMA and Prox1; the resulting three-dimensional reconstruction by Volocity software combined with *x* and *y* projections was used to highlight and calculate the smallest ( $d_s$ ) and largest ( $d_l$ ) diameters of the valve lumen. The values are obtained from calculation  $[(d_s+d_l)/2]$ . (n=4 mice per genotype at least 5 valves/mesentery were examined). \*, P<0.01. Scale bars, 25 $\mu$ m (A); (from Danussi et al., 2013).

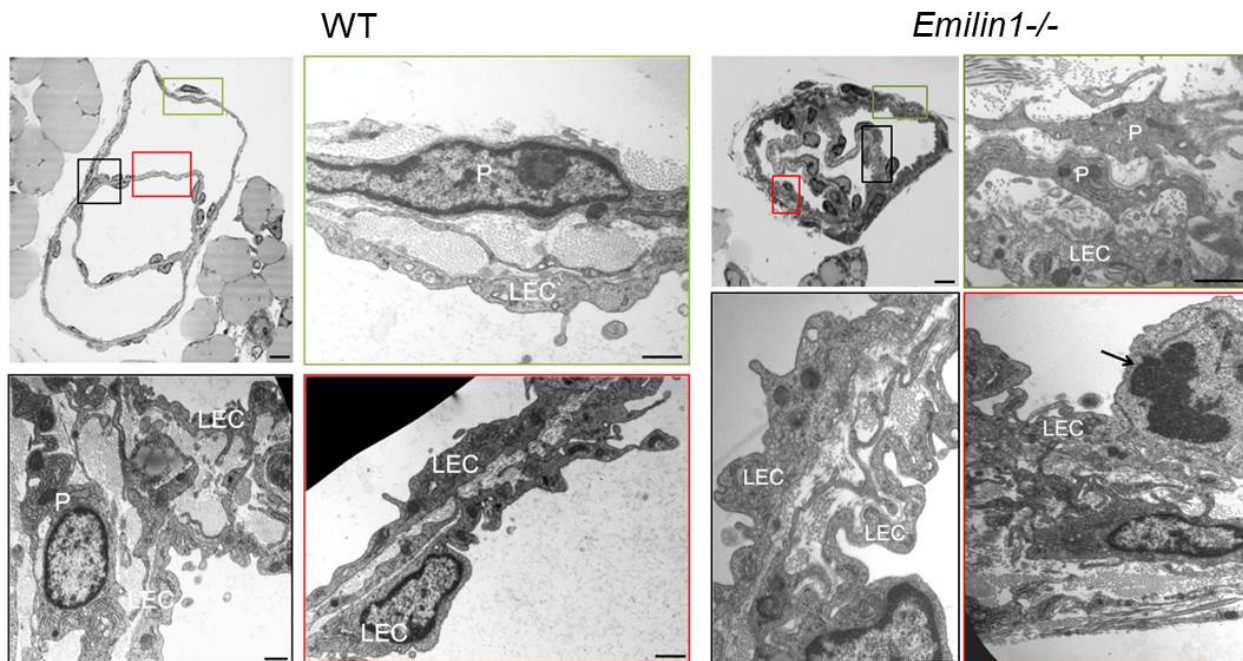


**Figure 16. *Emilin1*<sup>-/-</sup> collecting vessels coverage, semithin TEM analysis.** TEM analysis of P21 WT (left) and *Emilin1*<sup>-/-</sup> (right) mesenteric valves. The colored boxes in the semithin sections (upper left panels, corresponding to sections Aa and Ca, respectively, from Fig. 12) represent the areas that were selected for ultrathin sections. P indicate mural cells/pericytes which display a SMC/myofibroblast-like phenotype. The arrow indicates a mitotic LEC. Scale bars, 1  $\mu$ m; (from Danussi et al., 2013).

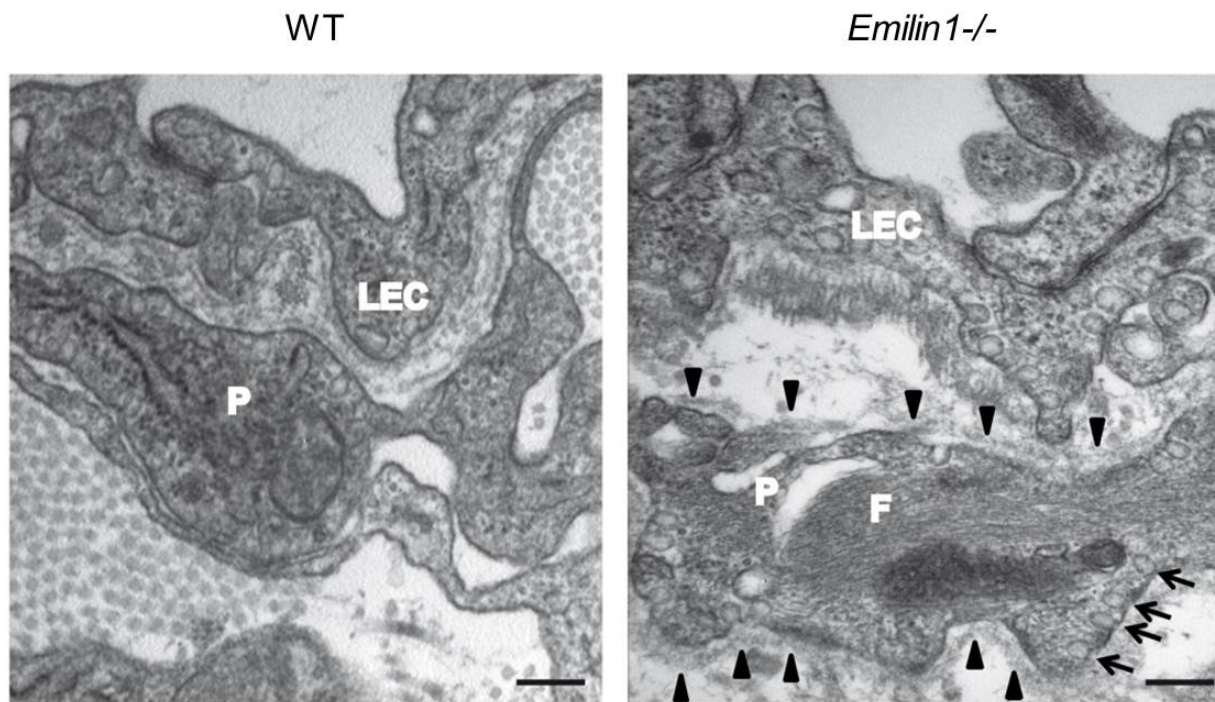


**Figure 17. *Emilin1*<sup>-/-</sup> collecting vessels coverage, ultrathin TEM analysis.** TEM analysis of P21 WT (left) and *Emilin1*<sup>-/-</sup> (right) mesenteric lymphatic vessel walls. Arrow indicate the caveolae, F the cytoplasmic filaments and arrowheads the basement membrane at the surface of one representative *Emilin1*<sup>-/-</sup> mural cell/pericyte. Scale bars, 500 nm; (from Danussi et al., 2013).

### 1.3 EMILIN1 deficiency impairs functionality of lymphatic valves.

The structural alterations due to EMILIN1 deficiency identified until now could be responsible for an impaired functionality. The loss of lymph uptake ability and the increase of leakage of *Emilin1*<sup>-/-</sup> lymphatic capillaries have been already demonstrated (Danussi et al., 2008). Here we focused our interest on collector functions using lymphangiography assay to investigate the effects on lymph transport ability. In particular, we evaluated the capability of collectors to drain lymph to the LNs with the aim to provide a more thorough explanation for the reduced functionality of the lymphatic circulatory system and the ensuing mild lymphedema in KO animals (Danussi et al., 2008). We injected subcutaneously large-molecular-weight-fluorescent dextran (FITC-dextran) in P21 and 6-months-old C57Bl/6 mice. At the beginning, to improve the technique, we tested two injection sites, forepad and tail, and we observed the spreading of the dye at different times. We noticed that the dye injected in forepad spread over very quickly (Fig. 18): after 5 minutes, the dye was drained to axillary and brachial LNs.

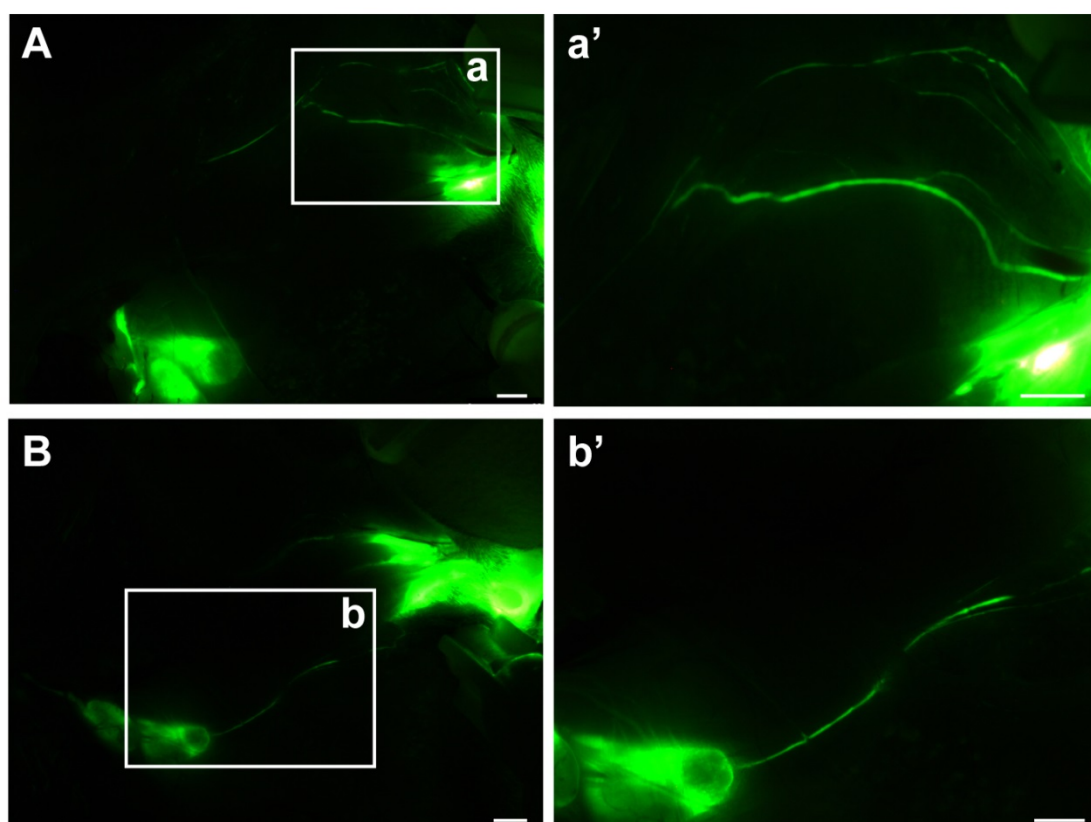


**Figure 18. Quick dye spreading from mouse forepad injection.** (A and B) FITC-dextran (2,000 kDa) spreading from forepad along forefoot till axillar and brachial LNs after 5 minutes from injection in two different WT C56Bl/6 mice at P21. Since the spreading is very quick it is impossible to record the initial phases of dye spreading. (a' and b') High magnification of the box in (A) and (B) highlight the dye spreading and the strong labeling of lymphatic collectors. Scale bar, 1mm.

Indeed we couldn't appreciate possible differences between two genotypes for the impossibility to record the initial phases of dye spreading (Fig. 19). The dye diffused along the forefoot and in all vessels network till the axillary LNs. This effect could be due to a very huge quantity of vessels in this relatively small area.

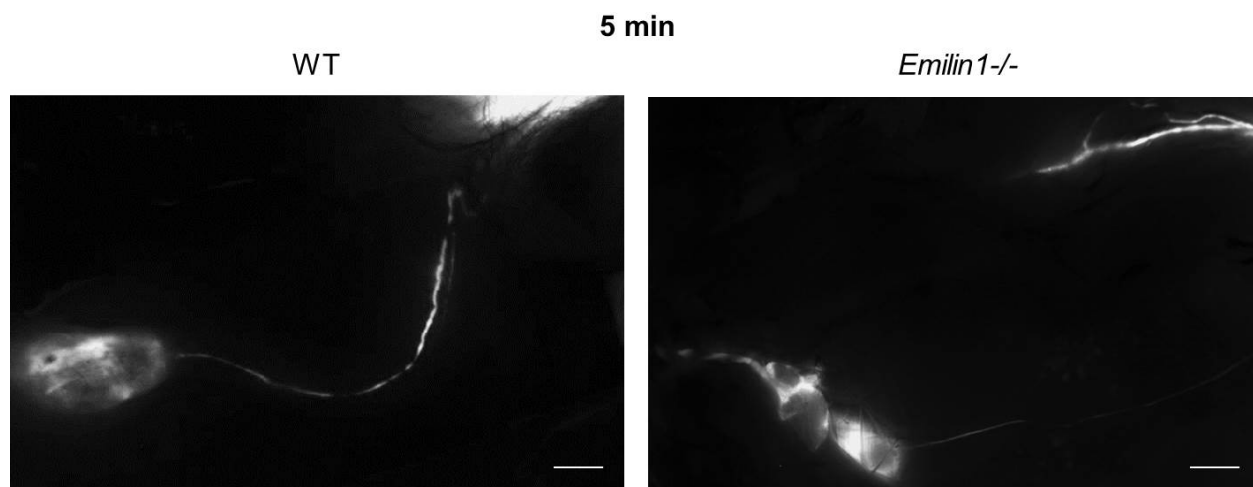


**Figure 19. Forepad injection in lymphangiography assay.** Lymphangiography assay was first of all tested using forepad as injection site of FITC-dextran (2,000 kDa) in WT and *Emilin1*<sup>-/-</sup> mice at P21. No differences were appreciable in dye spreading in two genotype; the axillary LNs are both labeled in WT and KO mice, with the similar intensity. Scale bar, 1mm.

We then decided to move to mouse tail as injection site for the following trials. In this set of experiments we considered the lymph spread through the entire mouse body, observing the lymphatic vessels and LNs labeled by dye, and not the local spreading close to tail injection site.

In Figure 20 the superficial network of lymphatic capillaries referred to tail injection is shown. For deeper collector drainage, we mainly considered two times, 5 and 30 minutes to evaluate lymph spread. The first time was important to have an idea of what happened in the very early steps from injection. On the other hand, at 30 minutes we wanted to see the spreading of dye before its return in the circulatory system and so not more visible in the lymphatic vessels. During this experimental procedure we noticed that the dye was drained preferentially through the principal longitudinal axis of animals (iliac, lumbar and mesenteric LNs) rather than diffused peripherally (popliteal and inguinal LNs) (Fig. 21).

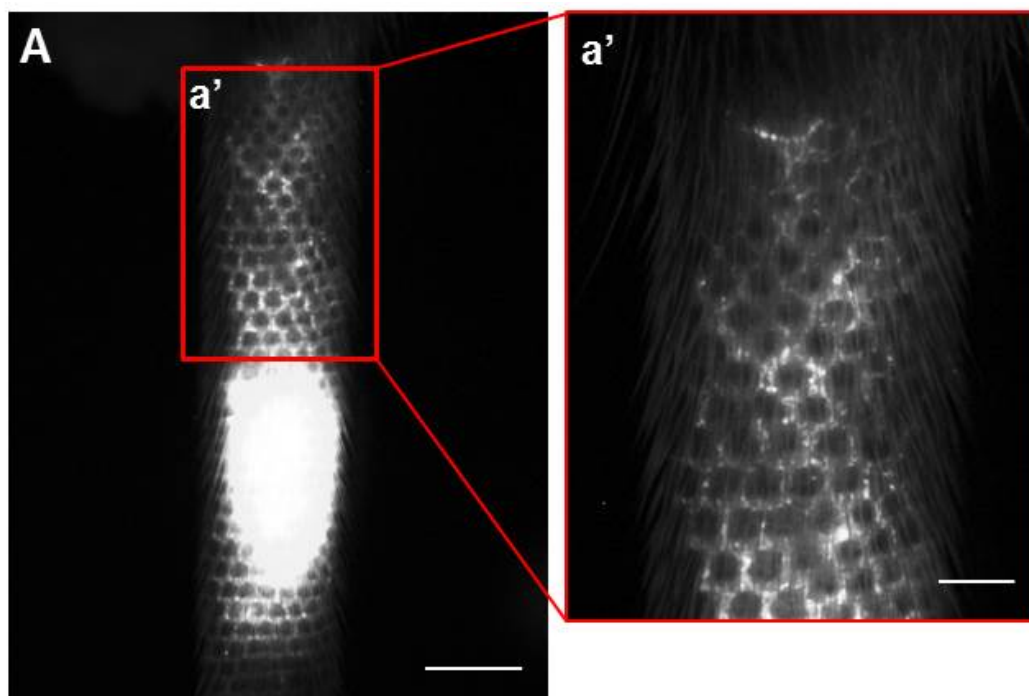


**Figure 20. FITC-dextran (2,000 kDa) diffusion in mouse tail.** (A) Injection site of FITC-dextran (2,000 kDa) in WT P21 C56Bl/6 tail mice. The stronger fluorescence indicate the injection site. (a') High magnification of the superficial lymphatic capillaries, which uptake the injected dye. The Scale bar, 2,5mm (A), 1mm (a').

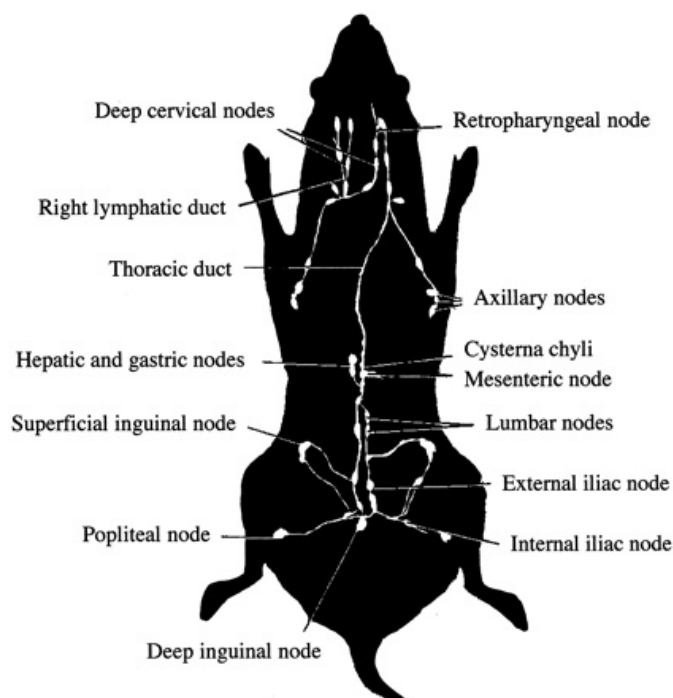


**Figure 21. Model of murine LNs localization.** LNs in mouse are easy to localize. They can be classified as superficial and deeper according to their localization. The nodes labeled after tail injection during lymphangiography assay are mainly deep LNs: iliac, lumbar and mesenteric. Sometimes even the superficial nodes among inguinal and axillary are labeled.

Moreover, we could observe that just after 5 minutes the WT iliac LNs were labeled and after 30 minutes even the mesenteric LNs (Fig. 22 and 23). In some cases we detected even the axillar nodes after 30 minutes (Fig. 22 A and B). Sometimes, popliteal and superficial inguinal LNs were positive for FITC-dextran (Fig. 22 C).

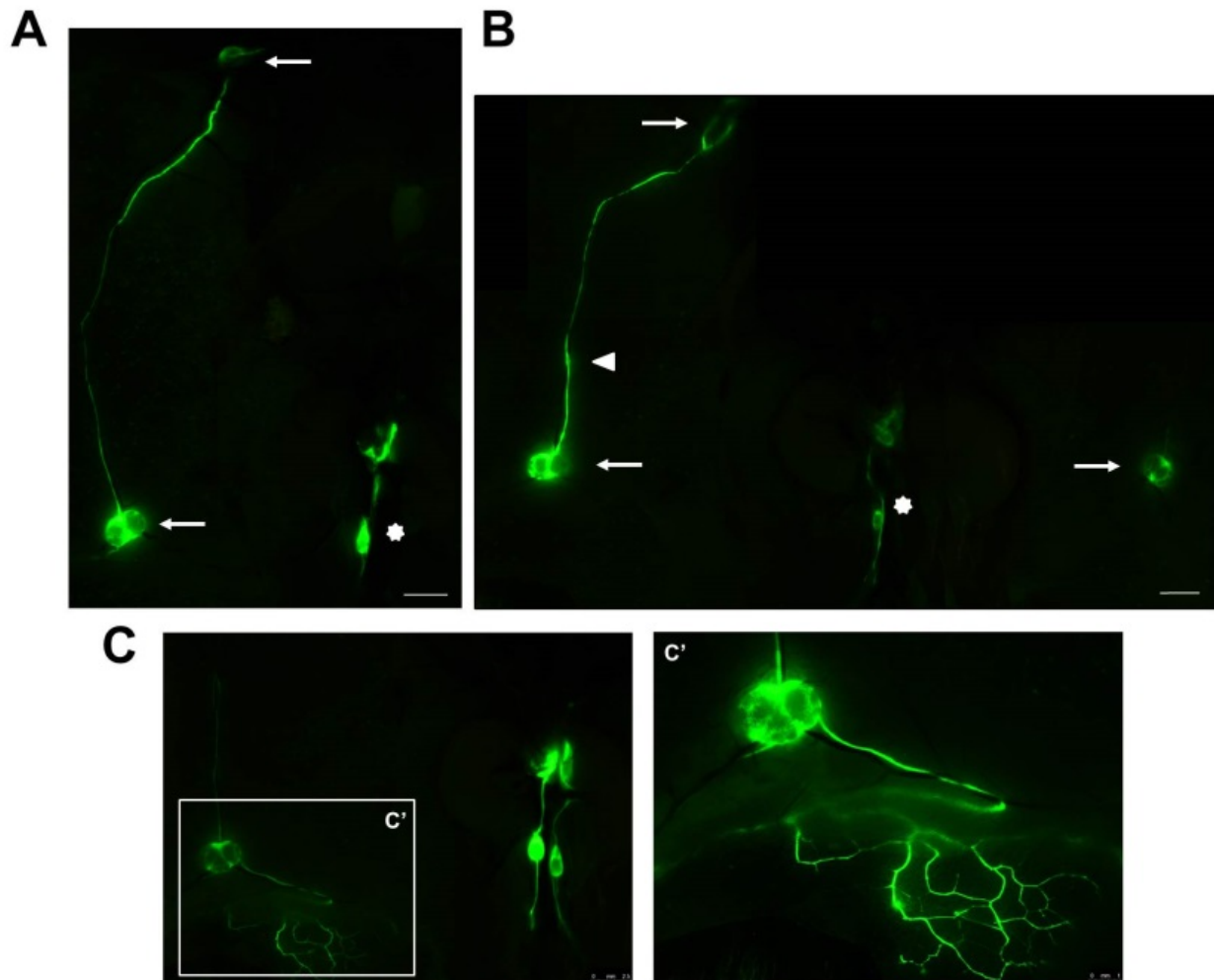


**Figure 22. Tail injection in lymphangiography assay.** FITC-dextran (2,000 kDa) was injected in mouse tails in WT P21 mice. (A and B) FITC-dextran (2,000 kDa) spreading in two different mice after 30 minutes from tail injection. Iliac (\*), inguinal and axillary (arrows) LNs are labeled. The arrowhead indicate V-shape valve. (C) Highlights the capillaries network close to inguinal LNs. (c') show a magnification of (C). Scale bar, 2,5mm.

---

On the contrary, in *Emilin1*<sup>-/-</sup> mice the FITC-dextran was less uptaken and not drained so fast. Indeed after 30 minutes from injection, just some iliac LNs were labeled. This technique allowed us to detect also the presence of the valves along the collectors: classical V-shape structures in WT mice and the ring-shape structures in *Emilin1*<sup>-/-</sup> collecting vessels were well evidenced (Fig. 23 A). A similar difference in dye spreading along collectors and LNs was evident even in 6-week-old mice (Fig. 23 B), indicating that the valve anomalies contributed to the persistence of reduced lymphatic functionality in young as well as in adult *Emilin1*<sup>-/-</sup> mice. Analyzing the FITC-dextran uptake and spreading velocity, we realized that both LNs and lymphatic vessels appeared fainter in *Emilin1*<sup>-/-</sup> animals. To demonstrate the differences in dye uptake we extracted the LNs labeled with dye and measured their fluorescence intensity. The measurements indicated that WT LNs were much more positive than *Emilin1*<sup>-/-</sup> LNs, indicating that they drained more lymph and in a faster way than KO. Indeed, kinetic analysis of FITC-dextran lymph node uptake confirmed slower dye transport in P21 *Emilin1*<sup>-/-</sup> mice than in WT littermates (Fig. 23 C). The delay in lymph transport and the reduction of LNs fluorescence in *Emilin1*<sup>-/-</sup> mice could be associated to a reduction of the lymphatic capillary permeability as already demonstrated (Danussi et al., 2008), but also to structural defects of *Emilin1*<sup>-/-</sup> lymphatic valves. The valves led to impaired lymph drainage because they weren't able to guarantee a correct thrust and unidirectional flow.

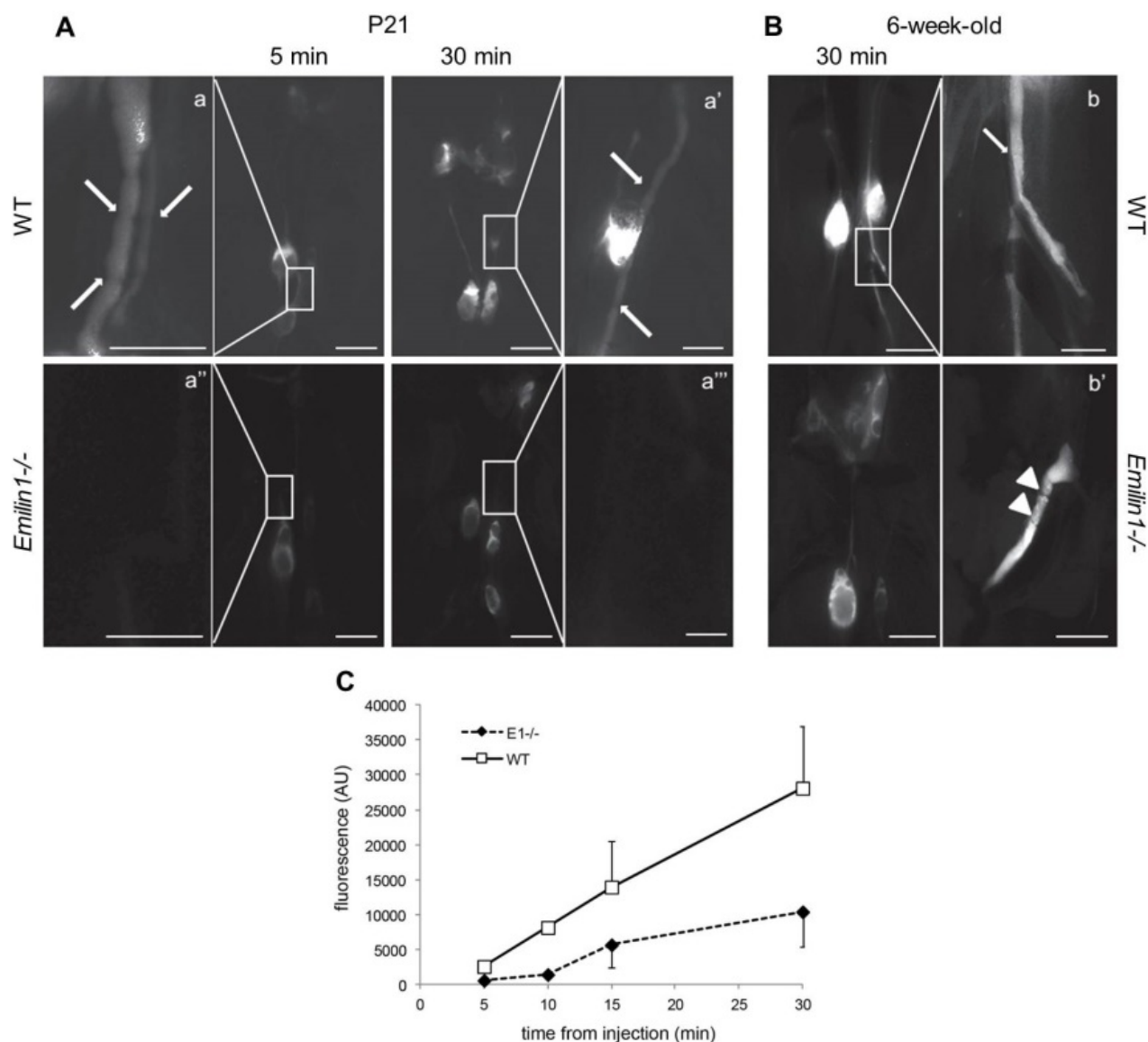
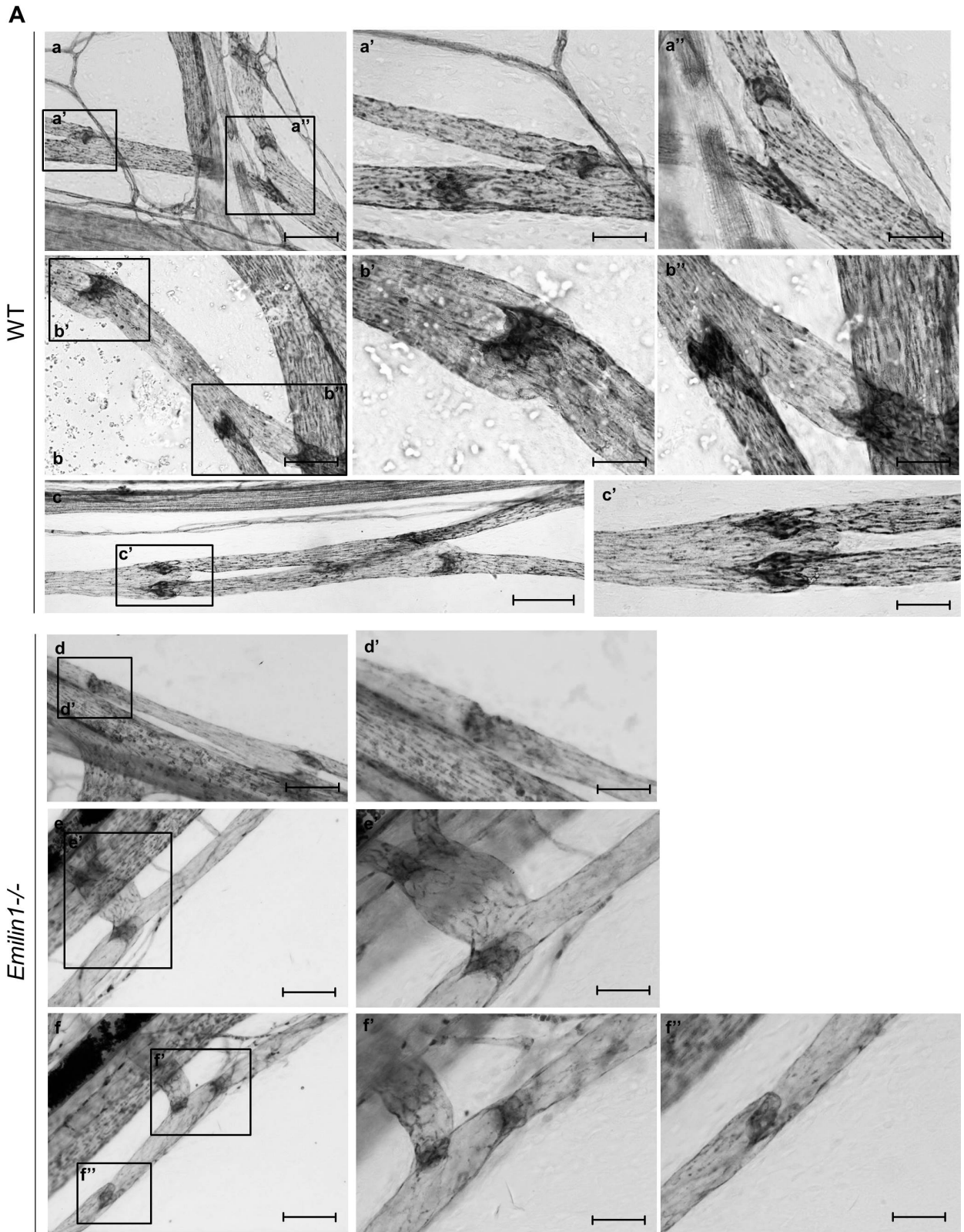


**Figure 23. Functional differences between WT and *Emilin1*<sup>-/-</sup> mice at P21 and 6-week-old.** Lymphangiography assay was performed in WT and *Emilin1*<sup>-/-</sup> mice at P21 (A) and at 6 weeks (B) injecting FITC-dextran (2,000 kDa) subcutaneously into the tails of mice to visualize the draining lymphatic vasculature and lymph nodes. Low-magnification images were taken to visualize lymph nodes, and high-magnification images (a, a', a'', a''', b and b''') were taken to detail collectors corresponding to the boxed areas. The arrows and arrowheads indicate v- and ring-shaped valves, respectively. (C) Draining lymph nodes (iliac, lumbar, mesenteric and inguinal) were removed 30min after injection and measured with a computer-interfaced GeniusPlus microplate reader (Tecan, Italy). Arbitrary fluorescence units (AU) in the graph represent the sums obtained from the fluorescence values of all draining lymph nodes/mouse. The graph reports the means  $\pm$  SD of three independent experiments (n=4 animals per genotype). Scale bar, 2 mm. Scale bar, 0.5 mm in a, a', a'', a''', b and b'''; (from Danussi et al., 2013).

#### 1.4 Phenotype differences are associated to different mouse strain.

The first studies about the role of EMILIN1 in lymphatic system were developed on CD1 mice (Danussi et al., 2008). We performed the lymphangiography assay in both CD1 and C57Bl/6 mouse strains to confirm that the lymphatic phenotype was really due to the absence of EMILIN1 in a wider background. As shown in Figure 12 B and C, CD1 and C57Bl/6 mice had a very similar trend about the percentage of V- vs ring-shape valves and the number of valves per vessel. Accordingly, the functionality of the collectors measured as FITC-dextran spreading was similarly impaired in both KO strains (data not shown). Since also FVB *Emilin1*<sup>-/-</sup> background were obtained in our laboratory after backcrossing, we examined also this inbred strain to improve our data and observations and to verify if a particular strain could be more suitable to perform functional studies.

We began with morphological analysis, extracting mesentery for staining with WMS technique. Surprisingly, whereas in CD1 strain as well as in C57Bl/6 *Emilin1*<sup>-/-</sup> LNs showed a 2-fold higher volume than WT LNs (Danussi et al., 2008), we didn't notice clear differences about LNs size between WT and KO in FVB mice. WMS on mesenteric lymphatic collecting vessels of P6 mice didn't display significant morphological differences between WT and *Emilin1*<sup>-/-</sup> samples (Fig. 24 A). In fact, in FVB KO animals the valves were often V-shaped. Moreover, FVB *Emilin1*<sup>-/-</sup> chyle-filled mesenteric vessels showed more valves with an elevated percentage of V-shape than KO mice of the other two mouse strains (Fig. 24 B). The resulting analysis from PECAM-1 staining in FVB mice about the valve number per vessel and their morphology revealed some quantitative differences (Fig. 24 C and D). The trend of FVB mice was the same of the CD1 and C57Bl/6 but the differences weren't significant. In fact, WT collecting vessels presented only 20% of V-shaped valves more than *Emilin1*<sup>-/-</sup> vessels at P6, whereas in the other two strains this difference was more or less of 50% (Fig. 12 B and C). Moreover and more importantly, the number of the valves along the vessel was very similar in WT and KO FVB mice.



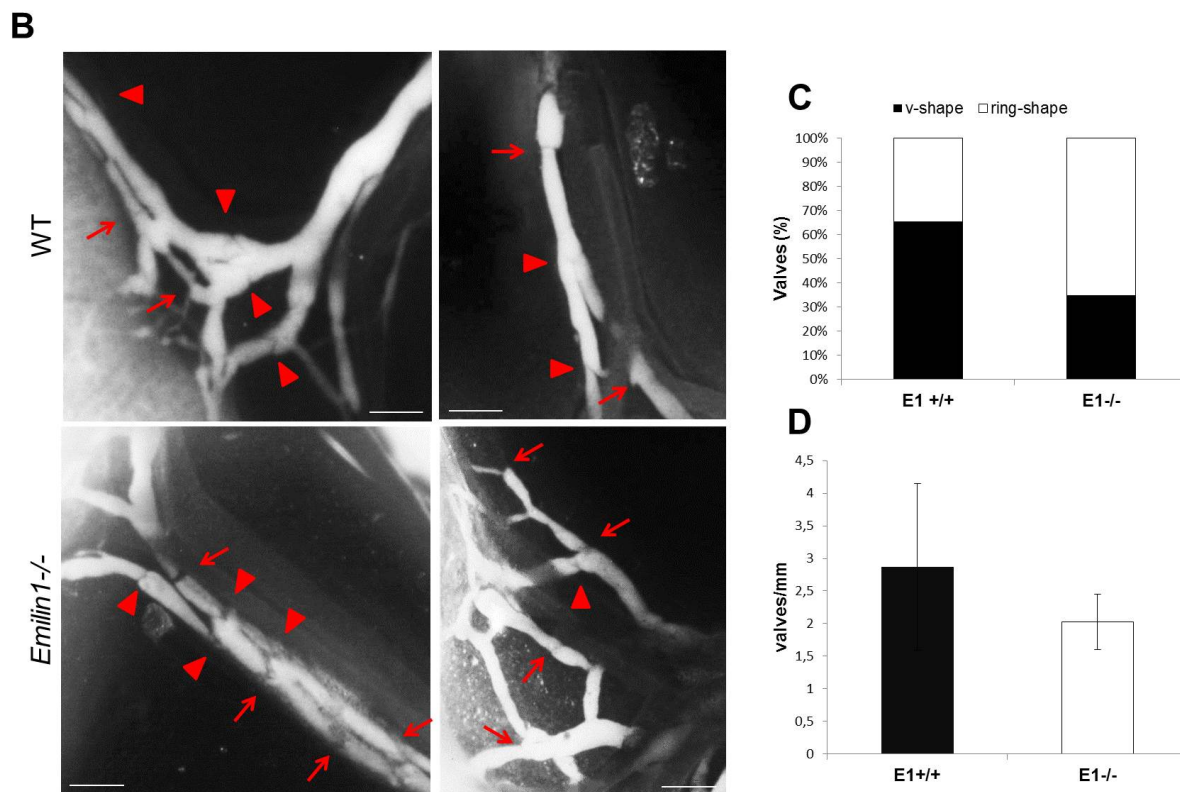
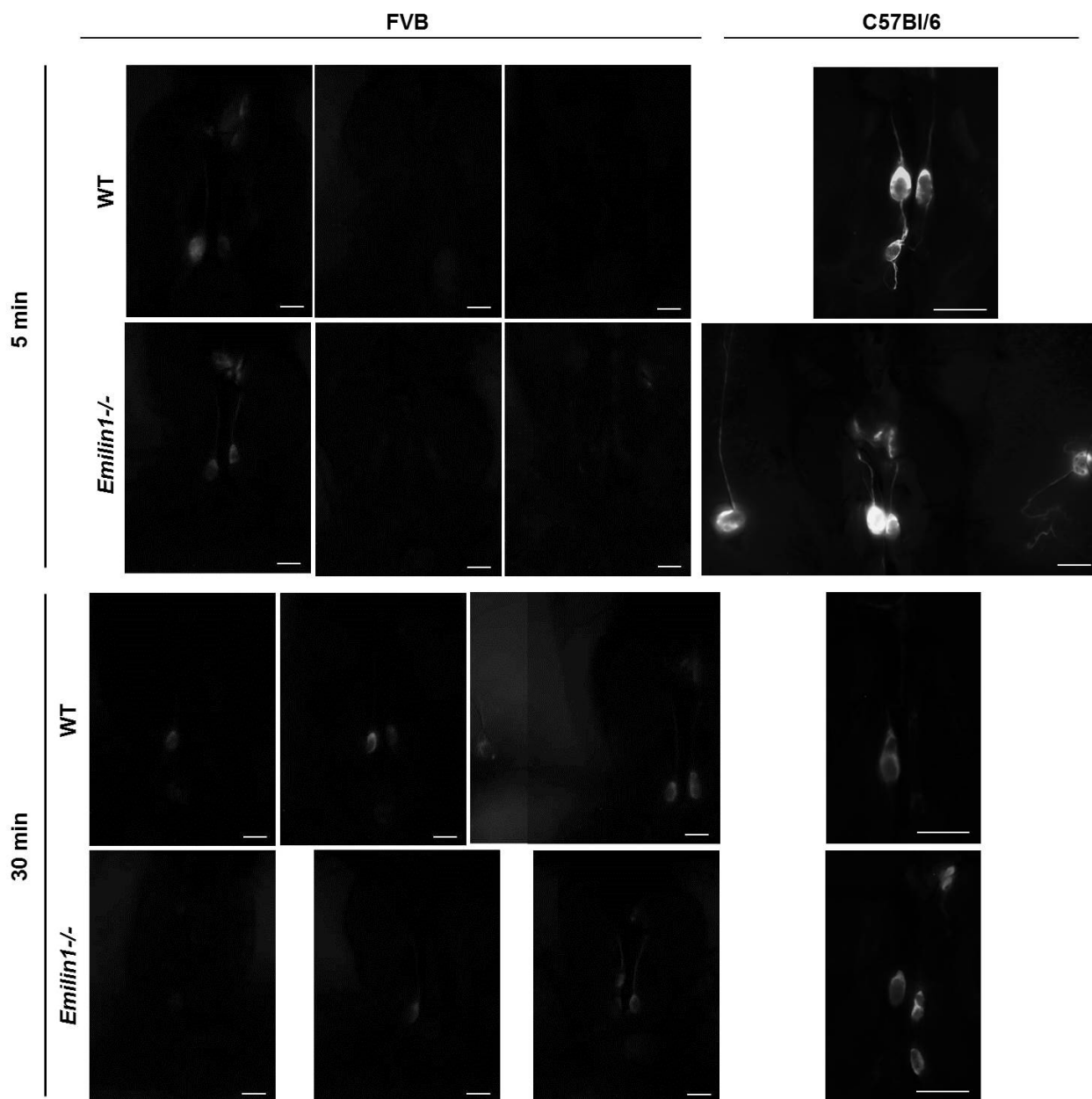


**Figure 24. Morphological phenotype of FVB strain.** (A) PECAM-1 immunohistochemistry of WT and *Emilin1*<sup>-/-</sup> mesenteric vessels and luminal valves at P6. The boxes (a-f) represent areas whose magnification is indicated in nearby images (a', a'', b', b'', c', d', e', f', f''). (B) Luminal valves in chyle-filled mesenteric P6 WT and *Emilin1*<sup>-/-</sup> mice. The arrowheads and arrows indicate normal (V-shaped) and abnormal (ring-shaped) valves, respectively. (C and D) Quantification of the luminal valves in P6 WT and *Emilin1*<sup>-/-</sup> FVB mesenteric lymphatic vessels (n=3 animals per genotype; P>0.05; Student's *t* test).

When the functionality of vessels in FVB mice was analyzed using lymphangiography assay (Fig. 25) the differences between two mouse strains weren't significant. These mice presented a very low uptake and flow rate: even after 30 minutes FVB WT mice were not able to display a FITC-dextran spread similar to C57Bl/6 (Fig. 23 and 25). Only in a very few WT FVB animals some iliac and sometimes some mesenteric LNs were labeled. Also in this case LN fluorescence was very difficult to detect. All these data showed drastic differences in lymphatic phenotype due to the mouse strain.

According to our data, we could conclude that FVB strain was not an useful strain to analyze some aspects of lymphatic system, in particular the evaluation of lymphatic vessel functionality. In our model FVB had not a behavior comparable to the other strains examined. Anyway, FVB mice could be a suitable model to study the lymphangiogenesis starting from pre-existing lymphatic vessels as described by Regenfuss et al. (2010). It was demonstrated that FVB strain have a good lymphangiogenic response in a corneal inflammatory model (Regenfuss et al., 2010).

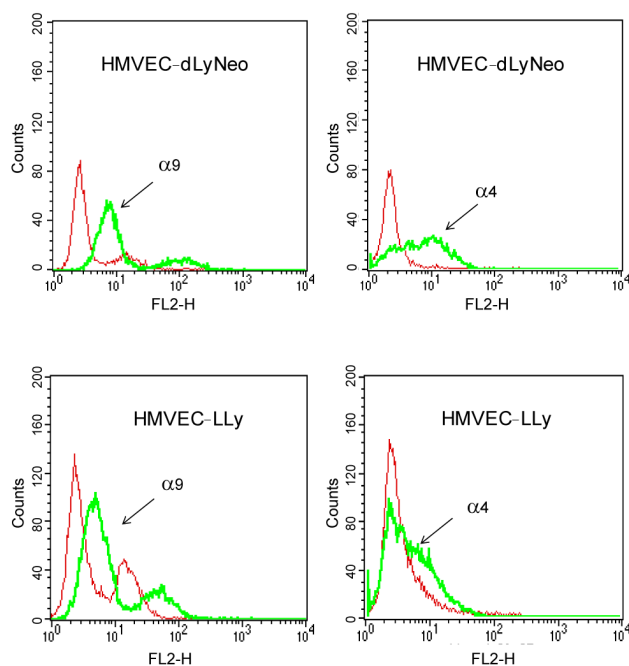
In conclusion, FVB strain is a suitable strain to study lymphangiogenesis in an inflammatory model in adult mice, but it is not a good tool to analyze the late stages of lymphangiogenesis in young mice.



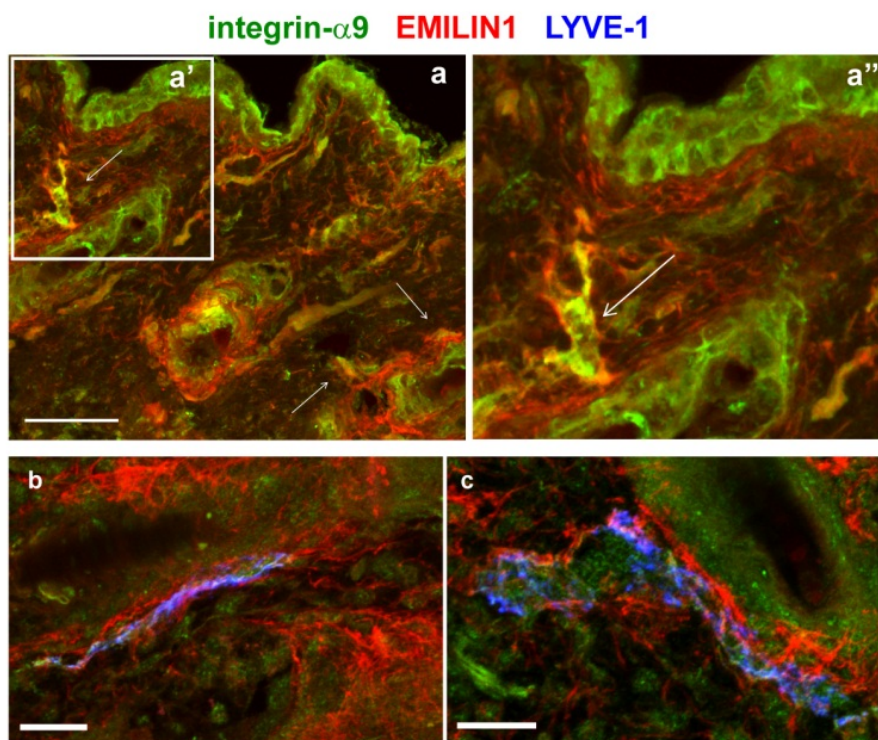
**Figure 25. Lymphatic vessels functionality in WT and *Emilin1*<sup>-/-</sup> mice at P6.** Lymphangiography assay was performed in WT and *Emilin1*<sup>-/-</sup> mice at P6 injecting FITC-dextran (2,000 kDa) subcutaneously into the tails of mice to visualize the draining lymphatic vasculature and lymph nodes. Scale bar, 200µm (FVB), 2,5mm (C57Bl/6).

### 1.5 EMILIN1 co-localizes with $\alpha 9$ integrin in the valve leaflets.

Our results demonstrated that EMILIN1 is crucial for the correct development and maintenance of the lymphatic structure and that its presence guarantees the functionality of the lymph uptake and transport. The mechanism responsible for EMILIN1 role in lymphatic valve formation and maintenance is not known. EMILIN1 is able to bind  $\alpha 4\beta 1$  and  $\alpha 9\beta 1$  integrins in a very specific way. Through this engagement the migratory and proliferative capability of the cells can be influenced (Danussi et al., 2011, 2012). Indeed, we have demonstrated the pro-adhesive and antiproliferative effects due to EMILIN1-  $\alpha 4/\alpha 9$  integrin interaction *in vitro* using different cells lines such as HT1080 and Caco-2 expressing  $\alpha 4\beta 1$  or  $\alpha 9\beta 1$  integrins respectively, and *in vivo* with a wound assay (Danussi, 2011). In the present study we characterized this engagement also for LECs in order to find out the molecules able to regulate lymphatic phenotype. We used human endothelial cells derived from lung (HMVEC-LLy) or dermal (HMVEC-dLyNeo) in flow cytometric analysis and we found that both cells lines express both  $\alpha 9$  and  $\alpha 4$  integrin but in different manner (Fig. 26). To verify if EMILIN1 could interact directly with  $\alpha 9$  integrin on tissue LECs we first verified if these two molecules co-localize in the lymphatic system and in particular in the valve leaflets. The immunofluorescence analysis on skin sections (Fig. 27) revealed that EMILIN1 and  $\alpha 9$  integrin presented the same localization. They often were expressed together around structures very similar to vessels, in fact when we used also LYVE-1 staining, all three molecules co-localized.



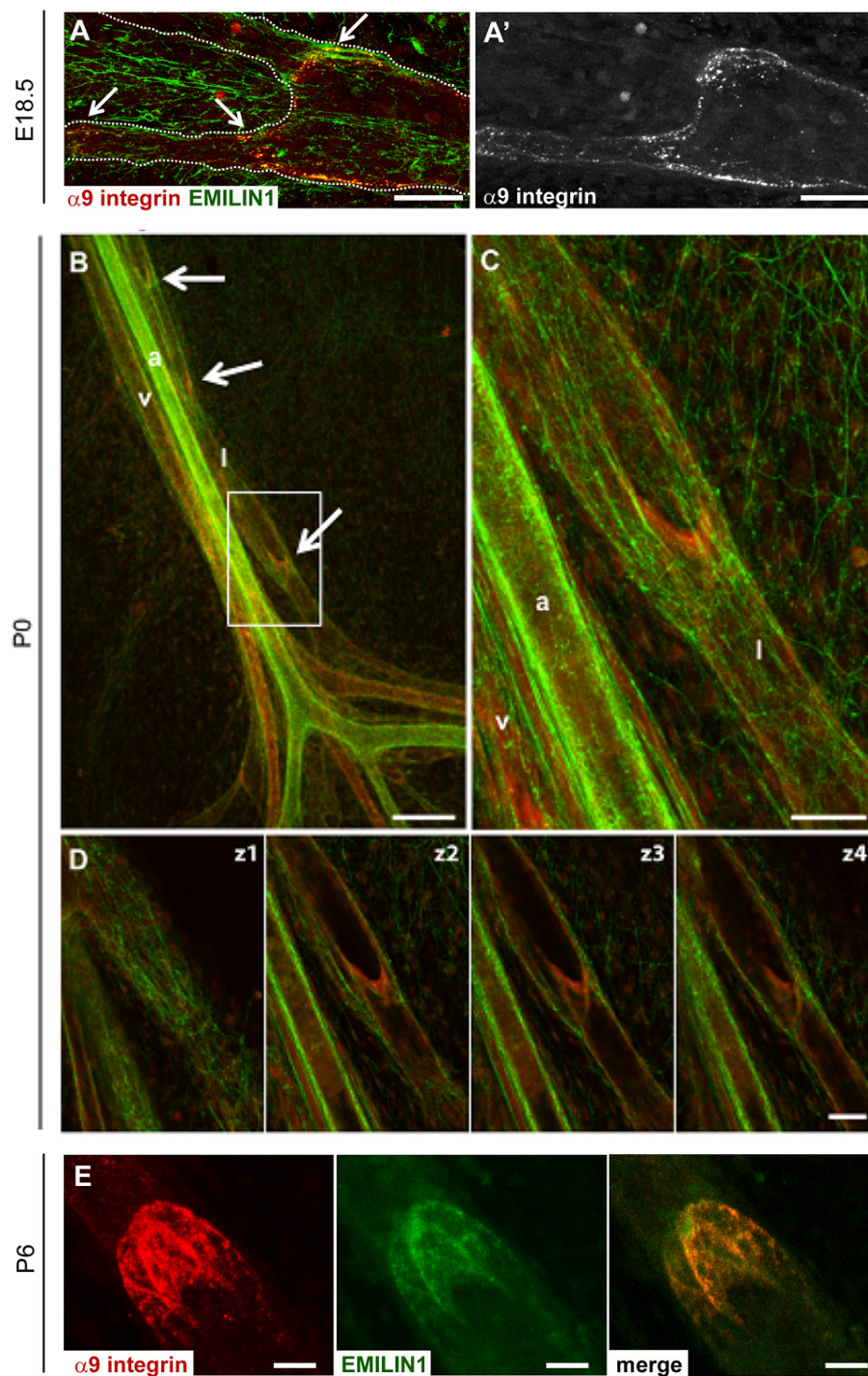
**Figure 26:  $\alpha 4$  and  $\alpha 9\beta 1$  integrin expression on HMVEC cell lines.** The graph reported FACS analysis of integrin- $\alpha 4$  and integrin- $\alpha 9$  expression levels in HMVEC-LLy and HMVEC-dLyNeo cells.



**Figure 27. EMILIN1- $\alpha 9\beta 1$  integrin co-localization in the skin.** Immunofluorescence staining for the localization of EMILIN1 (red),  $\alpha 9$  integrin (green) and LYVE-1 (blue) in 3-week-old mouse skin sections. The arrows indicate the sites in which the molecules co-localize close to dermal lymphatic capillaries. (a'') Magnification of boxed area in panel (a). It is well represented the co-localization of EMILIN1 and  $\alpha 9$  integrin next to vessels structure. Scale bar, 50 $\mu$ m.

This evidence supported the further investigation on the expression and localization of EMILIN1 and  $\alpha 9$  integrin in embryonic, neonatal and mature mesenteric lymphatic vessels. EMILIN1 was detected in both blood and lymphatic vessel structures from E18.5 as we have previously shown (Fig. 9 B). At this stage a clear association with  $\alpha 9$  integrin was detected along the wall vessels and in particular in the valve bumps (Fig. 28 A, arrows). At P0 EMILIN1 presented a strong positivity in lymphatic vessels, its fibers were thicker in the vessels and in the valves (arrows, Fig. 28 B and C), where there was a strong positivity for  $\alpha 9$  integrin. Moreover, it was possible to observe a thin network of fibers positive for EMILIN1 in the mesenteric membrane. Confocal longitudinal cross-sections of mesenteric valves revealed EMILIN1 deposition on both luminal and abluminal sides of the valves already at P0 (Fig. 28 D). The most evident co-localization of EMILIN1 and  $\alpha 9$  integrin was observed at P6 (Fig. 28 E). According to all data, EMILIN1 is expressed in the lymphatic vessels and valves since the first stages of embryonic development in close association with  $\alpha 9$  integrin. It is possible to speculate that EMILIN1 could sustain the lymphatic development interacting with LECs through direct binding of  $\alpha 9$  integrin.

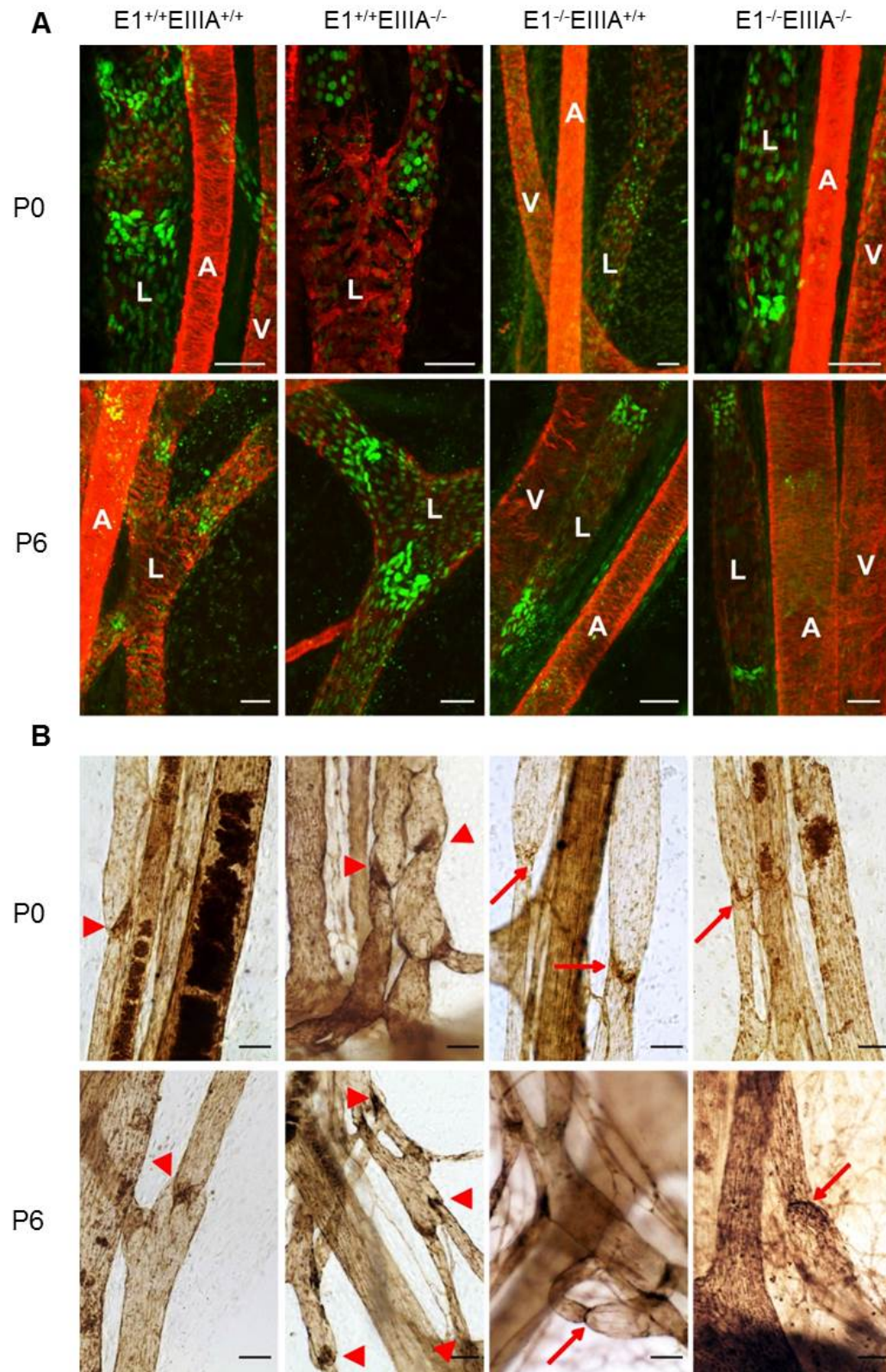
$\alpha 9$  integrin expression is crucial during lymphatic system development: its deficiency is sufficient to lead to a severe phenotype.  $\alpha 9$  integrin<sup>-/-</sup> mice die perinatal due to respiratory failure (Huang et al., 2000). Some of the lymphatic alterations of  $\alpha 9$  integrin<sup>-/-</sup> were very similar to those of *Emilin1*<sup>-/-</sup> collectors, with a reduced number of valves and with a ring-shape phenotype. In a previous study, Bazigou et al. (2009) demonstrated that  $\alpha 9$  integrin is highly expressed in the lymphatic valve leaflets and that it can bind to FN-EIIIA, the embryonic isoform of FN. This binding, according to the authors, is extremely important to allow correct setting and morphology of the valves during their formation.  $\alpha 9\beta 1$  integrin is responsible for FN fibrillogenesis and therefore necessary to create a proper scaffold for the valves. Bazigou et al., for the first time, indicated a mechanism to explain the altered lymphatic phenotype in  $\alpha 9$  integrin null mice, but they didn't answer to other important questions. FN-EIIIA, in fact, is progressively down-regulated after birth while  $\alpha 9$  integrin is constantly expressed in both embryonic and adult lymphatic cells. The authors showed that young *Fn-EIIIA*<sup>-/-</sup> mice displayed a phenotype similar but not so severe to  $\alpha 9$  integrin<sup>-/-</sup> background. Interestingly, *Fn-EIIIA*<sup>-/-</sup> mice rescue their phenotype in adulthood. FN-EIIIA is certainly important, especially during valves formation, but since in adulthood these KO mice are totally normal, another molecule, a cognate ligand for  $\alpha 9$  integrin, could be determinant for lymphatic structure and function. On the basis of already described evidences, we hypothesized that this ligand for  $\alpha 9$  integrin could be EMILIN1.



**Figure 28. EMILIN1- $\alpha 9\beta 1$  integrin co-localization in the lymphatic valve leaflets.** Immunofluorescence staining for the localization of EMILIN1 (green) and  $\alpha 9$  integrin (A', red or gray) in embryonic (E18.5) (A and A'), neonatal (P0) (B, C, and D), and mature (P6) (E) mesenteric lymphatic vessels. The arrows indicate lymphatic valves, which were positive for both EMILIN1 and  $\alpha 9$  integrin staining. (C) Magnification of the boxed area in panel B. The dotted lines in panel A outline the lymphatic vessels. (B and C) Mesenteric vessels are indicated as follow: a, artery; v, vein; l, lymphatic. (D) Four confocal longitudinal cross sections of a mesenteric valve showing EMILIN1 expression at both abluminal (z1) and luminal (z2, z3, and z4) sides of the valve and co-localization with  $\alpha 9$  integrin in the valve leaflets. (E) Representative P6 mesenteric lymphatic valve stained for EMILIN1 (green) and  $\alpha 9$  integrin (red). Scale bars, 150 $\mu$ m (B), 50 $\mu$ m (A, C, and D), and 25 $\mu$ m (E); (from Danussi *et al.*, 2013).

## 1.6 EMILIN1 contributes to valve formation, maintenance and function more than FN-EIIIA.

Starting from the evidences that: 1) *Emilin1*<sup>-/-</sup> and *Fn-EIIIA*<sup>-/-</sup> mice displayed a similar lymphatic alterations during lymphatic valve development; 2) *Fn-EIIIA*<sup>-/-</sup> valves rescued their abnormal phenotype in adulthood while defects in *Emilin1*<sup>-/-</sup> valves persisted; 3) FN-EIIIA was not expressed in adulthood and 4) both molecules (EMILIN1 and FN-EIIIA) were able to bind  $\alpha 9$  integrin, we decided to investigate the relative and peculiar contribution of EMILIN1 and FN-EIIIA in lymphatic valve formation and maintenance. More precisely, we asked which was the function of each single molecule during lymphatic development and whether one molecule could have a more penetrant phenotype. To clarify the specific role of FN-EIIIA and EMILIN1, we performed a genetic approach. Crossing *Emilin1*<sup>+/+</sup> and *Emilin1* null C57Bl/6 mice with *Fn-EIIIA*<sup>+/+</sup> and *Fn-EIIIA* null C57Bl/6 mice we obtained the following 4 genotypes of interest for our analysis: *EI*<sup>+/+</sup> *EIIIA*<sup>+/+</sup>, *EI*<sup>+/+</sup> *EIIIA*<sup>-/-</sup>, *EI*<sup>-/-</sup> *EIIIA*<sup>+/+</sup>, *EI*<sup>-/-</sup> *EIIIA*<sup>-/-</sup>. All these animals apparently seemed very similar to each other without evident macroscopic alterations. The observation from WMS revealed that collecting vessels of P0 and P6 mice expressing EMILIN1 (*EI*<sup>+/+</sup> *EIIIA*<sup>+/+</sup>, *EI*<sup>+/+</sup> *EIIIA*<sup>-/-</sup>) presented a higher valve number than EMILIN1 deficient mice (*EI*<sup>-/-</sup> *EIIIA*<sup>+/+</sup>, *EI*<sup>-/-</sup> *EIIIA*<sup>-/-</sup>). Moreover, these valves were very well formed and mature (red arrowheads) (Fig. 29 A and B). On the contrary, all valves in *Emilin1*<sup>-/-</sup> mice (*EI*<sup>-/-</sup> *EIIIA*<sup>+/+</sup>, *EI*<sup>-/-</sup> *EIIIA*<sup>-/-</sup>) appeared as immature horizontal constrictions. In the absence of FN-EIIIA (*EI*<sup>+/+</sup> *EIIIA*<sup>-/-</sup>) valve morphology appeared normal both at P0 and P6 (Fig. 29 A and B). Also semithin and ultrathin TEM section of *Fn-EIIIA*<sup>-/-</sup> P21 mesenteric collecting vessels (Fig. 29 C) displayed a morphology more similar to *Emilin1*<sup>+/+</sup> than *Emilin1*<sup>-/-</sup> vessels, with thin vessel walls and a normal lumen size in the valve area. Moreover, EMILIN1 WT (*EI*<sup>+/+</sup> *EIIIA*<sup>+/+</sup>) and *Fn-EIIIA*<sup>-/-</sup> (*EI*<sup>+/+</sup> *EIIIA*<sup>-/-</sup>) vessels were very similar for the presence of the smooth muscle cells and mural cells, and they did not show any caveolae nor cytoplasmic filaments nor a proper basement membrane as detected in *Emilin1*<sup>-/-</sup> mice (Fig. 17 and 29 C). This phenotype was independent from the presence or absence of FN-EIIIA indicating that this ECM molecule was not so significant in the valves formation process as previously suggested (Bazigou et al., 2009).



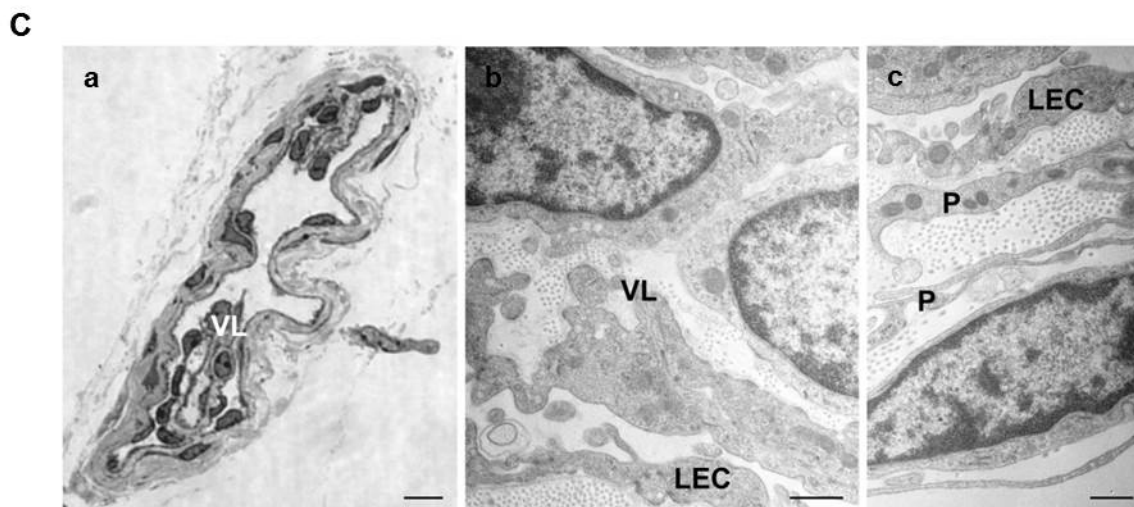


**Figure 29. EMILIN1 and Fn-EIIIA contribution in lymphatic valves formation.** (A) Mesenteric vessels stained for Prox-1 (green) and  $\alpha$ -sma ( $\alpha$ -smooth muscle actin, red) of P0 and P6 WT ( $E1^{+/+} EIIIA^{+/+}$ ),  $E1^{+/+} EIIIA^{-/-}$ ,  $E1^{-/-} EIIIA^{+/+}$  and double-KO ( $E1^{-/-} EIIIA^{-/-}$ ) mice. This staining allow to identify very well lymphatic vessels (L), arteries (A) and veins (V). (B) Mesenteric vessels stained for PECAM-1 of P0 and P6 WT,  $E1^{+/+} EIIIA^{-/-}$ ,  $E1^{-/-} EIIIA^{+/+}$  and double-KO mice. The arrowheads and arrows indicate normal V-shaped and abnormal ring-shaped valves, respectively. (C) Morphological analyses of semithin (a) and ultrathin (b and c) cross sections of mesenteric collecting vessels of  $E1^{+/+} EIIIA^{-/-}$  mice at P21 showing normal features of the valve leaflets (VL), endothelial cells (LEC), and mural cells/pericytes (P). Scale bars, 50 $\mu$ m (A and B), 20 $\mu$ m (C, a), and 1 $\mu$ m (C, b and c), (modified from Danussi et al., 2013)

Again, the quantitative analysis showed that the number and the morphology of the valves depend on EMILIN1 than FN-EIIIA expression. *Emilin1*<sup>-/-</sup> mice ( $E1^{-/-} EIIIA^{+/+}$ ,  $E1^{-/-} EIIIA^{-/-}$ ) displayed a number of valves of 58% lower when compared to WT mice at P0 and 64% at P6 (Fig. 30 A and B), confirming that these differences were not depending on the presence or absence of FN-EIIIA. Moreover, abnormal/immature valves were nearly double in *Emilin1*<sup>-/-</sup> and double KO mice compared to *Emilin1*<sup>+/+</sup> and *Fn-EIIIA*<sup>-/-</sup> mice at P0. At P6  $E1^{+/+} EIIIA^{-/-}$  mice displayed 43% ring valves vs 25% in  $E1^{+/+} EIIIA^{+/+}$  mice (P=0.05); on the other hand  $E1^{-/-} EIIIA^{+/+}$  and  $E1^{-/-} EIIIA^{-/-}$  had about 55% ring valves (P<0.01) (Fig. 30 C and D). In conclusion, FN-EIIIA could have a minimal protective role during valve maturation in young animals.

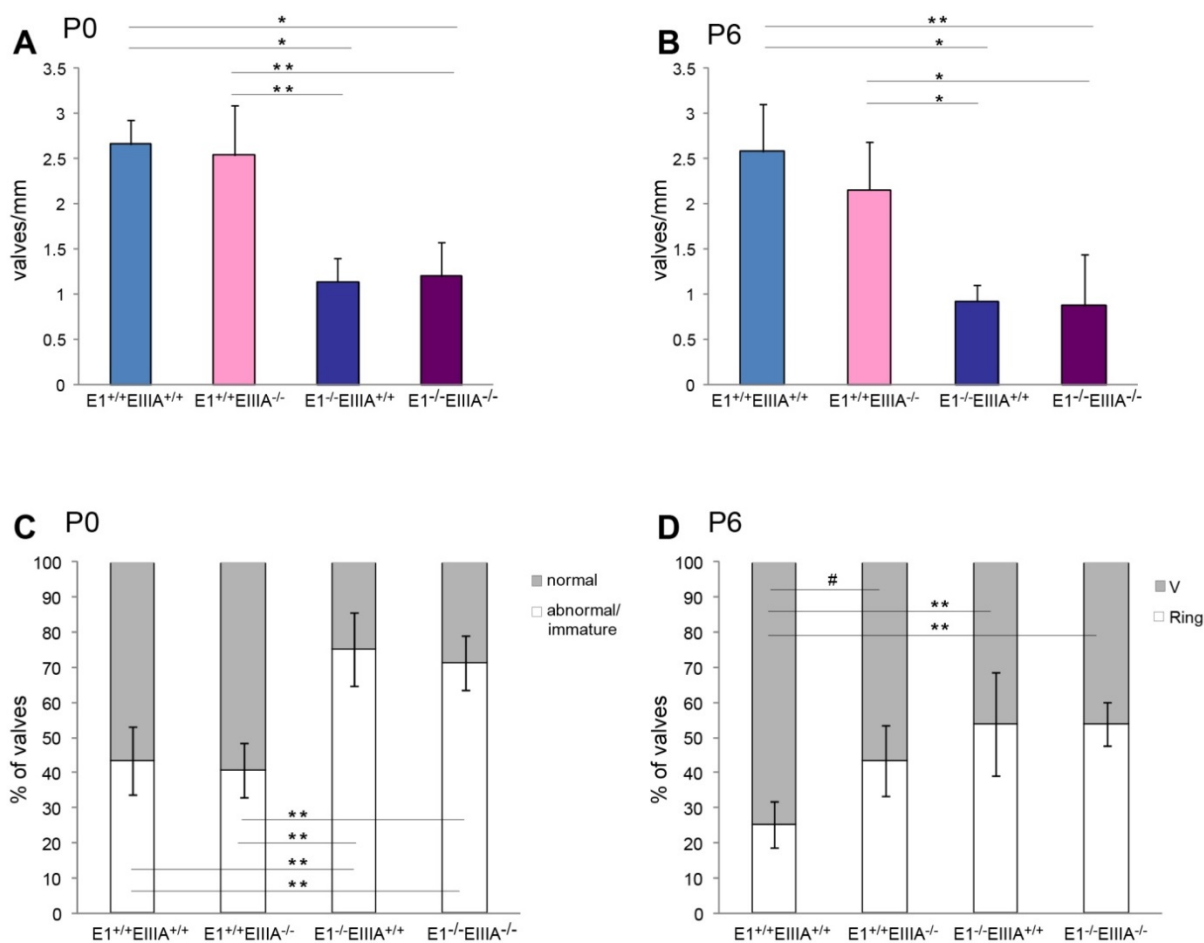


**Figure 30. E1 vs FN-E111A: differences in valves number and morphologies.** The luminal valve numbers (A and B) and morphological analyses (C and D) of mesenteric lymphatic vessels in neonatal (P0) (A and C) and postnatal (P6) (B and D) mice of the resulting genotypes are reported in the graphs. The data shown in panels A and B are the means and SD (n=3 to 6 animals per genotype with more than 10 vessels each). The data in panels C and D were obtained from 3 to 6 animals per genotype (more than 100 valves each). #, P=0.05; \*, P<0.05; \*\*, P<0.01 (a one-way analysis of variance followed by Tukey's post hoc test was performed), (from Danussi et al., 2013).

The FN-E111A marginal role was been demonstrated even by functional lymphangiography assay. We performed the assay in double WT and  $Fn-E111A^{-/-}$  ( $E1^{+/+} E111A^{+/+}$ ,  $E1^{+/+} E111A^{-/-}$ ) P21 mice. We observed that the FITC-dextran transport velocity and quantity were nearly equivalent in the  $E1^{+/+} E111A^{+/+}$  and  $E1^{+/+} E111A^{-/-}$  mice. Similarly to what we saw before (Fig. 23), after 5 minutes from injection, dye was been drained to the iliac LNs and after 30 minutes it reached even some mesenteric nodes in both genotypes. Moreover, the fluorescence intensity of LNs was very similar in the two genotypes. Also in this case it was possible to see V-shaped valves along the dye labeled vessels as indicated by arrows in Figure 31.

Altogether these data suggested that EMILIN1 is a key component regulating valve formation during developmental and maturation stages. Other ECM components certainly contribute to proper lymphatic development. Bazigou et al. (2009) identified, in developmental stage, FN-EIIIA as a crucial molecule, but our results, obtained from a larger number of animals, did not evidence severe alterations in newborn *Fn-EIIIA*<sup>-/-</sup> mice. On the other hand, *Emilin1*<sup>-/-</sup> mice showed a phenotype in newborn animals that persists even in the adult stage. Thus, we could conclude that EMILIN1 role is more crucial and penetrant for the proper lymphatic valve formation and maintenance than FN-EIIIA.

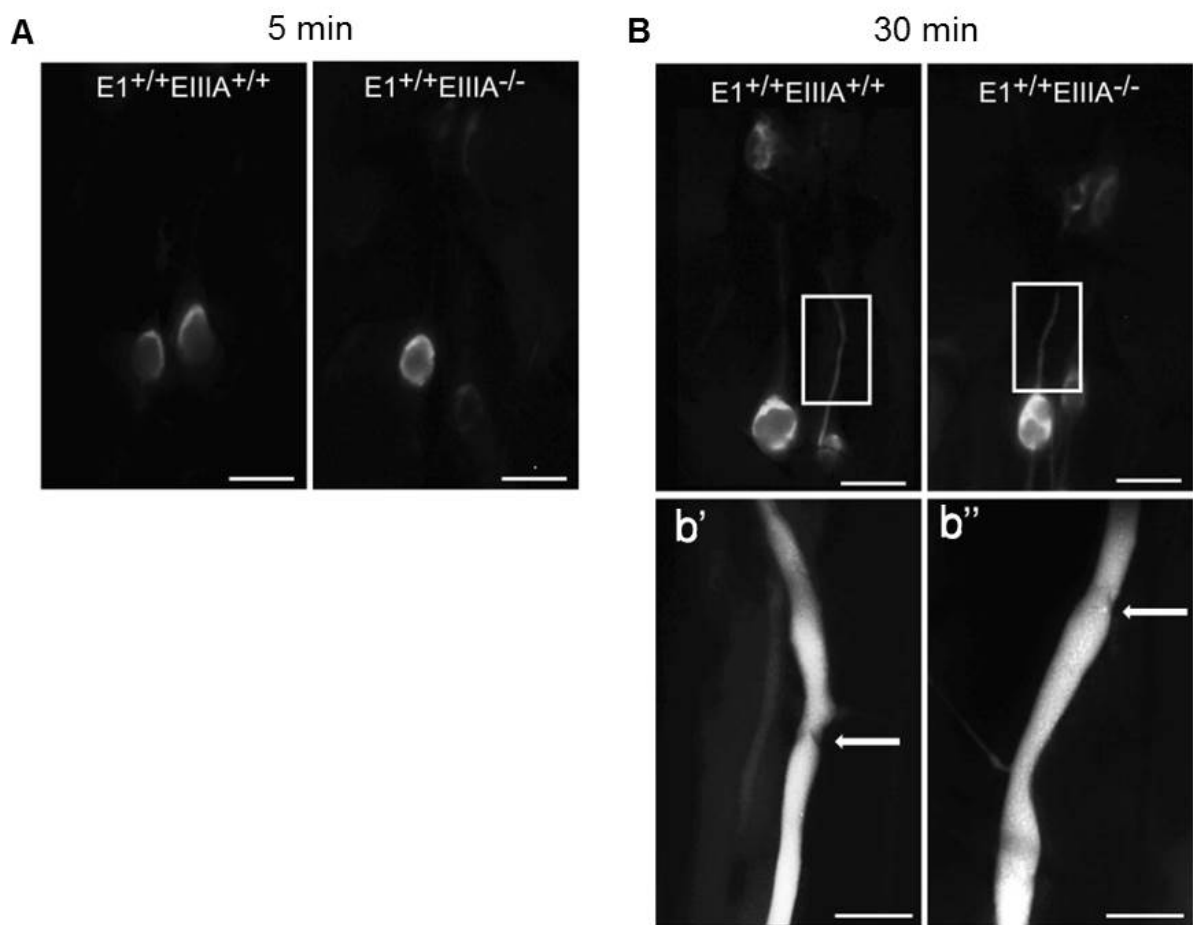


**Figure 31. EMILIN1 and FN-EIIIA contribution in lymphatic vessels functionality.** FITC-dextran (2000 kDa) was subcutaneously injected into the tail of  $E1^{+/+}EIIIA^{+/+}$  and  $E1^{+/+}EIIIA^{-/-}$  P21 mice to visualize the draining lymphatic vasculature and lymph nodes. Mice were sacrificed after 5 min (A) and 30 min (B) from injection. Low magnification images were taken to visualize above all lymph nodes and high magnification images were taken for detailing collectors corresponding to the area of the insets. White arrows indicate v- shaped valves. Scale bar: 2 mm (A and B) and 0.5 mm (b' and b'').

## 1.7 EMILIN1- $\alpha$ 9 $\beta$ 1 integrin interaction regulates LEC proliferation and migration.

We have previously demonstrated that EMILIN1 and its specific ligand expressed by LECs,  $\alpha$ 9 $\beta$ 1 integrin, co-localized in the valves leaflets at different ages, from embryonic to adult life (Fig. 28). But what is the meaning of the EMILIN1- $\alpha$ 9 $\beta$ 1 integrin interaction? We knew that the two molecules co-localize in the valves core and that  $\alpha$ 9 $\beta$ 1 integrin in other cell lines supports the adhesion on EMILIN1 (Danussi et al., 2011). First of all, we investigated if this happens also for LECs. We tested adhesion capability on EMILIN1 substrate of HMVEC-LLy and HMVEC-dLyNeo, expressing  $\alpha$ 9 integrin (Fig. 26). A very high amount of cells adhere on both EMILIN1 and its functional domain gC1q (Fig. 24 A). Since qC1q was the EMILIN1 domain responsible for the binding with  $\alpha$ 4 and  $\alpha$ 9 integrins, we tested the specificity of the interaction between EMILIN1 and  $\alpha$ 9 integrin using also a mutated form of gC1q, E933A. E933A has just one amino acid mutated in the binding site of gC1q domain. The adhesion assay showed that the HMVECs were able to bind EMILIN1 (Fig. 24 A) but not to E933A, through integrin. Since  $\alpha$ 4 and  $\alpha$ 9 integrins were highly homologous (Palmer et al., 1993), to demonstrate that the binding was  $\alpha$ 9 integrin dependent, we performed adhesion experiments using function-blocking antibodies against both  $\alpha$ 9 integrin (Y9A2) and  $\alpha$ 4 integrin (P1H4). In this type of experiments only human LECs were used because the function-blocking antibodies commercially available are specific for human but not for murine integrins. The adhesion assay showed a maintenance of the cell binding in control sample and when P1H4 antibodies were used, indicating that EMILIN1-LEC interaction is strictly  $\alpha$ 9 integrin dependent (Fig. 32 B). As positive control for  $\alpha$ 4 integrin expression we used Jurkat cell lines. In this model P1H4 antibodies, blocking  $\alpha$ 4 integrin activity induced loss of Jurkat cell adhesion (Fig. 32 B). Likely,  $\alpha$ 4 $\beta$ 1 receptor even if expressed (Fig. 26), was in an inactive status on LECs, and the cells utilize  $\alpha$ 9 $\beta$ 1 integrin for adhering to EMILIN1.

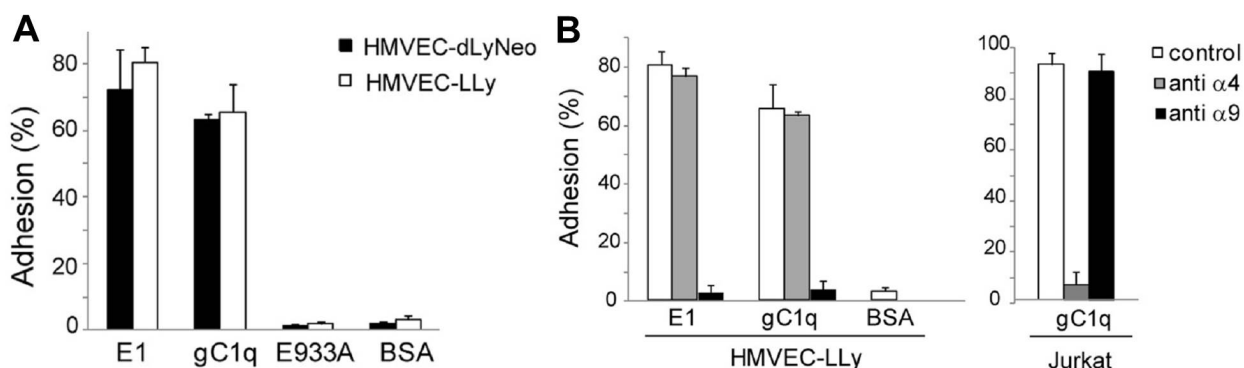


**Figure 32. The EMILIN1-LECs adhesion is  $\alpha$ 9 $\beta$ 1 integrin depended.** (A) Percentages of HMVEC-LLy and HMVEC-dLyNeo cells adhering to EMILIN1 (E1), gC1q, E933A, and bovine serum albumin (BSA). The data are expressed as means and SD of three independent experiments with 6 replicates. (B) Adhesion of HMVEC-LLy and Jurkat cells. The cells were preincubated with anti- $\alpha$ 4 integrin subunit monoclonal antibody (MAb) (P1H4) or anti- $\alpha$ 9 integrin subunit MAb (Y9A2). The data are expressed as means and SD of three independent experiments with 6 replicates. (from Danussi et al., 2013)

Since in other districts EMILIN1-integrin interaction was involved in regulation of cellular mechanism such as proliferation and migration (Spessotto et al., 2006, Danussi et al., 2011 and 2012), we wanted to verify whether also in lymphatic system this mechanism was regulated by this specific engagement. Since data obtained from WMS and TEM analysis evidenced the hyperplastic structures in the *Emilin1*<sup>-/-</sup> background, we investigated the possible effect of EMILIN1 on LEC proliferation. The proliferation rate of HMVEC cells was reduced when they were plated on EMILIN1 or gC1q domain, but any effect was recorded in contact with FN or EIIIA fragments (Fig. 33 A). Moreover, the cell proliferative activity was rescued preventing cell-EMILIN1/gC1q interaction using function-blocking antibodies against  $\alpha$ 9 integrin (Fig. 33 A). The additional proof of the antiproliferative effect of EMILIN1 came out from *ex vivo* observation: at P6 *Emilin1*<sup>-/-</sup> mice displayed a number of Ki67 positive cells in lymphatic valves 4-fold higher than WT counterpart (Fig 33 B and C). These data highlight for the first time that also in lymphatic system EMILIN1-  $\alpha$ 9 integrin interaction regulates the proliferation process.

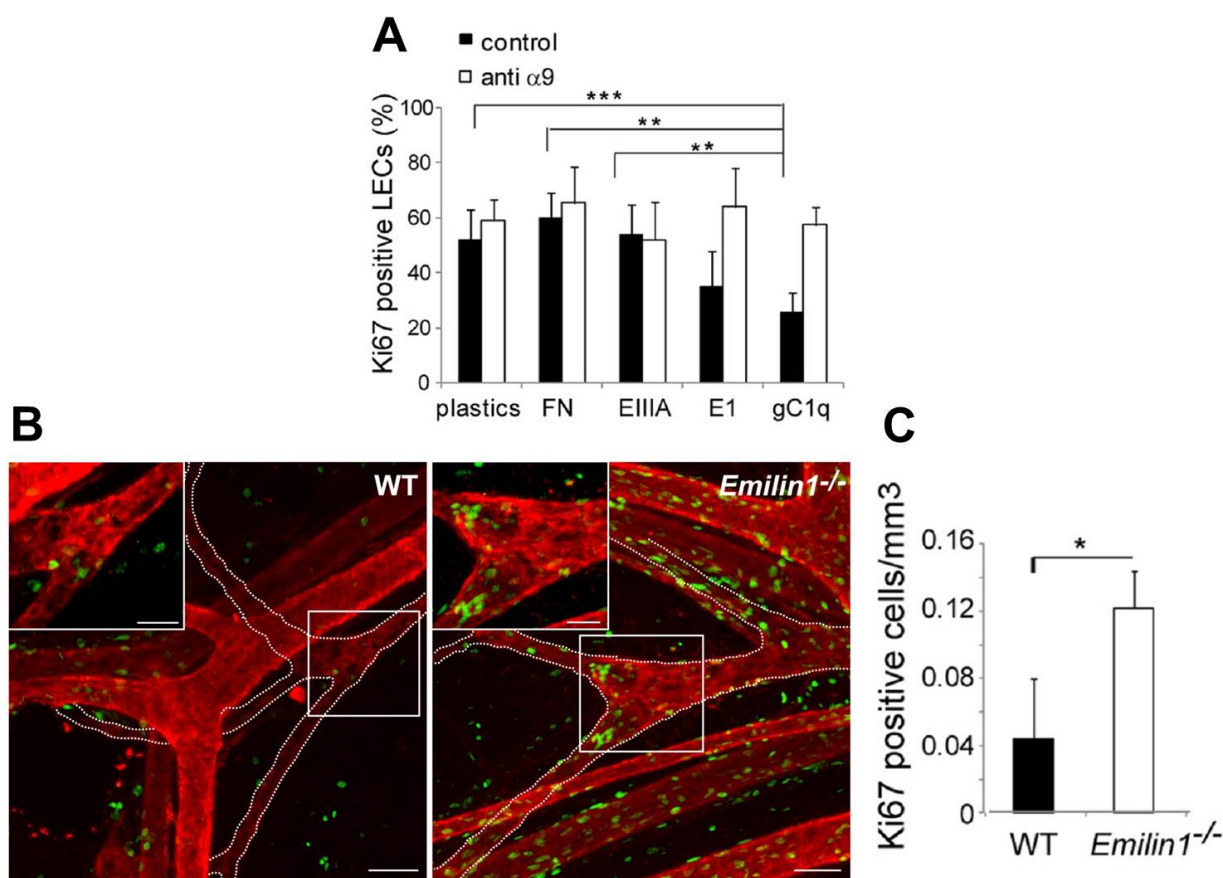


**Figure 33. EMILIN1 has an antiproliferative effect on HMVECs.** (A) Proliferation of HMVEC-LLy cells cultured on tissue culture plates (plastics) and incubated for 48 h in the presence of fibronectin, EIIIA, E1, or gC1q. The data are expressed as mean percentages and SD of the number of Ki67-positive cells of three independent experiments. Six fields were examined for each condition. (B) Representative images of Ki67 (green) and  $\alpha$ -SMA (red) staining of WT and *Emilin1*<sup>-/-</sup> P6 mesenteric vessels. The dotted lines outline the lymphatic vessels. The insets are magnifications of the boxed areas showing the presence of a higher number of Ki67-positive cells in *Emilin1*<sup>-/-</sup> lymphatic valves. (C) Quantification of the Ki67-positive cells of luminal valve-associated areas in WT and *Emilin1*<sup>-/-</sup> P6 mesenteric lymphatic vessels. Z-stack images were collected from whole-mount samples; the resulting 3D reconstruction by Volocity software was used to highlight and calculate the valve area and count the associated Ki67-positive cells. (n=4 mice per genotype at least 10 valves/mesentery were examined); (from Danussi et al., 2013).

During valve morphogenesis, migration of LECs, that will generate lymphangion structures, is a crucial process to ensure a correct setting and localization. As reported in the introduction section, at the moment *Foxc2* is the most important factor involved in this role (Norrmen et al., 2009). To test the hypothesis that EMILIN1 could affect LEC migration, we performed a haptotaxis assay with HMVEC-dLyNeo. For these assays the undersides of the transwell insert membranes were coated with gC1q or EIIIA recombinant fragments to create a concentration

gradient of ECM molecules. Fluorescently tagged cells were added into the transwell inserts and after 8 h, the membranes were cut off, mounted and the transmigrated cells counted under a fluorescence microscope. The LECs were able to migrate towards gC1q domain but not to EIIIA fragment (Fig. 34 A). This behavior in triggering LEC movements was not due to a defective binding ability: LECs were able to adhere with similar extent on FN and EMILIN1 as well as on their binding domains EIIIA and gC1q respectively (Fig. 34 B). Additional evidences on the influence of EMILIN1- $\alpha 9$  integrin engagement in cell migration were obtained in wound-healing assays. We investigated the behavior of cells in normal condition and in presence of function-blocking antibodies against  $\alpha 9$  integrin or against gC1q (Fig. 34 C). These experiments confirmed that cells migrated in a specific way depending on EMILIN1-integrin interaction: antibodies against  $\alpha 9$  integrin or gC1q reduced the movement by blocking the engagement. To further confirm the pro-migratory effect of EMILIN1 we tested also murine endothelial lymphatic cells, LAECs, in a wound-healing assay (Fig. 35). These LAECs were obtained from lymphangiomas induced in WT and KO mice as previously described (Danussi et al., 2012). Wild-type cells moved to close the wound more rapidly than *Emilin1*<sup>-/-</sup> cells: after 20 hours from scratch WT LAECs were able to close the wound in an almost complete way. The difference was more evident when the cells were cultured without LEC supplements and growth factors (Fig. 36).

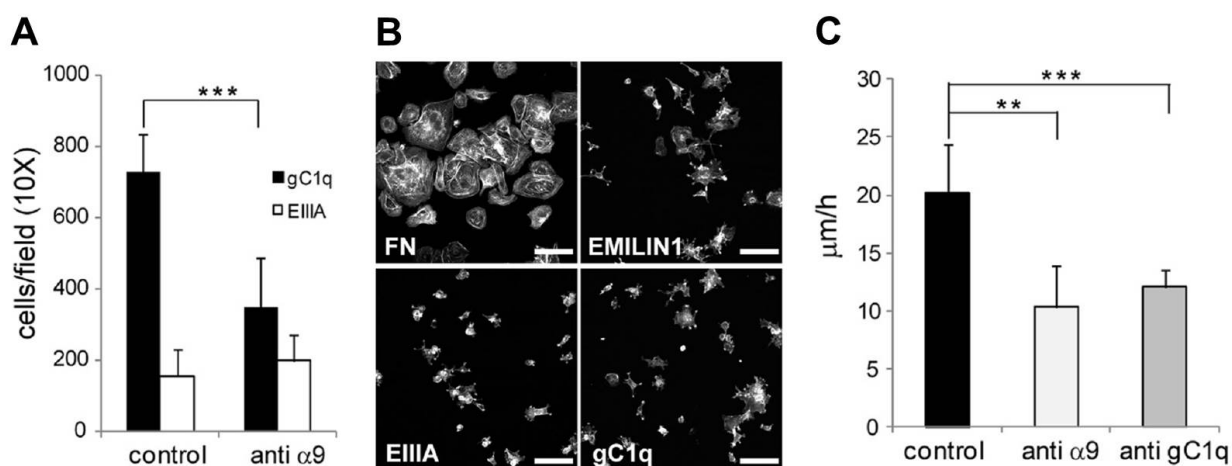


**Figure 34. EMILIN1 has pro-migratory effect on HMVEC.** (A) Haptotactic movement of HMVEC-dLyNeo cells toward C1q or EIIIA in the presence or absence of the function-blocking monoclonal anti- $\alpha 9$  integrin subunit. (B) Phalloidin staining for actin cytoskeleton visualization of HMVEC-dLyNeo after 1h of adhesion on FN, EMILIN1, EIIIA, or gC1q. (C) Wound-healing scratch performed on HMVEC-dLyNeo in the presence of the function-blocking monoclonal anti- $\alpha 9$  integrin subunit or of the monoclonal antibody anti-gC1q. Scratch healing was determined by measuring the shortest distance between scratch edges at 0 and 20 h in each field of view. At least 3 different fields were measured per scratch. Scale bar, 50 $\mu\text{m}$  (B); (from Danussi et al., 2013).

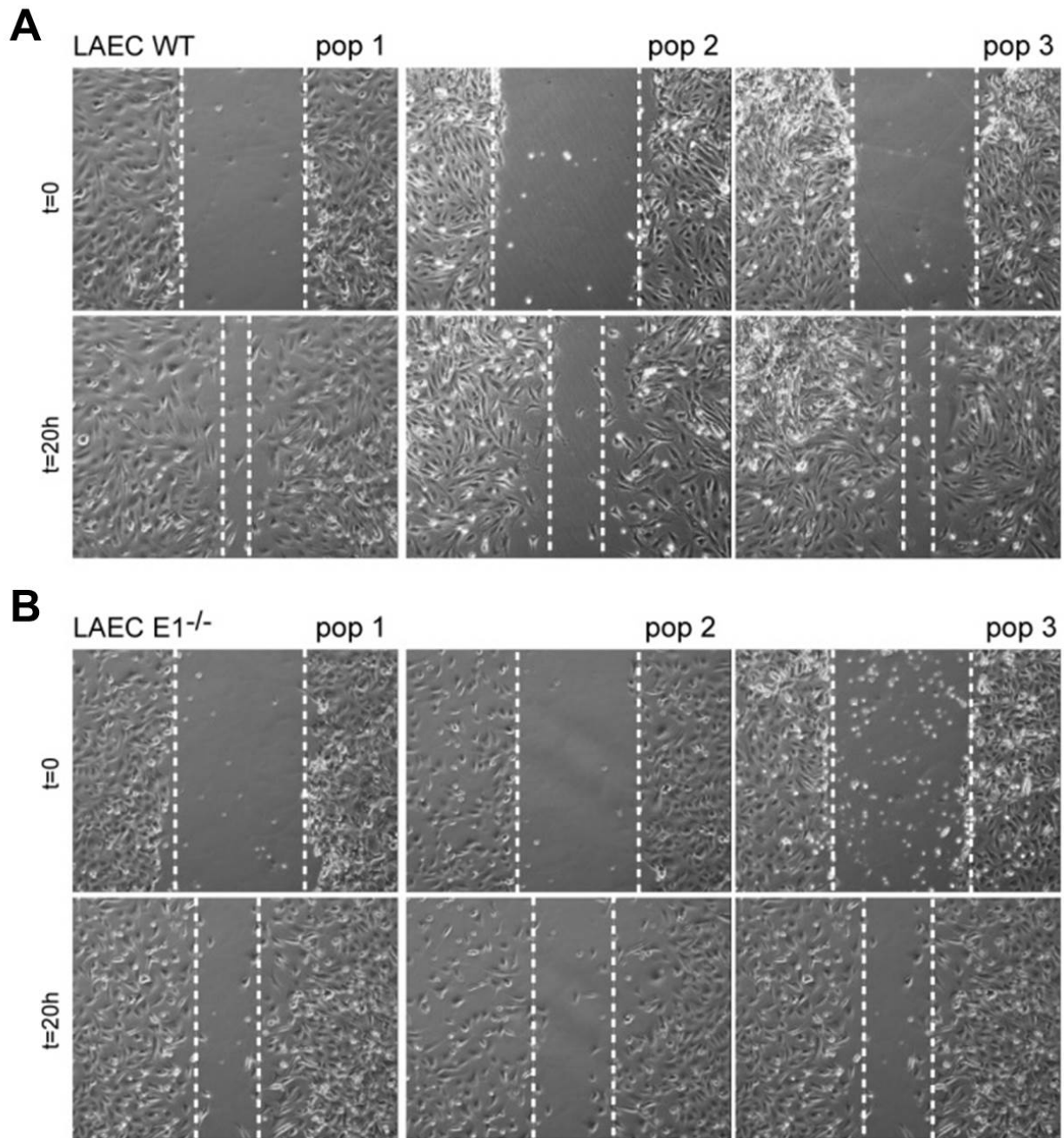


**Figure 35. EMILIN1 has pro-migratory effect on LAECs.** (A and B) Wound-healing assays of WT and Emilin1<sup>-/-</sup> (E1<sup>-/-</sup>) LAECs. The scratch assay was made on confluent LAECs by drawing a line across the bottom of the dish. The figure shows representative micrographs of three different population of LAECs immediately after scratch (t = 0) and the extent of closure after 20 hours.

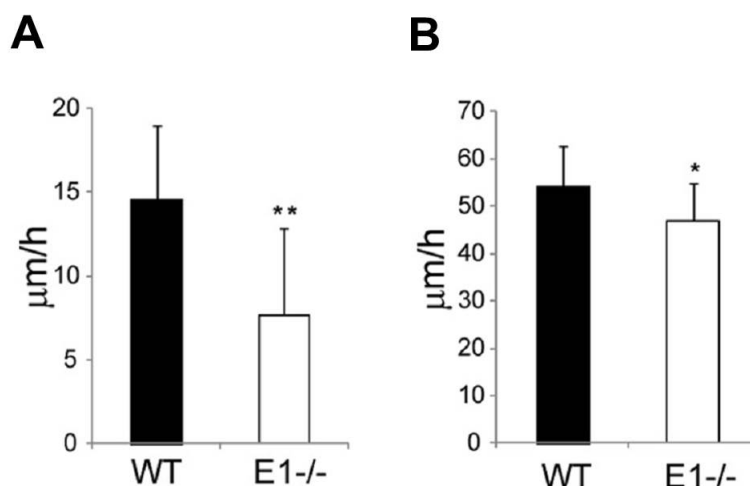


**Figure 36. Speed of closure of WT and *Emilin1*<sup>-/-</sup> LAECs.** The graphs report the speed of closure ( $\mu\text{m}/\text{h}$ ) of WT and *Emilin1*<sup>-/-</sup> LAECs in the presence of culture medium without (A) or enriched with (B) supplements and growth factors; (from Danussi et al., 2013).

In another set of experiments we silenced EMILIN1 expression in LAECs by lentiviral system to verify if the results obtained were dependent only on EMILIN1 (Fig. 37 A). Again, WT cells migrated faster than silenced cells, closing almost completely the wound after 20 hours. The absence of supplements and growth factors increased the difference between WT and silenced LAECs (Fig. 37 B). The results obtained from migration approaches indicate that EMILIN1 could be the “guiding” ECM molecule for the proper localization of the LECs along the valves leaflets during lymphangiogenesis.

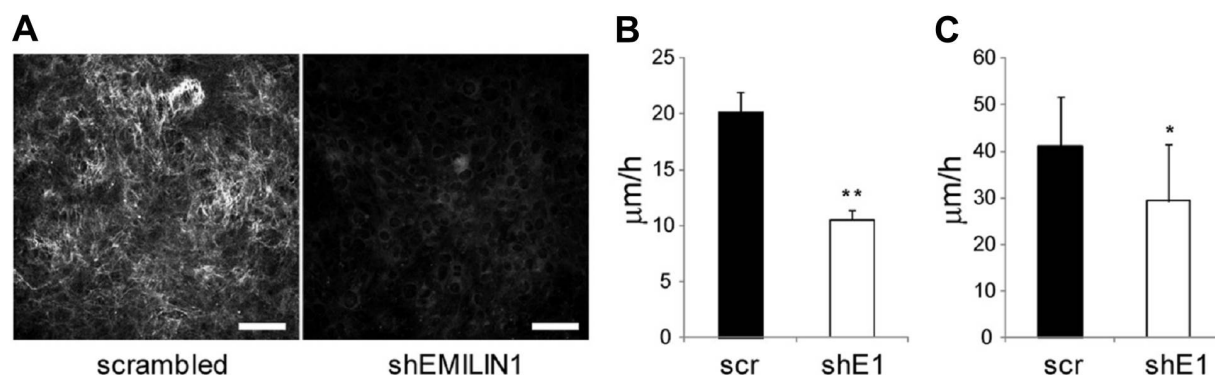


**Figure 37. LAEC WT close the wound more rapidly than LAEC silenced for EMILIN1.** (A) Immunodetection for EMILIN1 staining of LAEC transduced with scrambled or short hairpinRNA EMILIN1 (shEMILIN1) lentiviral particles. (B and C) Velocity of scrambled (scr) and EMILIN1 silenced (shE1) LAECs in a scratch assay in the presence of culture medium without (B) or enriched with (C) supplements and growth factors. The data shown in the graphs are the means and SD of three independent experiments each. \*,  $P < 0.05$ ; \*\*,  $P < 0.02$ ; \*\*\*,  $P = 0.0001$ . Scale bars,  $50\mu\text{m}$ . (from Danussi et al., 2013)

## 2 EMILIN1 DEFICIENCY PROMOTES CELL PROLIFERATION IN THE SKIN

EMILIN1 is expressed in several districts such as lung, cornea, kidney, intestine, lymph nodes, lymphatic vessels and skin. The EMILIN1-integrin interaction in lymphatic system characterized in this thesis was supported by strong evidences obtained with a previous study on the skin phenotype of *Emilin1*<sup>-/-</sup> mice. We demonstrated that EMILIN1 was produced by dermal fibroblasts and that EMILIN1 fibril reached the basal keratinocytes to regulate their proliferation (Danussi et al., 2011). In fact, both epidermis and dermis compartment displayed a significant increase of thickness due to an increase of proliferation rate (Fig. 38 and 39). No differences were found about the apoptosis rate between WT and *Emilin1*<sup>-/-</sup> skin. *In vitro* proliferation assays showed that *Emilin1*<sup>-/-</sup> dermal fibroblasts extracted from *Emilin1*<sup>-/-</sup> mice had a higher proliferation rate compared with fibroblasts isolated from WT mice (Danussi et al., 2011). Moreover, *Emilin1*<sup>-/-</sup> fibroblasts, isolated or silenced by specific short hairpin RNA sequence, were able to enhance proliferation of keratinocytes when co-cultivated in the same plate. In a full-thickness excisional wound, to evaluate the antiproliferative activity of EMILIN1 *in vivo*, *Emilin1*<sup>-/-</sup> mice skin wound closed faster than in WT mice, and the differences were significant already at early phases. The faster closure was due by the hyperproliferative phenotype of *Emilin1*<sup>-/-</sup> mice: in the wound site of KO mice more ki67-positive cells were counted (Danussi et al., 2011).

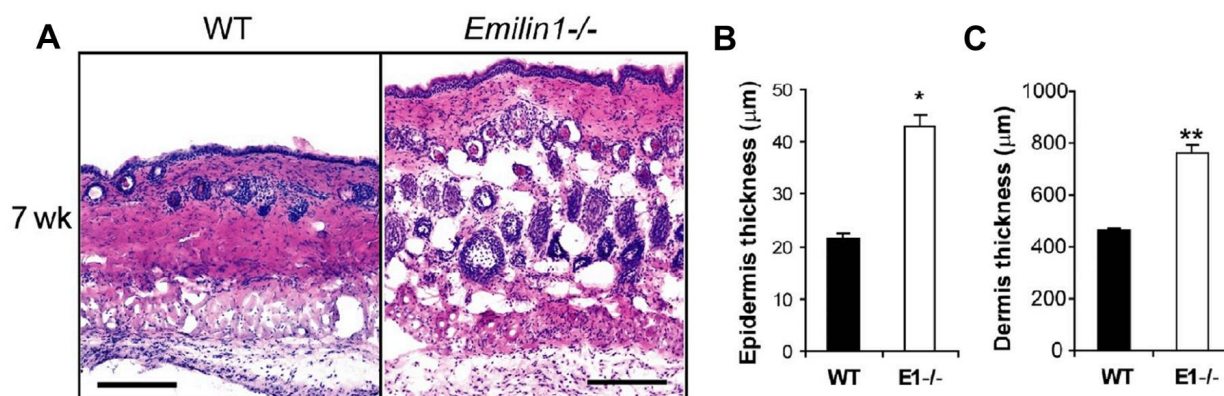


**Figure 38. Skin hyperplastic phenotype in *Emilin1*<sup>-/-</sup> mice.** (A) Cross sections of 7-wk-old skin. Bars, 100 µm. (B and C) ImageJ quantification of epidermis and dermis thickness of 7-wk-old WT (n= 5) and *Emilin1*<sup>-/-</sup> (n= 5) mice. Three H/E-stained sections for each mouse were examined. Mean values ± SD are reported. \*, P = 1 × 10<sup>-14</sup>; \*\*, P = 2 × 10<sup>-12</sup>; (from Danussi et al. 2011).

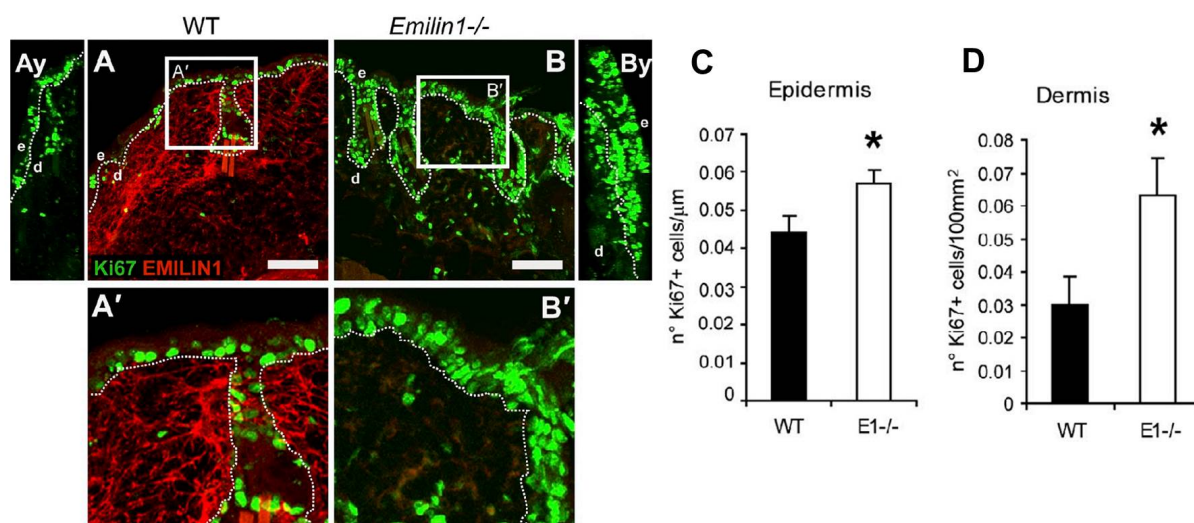


**Figure 39. *Emilin1*<sup>-/-</sup> mice display epidermal and dermal hyperproliferation.** (A and B) Representative images of WT (A) and *Emilin1*<sup>-/-</sup> (B) mouse skin cryostat sections stained for EMILIN1 and for the proliferation marker Ki67. Bars, 75 $\mu$ m. (A<sub>y</sub> and B<sub>y</sub>) yz sections of the confocal images shown in A and B. (A' and B') Zoomed images of the boxed areas in A and B. d, dermis; e, epidermis. The dashed lines denote the basal membrane. (C and D) ImageJ analysis of the number of epidermal Ki67-positive cells/micrometer and dermal Ki67-positive cells/100  $\mu$ m<sup>2</sup>. Mean values  $\pm$  SD are reported. \*, P<0.02. For these quantitative analyses, three different cryostat sections of 7-wk-old WT (n= 5) and *Emilin1*<sup>-/-</sup> (n=5) mice were examined; (from Danussi et al. 2011).

The pathway involved in the proliferative process was mainly characterized and the results evidenced an upregulation of pERK and reduced levels of PTEN (Fig. 40). This pathway was enhanced also from increased levels of TGF $\beta$  detectable in a *Emilin1*<sup>-/-</sup> background. My personal contribution in this study was just to demonstrate that PTEN was the central molecule regulating the pathway activated by EMILIN1/ $\alpha$ 4 or  $\alpha$ 9 integrin engagement. To this aim I silenced PTEN expression using lentiviral system in epidermal cells lines (Caco-2 and HaCaT) and therefore I analyzed the expression levels of the molecules involved in the pathway (Fig. 41).

The results highlighted and defined that the proliferative behavior depended on the signals derived from integrin engagement by EMILIN1. When this engagement was lost the cell proliferation increased, whereas when the integrins were bound to EMILIN1 a homeostatic cell growth was maintained. The EMILIN1-integrin ligation induced a significant increase of PTEN activity that leads to the reduction of proliferative rate by controlling PI3K, Erk, Smad2 and Akt activation. Moreover, this work identified for the first time that  $\alpha$ 9 integrin, expressed by keratinocytes, was a new ligand for EMILIN1 (Danussi et al., 2011).

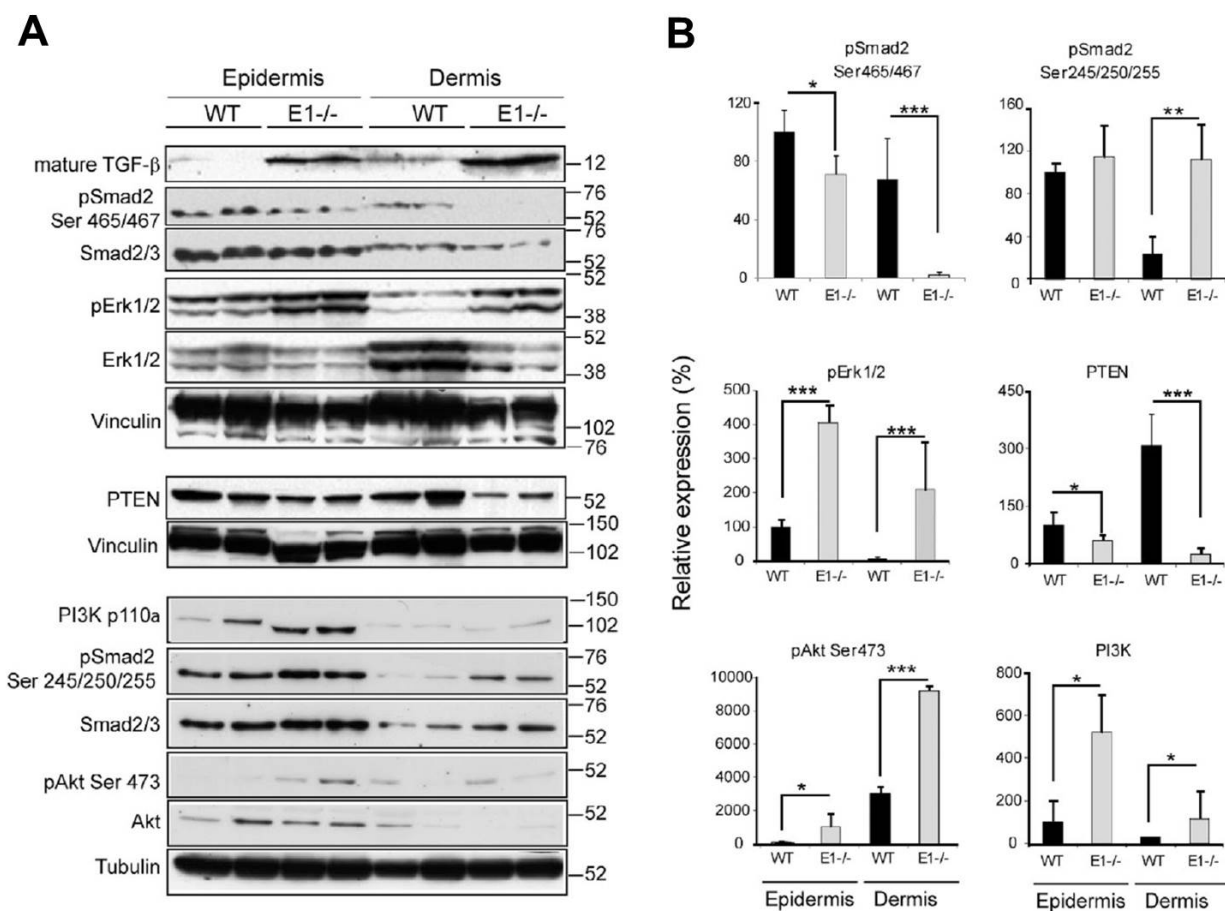


**Figure 40. EMILIN1 deficiency up-regulates PI3K/Akt and Erk1/2 and down-regulates PTEN.** (A) Western blot analysis of epidermis and dermis of 7-wk-old WT and *Emilin1*<sup>-/-</sup> mice. Molecular mass is indicated in kilodaltons. (B) Quantification of Western blot analysis by Quantity One software. The mean values ( $\pm$ SD) of pSmad2 (Ser465/467 and Ser245/250/255), pErk1/2, PTEN, pAkt (Ser473), and PI3K relative expression levels of WT (n = 4) and *Emilin1*<sup>-/-</sup> (n = 4) mice are reported. \*, P=0.05; \*\*, P<0.05; \*\*\*, P<0.01; (from Danussi et al. 2011).

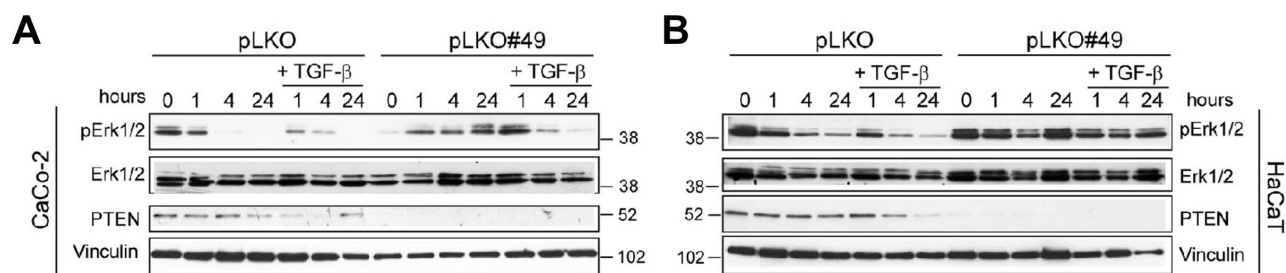


**Figure 41. PTEN down-regulates pErk1/2.** Western blot analysis of control (pLKO) or PTEN-silenced (pLKO#49) CaCo-2 and HaCaT cell extracts after adhesion for different lengths of time on gC1q in the presence or absence of 10 ng/ml TGF- $\beta$ 1; (from Danussi et al. 2011).

### 3. EMILIN1 AND SKIN CARCINOGENESIS

#### 3.1 *Emilin1*<sup>-/-</sup> mice were more susceptible to chemically induced skin carcinogenesis

We demonstrated that EMILIN1 influences cell adhesion, proliferation, migration and that it is a crucial ECM component of lymphatic vessels. For all these properties, its absence or degradation could be crucial in generating or increasing severe alterations as happens in pathological conditions, from inflammation to tumorigenesis. As first approach we investigated EMILIN1 influence on cell behavior, inducing tumorigenesis with a skin carcinogenesis well established protocol. We treated mice with DMBA and TPA reagents to chemically induce skin papillomas. As expected, *Emilin1*<sup>-/-</sup> mice showed accelerated formation of skin papillomas with a lower average latency period than WT mice. Moreover, 100% of *Emilin1*<sup>-/-</sup> mouse and only 60% of WT mice developed tumors, after 20 weeks from first TPA application. In *Emilin1*<sup>-/-</sup> mice more and larger papillomas grown than in WT littermates (Danussi et al., 2012). Since EMILIN1 directly inhibits cell proliferation by engaging  $\alpha 4\beta 1$  integrin expressed on dermal fibroblasts or  $\alpha 9\beta 1$  integrin expressed on basal keratinocytes as reported before (Danussi et al., 2011), we analyzed if the increased growth rate of papillomas in *Emilin1*<sup>-/-</sup> mice was due to the loss of integrin engagement by EMILIN1. *Emilin1*<sup>-/-</sup> skin tumors showed a considerable increase of epidermal as well as dermal Ki67-positive cells compared with WT mice. Also in the tumor microenvironment the lack of EMILIN1– $\alpha 4/\alpha 9$  integrin interaction in *Emilin1*<sup>-/-</sup> mice promoted cell hyperplasia because of the reduction of PTEN, and the consequent activation of PI3K/Akt and Erk1/2 pathways, and hence increased proliferation as well as normal skin (Danussi et al., 2011 and 2012). This suggested that aberrant skin homeostasis generated by EMILIN1 deficiency, and consequent positive regulation of signal pathways involved in cell proliferation, induced a protumorigenic environment.

### 3.2 In *Emilin1*<sup>-/-</sup> mice lymphangiogenesis and metastatization increase

In this neoplastic model my effort was focused above all on lymphangiogenesis and lymphatic spread in association to EMILIN1 presence or absence. First of all, vessel density in skin papillomas and in inguinal and axillary LNs after treatment for skin carcinogenesis induction was analyzed (Fig. 42). In both sites we saw a great variability in vessel density but whereas blood vessels (MMRN2-positive cells) didn't show differences between WT and *Emilin1*<sup>-/-</sup> littermates, lymphatic vessels (LYVE-1-positive cells) displayed a significant increase in *Emilin1*<sup>-/-</sup> than in WT mice in both papillomas and LNs. In *Emilin1*<sup>-/-</sup> draining LNs, lymphatic vessels appeared more dense and thicker compared with those of WT littermates (Fig. 43 C and D). Moreover, we found that *Emilin1*<sup>-/-</sup> mice treated with skin carcinogenesis protocol, presented LNs larger (almost 2-fold) compared to WT mice (Fig. 43 A, B, C). Sometimes they displayed wide hemorrhagic foci (Fig. 43 B).

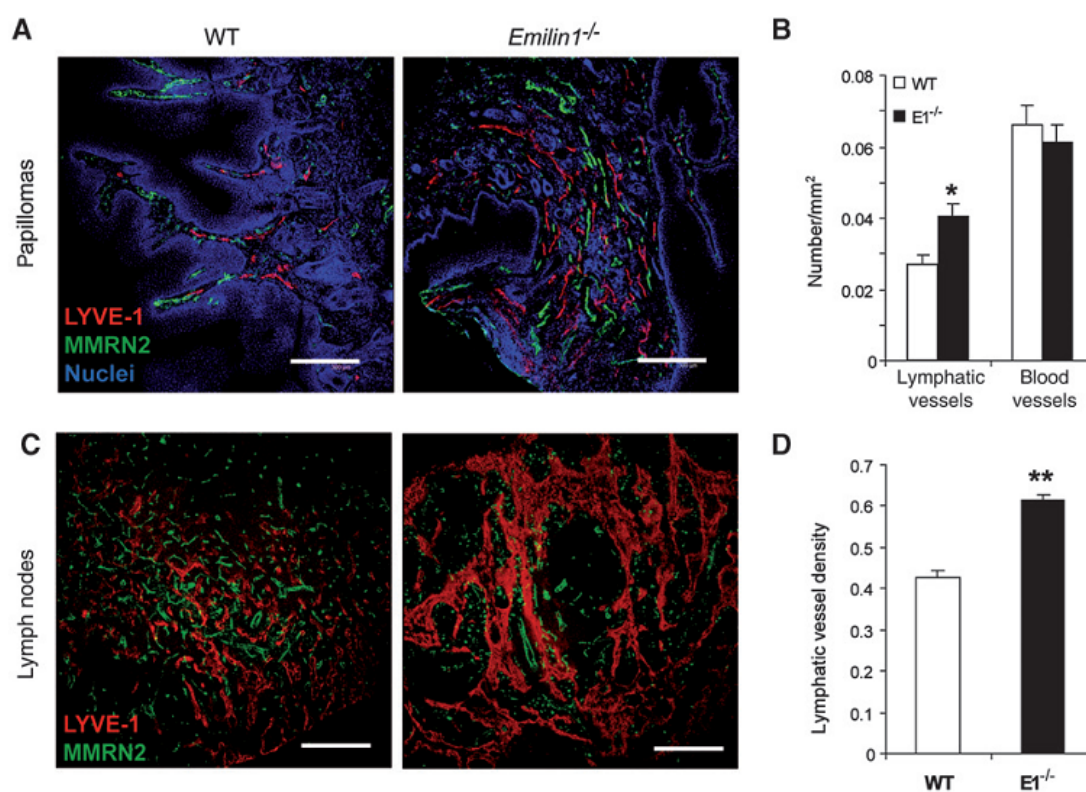


**Figure 42. Enhanced tumor and sentinel lymph node lymphangiogenesis in tumor-bearing *Emilin1*<sup>-/-</sup> mice.** (A) Immunofluorescence analysis of cryostat sections of WT and *Emilin1*<sup>-/-</sup> papillomas. Lymphatic vessels are LYVE-1-positive (red) and blood vessels are MMRN2-positive (green). Nuclei are labeled by ToPro (blue). Scale bar: 300 mm. (B) Computer-assisted morphometric analysis of tumor-associated lymphatic and blood vessels. Three representative images of papillomas (n=6) for each genotype were analyzed. The values represent the mean $\pm$ SD of vessels per unit area (mm<sup>2</sup>). \*,P=0.003. (C) Representative immunofluorescence images of inguinal lymph node cryostat sections stained for LYVE-1 (red) and MMRN2 (green) excised from papilloma-bearing WT and *Emilin1*<sup>-/-</sup> mice. Scale bar: 300mm. (D) Computer-assisted morphometric analysis of lymph node lymphatic and blood vessels. \*\*, P=1x10<sup>-8</sup>; (from Danussi et al. 2012).

We also tested the presence of metastases by PCR analysis and immunostaining for the epithelial markers (Keratins 8 and Keratins 14) (Fig. 43 D). *Emilin1*<sup>-/-</sup> LNs displayed higher percentage of epithelial metastatic cells. The dissemination of metastatic cells was certainly allowed by a higher number of lymphatic vessels but maybe also by the increased vessel permeability (Danussi et al., 2008). We therefore verified if metastatic spread was due to lymphatic vessel alterations and so if LECs were differently permissive for tumor cells passage. Performing a transmigration assay on a monolayer of WT or *Emilin1*<sup>-/-</sup> LAECs and using several tumor cells lines, we observed that the percentage of migrated cells through *Emilin1*<sup>-/-</sup> LAECs was higher in both intra- and extravasation models (Fig. 44). This migration assay demonstrated that the cell migration was not dependent on  $\alpha 4\beta 1$  integrin expressed on tumor cells (as reported by Rebhun et al., 2010), suggesting that this integrin was not playing a primary role in tumor cell dissemination and that the spreading was due to the structural properties of LAECs.

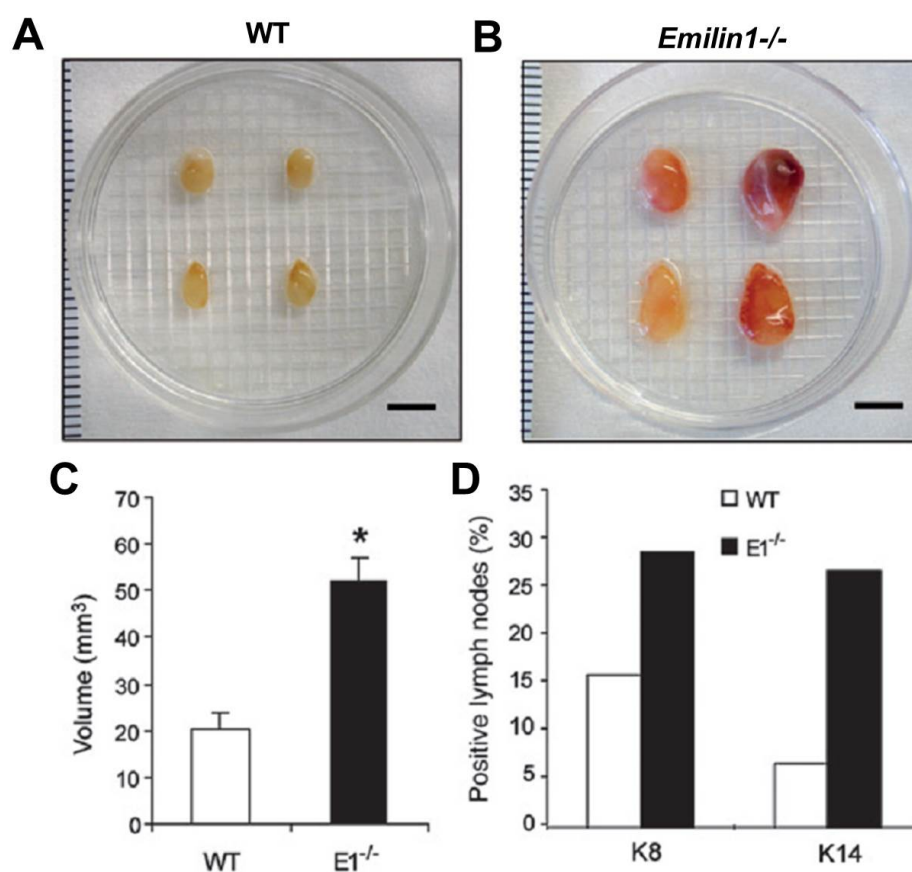


**Figure 43. Increased lymph nodes volume and metastasis in *Emilin1*<sup>-/-</sup> mice.** (A and B) WT and *Emilin1*<sup>-/-</sup> excised inguinal and axillary LNs. (C) Inguinal and axillary LNs volume, mean  $\pm$ SD of WT (n=34) and *Emilin1*<sup>-/-</sup> (n=38). Larger ( $d_L$ ) and smaller distance ( $d_S$ ) of lymph nodes were measured with ImageJ software and volume was calculated by the formula  $V=0.5 \times d_L \times d_S^2$ . \*,  $P < 4.5 \times 10^{-6}$ . (D) Number of K8- and K14-positive or negative lymph nodes evaluated by RT-PCR analysis. Scale bar: 5 mm(A, B); (from Danussi et al. 2012).

All these findings indicated that: 1) the lack of antiproliferative effect of EMILIN1/ $\alpha$ 4 or  $\alpha$ 9 integrin interaction, which led to higher lymphatic vessel density within the tumors as well as in the draining LNs, and 2) the structural defect due to EMILIN1 deficiency, such as a reduction of anchoring filaments and the presence of abnormal intercellular junctions (Danussi et al., 2011), generate a lymphatic pro-metastatic environment facilitating tumor cells dissemination to LNs.

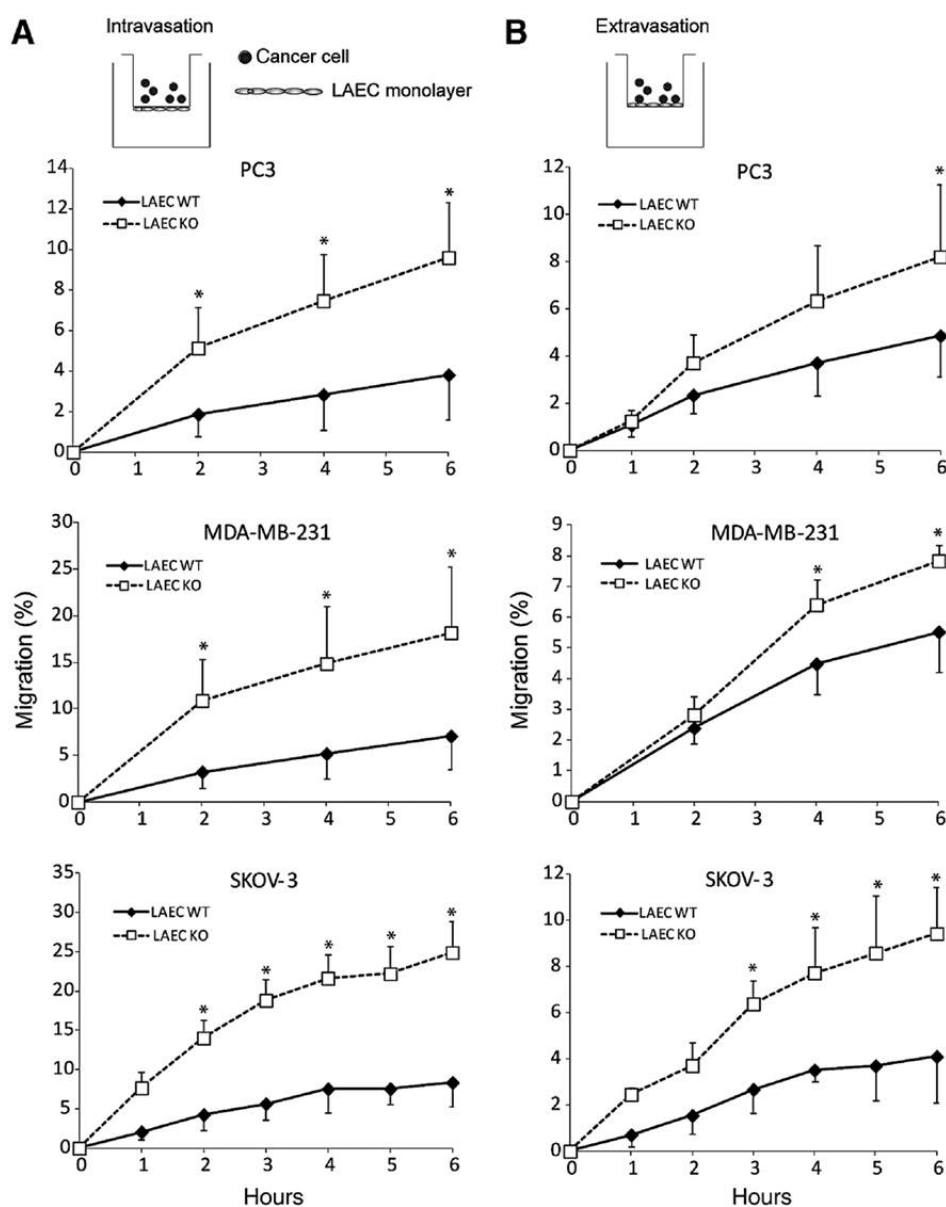


**Figure 44. Tumor cell transmigration.** (A and B) Transmigration assays of PC3, MDA-MB-231, and SKOV-3 cells expressing  $\alpha$ 4 integrin were conducted growing WT and *Emilin1*<sup>-/-</sup> LAECs on the lower-side or on the upper-side of Transwell filters to mimic lymphatic intra- (A) and extravasation (B). The values report the mean migration percentages SD obtained in 3 separate experiments conducted in triplicate. \*,  $P < 0.05$ ; (from Danussi et al. 2012).

# **DISCUSSION**

The cells of the microenvironment are embedded in a supporting network of ECM constituents that include collagens, elastin, proteoglycans, and glycoproteins (Li et al., 2007; Zhang and Huang, 2011). The ECM does not constitute a mere structural scaffold but it elicits profound influences on cell behavior and affects cell growth, differentiation, motility, and viability (Bissell et al., 2005; Marastoni et al., 2008; Hynes, 2009; Cukierman and Bassi, 2010; Colombatti et al., 2012). EMILIN1 is a glycoprotein of ECM associated to elastic fibers expressed in several tissues displaying several function.

The scheme in Figure 45 summarizes the principal results illustrated in this study. According to the results obtained in Danussi et al. (2008), we extended the analysis about the role of EMILIN1 in the lymphatic system. Through above all *ex vivo* analysis we demonstrated that the presence of this ECM protein is crucial for the proper formation of lymphatic vessels and valves. Performing analyses on two different mouse strains we showed that EMILIN1 is expressed along lymphatic collectors and especially in the core of the intraluminal valves. Its expression leads to well organized structures, with a high number of intraluminal valves which present mostly the classical V-shape. On the contrary, *Emilin1*<sup>-/-</sup> vessels appeared convoluted and twisted with a reduced number of valves. Moreover, *Emilin1*<sup>-/-</sup> valves appear as constrictions along the vessels or with immature shape. Another important evidence is the increased proliferation of cells of lymphatic *Emilin1*<sup>-/-</sup> collectors. The consequence is the enlargement of the thickness of wall vessel but even of the valve leaflets and a decreased vascular lumen. The abnormal structures in *Emilin1*<sup>-/-</sup> lymphatic system don't ensure an efficient lymph drainage. Previous functional studies revealed a considerable delay in *Emilin1*<sup>-/-</sup> mice in the lymph transport associated to an impair of lymph uptake from interstitium (Danussi et al., 2008). The studies reported also a reduction of lymph flow into the collectors. In fact, in *Emilin1*<sup>-/-</sup> environment the immature valves are unable to push the lymph through lymphangions and they can't prevent the backflow. The lymphatic anomalies should lead a severe phenotype, but KO mice do not exhibit an evident pathological condition. These mice look healthy, fertile and with a long lifespan. They just present a mild lymphedema. We have hypothesized a compensatory effect, considering another important observation detected in TEM and WMS analysis. Usually collecting vessels are characterized by the presence of a basement membrane and of a SMC coverage that is not so dense in valve area. *Emilin1*<sup>-/-</sup> vessels displayed an enhanced and pronounced the coverage of mural cells/pericytes with a myofibroblast-like phenotype if compared with WT littermate. This hypothesized compensatory mechanism could also be induced by the increase of mature TGFβ1

levels in KO mice. EMILIN1, in fact, inhibits TGF $\beta$ 1 maturation (Zacchigna et al., 2006). The enhanced TGF $\beta$ 1 signaling could be crucial because TGF $\beta$ 1 is a strong inducer of fibroblast-myofibroblast terminal differentiation (Evans et al., 2003). Other molecules are involved in the establishment and maintenance of lymphatic collectors such as Sema3A, which plays a role in regulating coverage by SMC/mural cells (Jurisic et al., 2012). Sema3a-null mice exhibit a change in the lymphatic vessel morphology and an abnormal SMC coverage. Moreover, recently it has been demonstrated that Reelin is important during lymphatic vessels formation (Lutter et al., 2012). Reelin is deposited by LECs, associated to specific matrix components, in the valve regions. SMC recruitment to the collecting lymphatic vessels activates Reelin signaling, and the same Reelin acts in an autocrine way to regulate SMC recruitment and collecting vessels differentiation. Reelin null mice display irregular lymphatic vessel diameter, with abnormal constrictions and swellings (Lutter et al., 2012).

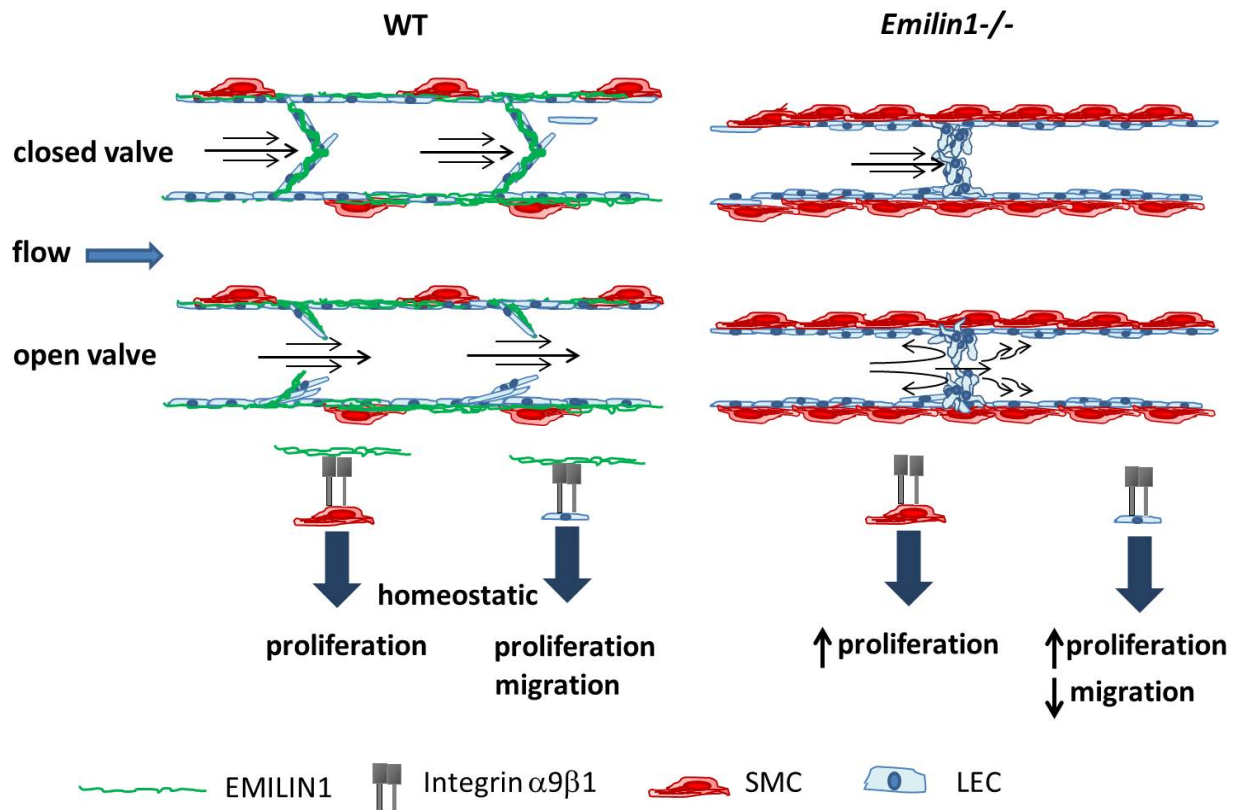


**Figure 45. Schematic overview of WT and *Emilin1*<sup>-/-</sup> collecting lymphatic vessel.** A correct lymph transport is warranted by the proper structure of the valves and positioning of SMCs along the collectors in WT mice. On the contrary, in *Emilin1*<sup>-/-</sup> mice the abnormal coverage of SMCs in the proximity of the valves and valve abnormal morphology cause flow defects and delays in lymph transport (A). These impairments are due to the lack of EMILIN1- $\alpha$ 9 integrin interaction that leads to increased proliferation of SMCs and LECs (B). Moreover, if EMILIN1 is absent, a proper extracellular component in guiding the migration of LECs to form functional valve leaflet runs out with the consequence of a reduced number of valves and the persistence of ring-unfunctional valves in adulthood.

The first evidences in which an ECM protein is involved in a specific way in valve development, regard the embryonic isoform of fibronectin, FN-EIIIA. Bazigou et al., showed an altered morphological formation of the valve leaflet in *Fn-EIIIA*<sup>-/-</sup> mice with a consequent impairment of lymphatic function. *Fn-EIIIA*<sup>-/-</sup> valves, according to these authors, show valve anomalies, but this phenotype is completely rescued in adulthood. Crossing *Emilin1*<sup>-/-</sup> with *Fn-EIIIA*<sup>-/-</sup> mice we have established the relative role of this two ECM molecules in valve formation and maturation. Our data highlight the lower penetrance of FN-EIIIA if compared with EMILIN1 phenotype. *Fn-EIIIA*<sup>-/-</sup> valves, even in newborn mice, didn't display a severe phenotype as well as *Emilin1*<sup>-/-</sup> structures. Since FN-EIIIA deficiency induce a mild lymphatic phenotype and its altered phenotype is rescued in adulthood, but the role of EMILIN1 in the proper formation of lymphatic intraluminal valves is predominant.

A lot of evidence confirms the crucial role of ECM compartment as regulator of lymphatic development, but the mechanisms are poorly known. Usually the regulatory interaction between ECM and cells occurs through transmembrane proteins such as integrins. The ECM-integrin engagement can regulate several cell features among morphology, migration, proliferation and apoptosis. In particular, it is known that gC1q domain of EMILIN1 has two specific ligands:  $\alpha4\beta1$  and  $\alpha9\beta1$  integrins (Verdone et al., 2008, Danussi et al., 2008, 2011). In this thesis we demonstrated that  $\alpha9\beta1$  integrin is expressed by LECs and that the binding with EMILIN1 is involved in lymphatic vessel developing and maintenance. Moreover, many findings related  $\alpha9\beta1$  integrin to the development of the lymphatic vascular system (Bazigou et al., 2009, Huang et al. 2000, Vlahakis et al., 2005, Kajiya et al., 2005, Mishima et al., 2007).  $\alpha9\beta1$  null mice die perinatally of chylothorax due to impaired lung functions. Bazigou et al. demonstrated that they have specific defects in lymphatic valves, which appear as horizontal constrictions rather than V-shaped, whereas the lymphatic vasculature apparently undergoes normal development (Huang et al. 2000).  $\alpha9\beta1$  integrin interacts with a relatively large number of ECM ligands including tenascin C, osteopontin, VCAM-1, FN-EIIIA (Bazigou et al., 2009, Taooka et al., 1999, Yokosaki Yet al., 1994, 1999, Eto et al., 2000, Majumdar et al., 2004). Null mutations in some of these  $\alpha9\beta1$  ligands didn't affect the development of a normal lymphatic phenotype (Gurtner et al., 1995, Forsberg et al., 1996, Fukamauchi et al., 1996, Liaw et al., 1998) except FN-EIIIA and EMILIN1, as demonstrated by this study. Since EMILIN1–integrin interaction regulates adhesion and proliferation of different cell system, we investigated if the engagement of  $\alpha9\beta1$  integrin by

EMILIN1 could regulated proliferation even in the lymphatics (Fig. 45). The results obtained in skin revealed that  $\alpha 9\beta 1$  integrin, expressed by basal keratinocytes, is a EMILIN1 receptor and that the lack of engagement lead to a hyperproliferative environment (Danussi et al., 2011). Similarly, the lack of EMILIN1- $\alpha 9$  integrin interaction induces an increase the proliferation rate also in LECs.

During vessel formation and remodeling, cell proliferation is an important process, but even the migratory ability plays a crucial role to guarantee the proper setting of the cells along the vessels and on the valve leaflets. We observed that during embryonic development EMILIN1 was upregulated in specific sites along the lymphatic vessels, which represent valve buds. Moreover, we showed that EMILIN1 by  $\alpha 9$  integrin engagement has a pro-migratory effect *in vitro*. The EMILIN1 core in the valve leaflets and along the vessels could indicate the site of valve formation, so that LECs localize and set to create a functional structure. In this way EMILIN1 could co-operate, in the organization of intraluminal valves and of lymphatic vessels, with important lymphangiogenic factors such as Foxc2, Podoplanin, EphrinB2 and Angiopoietins.

Altogether, these results suggest that EMILIN1 and its cognate receptor  $\alpha 9\beta 1$  integrin play a dual role in valve morphogenesis: not only in contributing to the structural integrity of the valve core but also in “guiding” the migration of LECs and controlling proliferation to form functional valve leaflets.

Moreover, according to the results obtained in this and previous works for which I contributed for a partial part (Danussi et al., 2011, 2012), we could suppose that EMILIN1, inhibiting cell proliferation, sustains the differentiation process for lymphatic endothelial and surrounding cells and indicates the proper localization and orientation along the vessels and in valves leaflets.

Usually an inflammatory or tumor environment is rich in pro-lymhangiogetic factors such as VEGF-C/D/A. This background could enhance the hyperproliferative effect of *Emilin1*<sup>-/-</sup> environment. Indeed we showed that *Emilin1*<sup>-/-</sup> mice were more susceptible to develop papillomas during skin carcinogenesis chemical treatment. According to the hyperproliferative phenotype, in *Emilin1*<sup>-/-</sup> microenvironment, lymphangiogenesis is promoted not only in the tumor site but also in the lymph nodes. In KO lymph nodes and papillomas there is a higher percentage of formation of new and larger lymphatic vessels when compared to WT. The absence of EMILIN1 leads to changes in integrity of the vessels, indeed increase the vessel permeability. This finding could explain the major number of metastatic cells and foci revealed in KO lymph nodes. The lack of EMILIN1 expression may lead to alteration in cell-ECM molecular

architecture and provide enhanced opportunity for tumor cell proliferation and migration through the disrupted barriers of the altered morphofunctional lymphatic vessels. In conclusion EMILIN1, exerts a suppressive function on tumor growth, tumor lymphatic vessel formation, as well as tumor cell spread to lymph nodes. These properties are crucial and important for an ECM component, since the majority of ECM molecules have opposite effects, such as stimulation of cell proliferation and invasion. Very few molecules (thrombospondin-1, transforming growth factor  $\beta$  binding protein-2, fibulin-5 and -3, CCN1, decorin and EMILIN2) exert inhibitory effect in a tumorigenic context (Mirochnik Y et al. 2008, Albig et al., 2004, 2005, 2006, Todorovic et al., 2005, Seidler et al., 2006 and Mongiat et al., 2007, Hyytiäinen et al., 2003).

In conclusion EMILIN1 is a key regulator of the development, maturation and maintenance of lymphatic capillaries, lymphatic collectors and their intraluminal valves. This work highlights the regulatory function of the EMILIN1, an ECM glycoprotein, on proliferation and migration to guarantee the proper lymphatic vessels formation and functionality. The results presented in this study are useful for the comprehension of the regulatory processes in the normal development and function of the lymphatic system. It is building fundamental basis to understand the mechanisms of several human diseases, including lymphedema and cancer metastasis, and to provide clues to develop new therapeutic strategies.

# **REFERENCES**

- Aalami, O. O.**, Allen, D. B. & Organ, C. H. Jr. 2000 Chylous ascites: a collective review. *Surgery* 128, 761–778.
- Abtahian, F**, Guerriero A, Sebzda E, Lu MM, Zhou R, Mocsai A, Myers EE, Huang B, Jackson DG, Ferrari VA, Tybulewicz V, Lowell CA, Lepore JJ, Koretzky GA, Kahn ML. 2003 Regulation of blood and lymphatic vascular separation by signalling proteins SLP-76 and Syk. *Science* 299, 247–251.
- Albig AR**, Neil JR, Schiemann WP. 2006 Fibulins 3 and 5 antagonize tumor angiogenesis in vivo. *Cancer Res* 66: 2621-2629.
- Albig AR**, Schiemann WP. 2005 Fibulin-5 function during tumorigenesis. *Future Oncol* 1: 23-35.
- Albig AR**, Schiemann WP. 2004 Fibulin-5 antagonizes vascular endothelial growth factor (VEGF) signaling and angiogenic sprouting by endothelial cells. *DNA Cell Biol* 23: 367-379.
- Alitalo K**, Tammela T, Petrova TV. 2005 Lymphangiogenesis in development and human disease. *Nature* 438(7070):946-53.
- Allen MD**, Vaziri R, Green M, Chelala C, Brentnall AR, et al. 2011 Clinical and functional significance of alpha9beta1 integrin expression in breast cancer: a novel cell-surface marker of the basal phenotype that promotes tumour cell invasion. *J Pathol* 223: 646-658.
- Baldwin, M.E.** Halford MM, Roufail S, Williams RA, Hibbs ML, Grail D, Kubo H, Stacker SA, Achen MG. 2005 Vascular endothelial growth factor D is dispensable for development of the lymphatic system. *Mol. Cell Biol.* 25, 2441–2449.
- Baluk P**, Fuxe J, Hashizume H, Romano T, Lashnits E, Butz S, Vestweber D, Corada M, Molendini C, Dejana E, McDonald 2007 Functionally specialized junctions between endothelial cells of lymphatic vessels. *DMJ Exp Med.*; 204(10):2349-62.
- Bazigou E**, Xie S, Chen C, Weston A, Miura N, Sorokin L, Adams R, Muro AF, Sheppard D, Makinen T. 2009. Integrin-alpha9 is required for fibronectin matrix assembly during lymphatic valve morphogenesis. *Dev. Cell* 17:175–186.
- Bissell, M. J.**, Kenny, P. A., and Radisky, D. C. 2005 Microenvironmental regulators of tissue structure and function also regulate tumor induction and progression: the role of extracellular matrix and its degrading enzymes. *Cold Spring Harb. Symp.*
- Braghetta P**, Ferrari A, De Gemmis P, Zanetti M, Volpin D, Bonaldo P, Bressan GM. 2004 Overlapping, complementary and site-specific expression pattern of genes of the EMILIN/Multimerin family. *Matrix Biol.* 22(7): 549-56.
- Bressan GM**, Castellani I, Colombatti A, Volpin D. 1983 Isolation and characterization of a 115,000-dalton matrix-associated glycoprotein from chick aorta. *J of biological chemistry*, 258(21):13262-13267.

- Bressan GM**, Daga-Gordini D, Colombatti A, Castellani I, Marigo V, Volpin D. 1993 Emilin, a component of elastic fibers preferentially located at the elastin-microfibrils interface. *J Cell Biol.*121(1):201-12.
- Christian S**, Ahorn H, Novatchkova M, Garin-Chesa P, Park JE, Weber G, Eisenhaber F, Rettig WJ, Lenter MC. 2001 Molecular cloning and characterization of EndoGlyx-1, an EMILIN-like multisubunit glycoprotein of vascular endothelium. *J Biol Chem.*;276(51):48588-95.
- Colombatti A**, Bressan GM, Castellani I, Volpin D. 1985 Glycoprotein 115, a glycoprotein isolated from chick blood vessels, is widely distributed in connective tissue. *J Cell Biol.*; 100(1):18-26.
- Colombatti A**, Doliana R, Bot S, Canton A, Mongiat M, Mungiguerra G, Paron-Cilli S, Spessotto P. 2000 The EMILIN protein family. *Matrix Biol.*; 19(4):289-301.
- Colombatti A**, Spessotto P, Doliana R, Mongiat M, Bressan GM and Esposito G. 2012 The EMILIN/multimerin family. *Front. Immun.*2:93.
- Cueni, L. N.**, and M. Detmar. 2006. New insights into the molecular control of the lymphatic vascular system and its role in disease. *J. Investig. Dermatol.* 126:2167–2177.
- Cueni LN**, Detmar M. 2008. The lymphatic system in health and disease. *Lymphat. Res. Biol.*6:109–122.
- Cukierman, E.**, and Bassi, D. E. 2010 Physico-mechanical aspects of extracellular matrix influences on tumorigenic behaviors. *Semin. Cancer Biol.*20, 139–145.
- Danussi C**, Spessotto P, Petrucco A, Wassermann B, Sabatelli P, Montesi M, Doliana R, Bressan GM, Colombatti A. 2008 Emilin1 deficiency causes structural and functional defects of lymphatic vasculature. *Mol Cell Biol.*; 28(12): 4026-39.
- Danussi C**, Petrucco A, Wassermann B, Pivetta E, Modica TM, Del Bel Belluz L, Colombatti A, Spessotto P. 2011 EMILIN1- $\alpha$ 4/ $\alpha$ 9 integrin interaction inhibits dermal fibroblast and keratinocyte proliferation. *J. Cell Biol.*195:131–145.
- Danussi C**, Petrucco A, Wassermann B, Modica TM, Pivetta E, Del Bel Belluz L, Colombatti A, Spessotto P. 2012 An EMILIN1-negative microenvironment promotes tumor cell proliferation and lymph node invasion. *Cancer Prev. Res.*5:1131–1143.
- Danussi C**, **Del Bel Belluz L**, Pivetta E, Modica TM, Muro A, Wassermann B, Doliana R, Sabatelli P, Colombatti A, Spessotto P. 2013 EMILIN1 / $\alpha$ 9 $\beta$ 1 integrin interaction is crucial in lymphatic valve formation and maintenance. *Mol Cell Biol.*; 33(22):4381-94. doi: 10.1128/MCB.00872-13.
- De Cock**, H. E., Affolter, V. K., Farver, T. B., Van Brantegem, L., Scheuch, B., and Ferraro, G. L. 2006 Measurement of skin desmosine as an indicator of altered cutaneous elastin in draft horses with chronic progressive lymphedema. *Lymphat. Res. Biol.* 4, 67–72.

- Doliana R**, Mongiat M, Bucciotti F, Giacomello E, Deutzmann R, Volpin D, Bressan GM, Colombatti A. 1999 EMILIN, a component of the elastic fiber and a new member of the C1q/tumor necrosis factor superfamily of proteins. *J Biol Chem.*;274(24):16773-81.
- Doliana R**, Bot S, Bonaldo P, Colombatti A. 2000 EMI, a novel cysteine-rich domain of EMILINs and other extracellular proteins, interacts with the gC1q domains and participates in multimerization. *FEBS Lett.*;484(2):164-8.
- Doliana R**, Bot S, Mungiguerra G, Canton A, Cilli SP, Colombatti A. 2001 Isolation and characterization of EMILIN-2, a new component of the growing EMILINs family and a member of the EMI domain-containing superfamily. *J Biol Chem.*;276(15):12003-11.
- Dumont, D. J.**, Jussila L, Taipale J, Lymboussaki A, Mustonen T, Pajusola K, Breitman M, Alitalo K. 1998 Cardiovascular failure in mouse embryos deficient in VEGF receptor-3. *Science*282, 946–949.
- Ebata, N.**, Y. Nodasaka, Y. Sawa, Y. Yamaoka, S. Makino, Y. Totsuka, and S. Yoshida. 2001. Desmoplakin as a specific marker of lymphatic vessels. *Microvasc. Res.* 61:40–48.
- Eto K**, Puzon-McLaughlin W, Sheppard D, Sehara-Fujisawa A, Zhang XP, Takada Y. 2000 RGD-independent binding of integrin alpha9beta1 to the ADAM-12 and -15 disintegrin domains mediates cell-cell interaction. *J. Biol. Chem.*275:34922–34930.
- Evans RA**, Tian YC, Steadman R, Phillips AO. 2003 TGF-beta1-mediated fibroblast-myofibroblast terminal differentiation—the role of Smad proteins. *Exp. Cell Res.*282:90–100.
- Ferrell RE**. 2002 Research perspectives in inherited lymphatic disease. *Ann N Y Acad Sci.*;979:39-51.
- Forsberg E**, Hirsch E, Frohlich L, Meyer M, Ekblom P, Aszodi A, Werner S, Fassler R. 1996 Skin wounds and severed nerves heal normally in mice lacking tenascin-C. *Proc. Natl. Acad. Sci. U. S. A.*93:6594– 6599.
- Fukamauchi F**, Mataga N, Wang YJ, Sato S, Youshiki A, Kusakabe M. 1996. Abnormal behavior and neurotransmissions of tenascin gene knockout mouse. *Biochem. Biophys. Res. Commun.*221:151–156.
- Gale, N. W.** Thurston G, Hackett SF, Renard R, Wang Q, McClain J, Martin C, Witte C, Witte MH, Jackson D, Suri C, Campochiaro PA, Wiegand SJ, Yancopoulos GD. 2002 Angiopoietin-2 is required for postnatal angiogenesis and lymphatic patterning, and only the latter role is rescued by Angiopoietin-1. *Dev. Cell* 3,411–423.
- Garmy-Susini B**, Avraamides CJ, Schmid MC, Foubert P, Ellies LG, et al. 2010 Integrin alpha4beta1 signaling is required for lymphangiogenesis and tumor metastasis. *Cancer Res* 70: 3042-3051.

- Gerli, R.**, L. Ibba, and C. Fruschelli. 1990 A fibrillar elastic apparatus around human lymph capillaries. *Anat. Embryol.* 181:281–286.
- Gurtner GC**, Davis V, Li H, McCoy MJ, Sharpe A, Cybulsky MI. 1995 Targeted disruption of the murine VCAM1 gene: essential role of VCAM-1 in chorioallantoic fusion and placentation. *Genes Dev.*9:1–14.
- Harvey, N. L.**, Srinivasan RS, Dillard ME, Johnson NC, Witte MH, Boyd K, Sleeman MW, Oliver G. 2005 Lymphatic vascular defects promoted by Prox1 haploinsufficiency cause adult-onset obesity. *Nature Genet.* 37, 1072–1081.
- Hayward CP.** 1997 Multimerin: a bench-to-bedside chronology of a unique platelet and endothelial cell protein--from discovery to function to abnormalities in disease. *Clin Invest Med.*;20(3):176-87.
- Hyytiäinen M**, Keski-Oja J. 2003 Latent TGF-beta binding protein LTBP-2 decreases fibroblast adhesion to fibronectin. *J Cell Biol* 163: 1363-1374.
- Hong, Y. K.** Harvey N, Noh YH, Schacht V, Hirakawa S, Detmar M, Oliver G. 2002 Prox1 is a master control gene in the program specifying lymphatic endothelial cell fate. *Dev. Dyn.*225,351–357
- Høye AM**, Couchman JR, Wewer UM, Fukami K, Yoneda A. 2012 The newcomer in the integrin family: integrin  $\alpha 9$  in biology and cancer. *Adv Biol Regul* 52: 326-339.
- Huang XZ**, Wu JF, Ferrando R, Lee JH, Wang YL, Farese RV, Jr, Sheppard D. 2000. Fatal bilateral chylothorax in mice lacking the integrin  $\alpha 9\beta 1$ . *Mol. Cell. Biol.*20:5208–5215.
- Hynes, R. O.** 2009 The extracellular matrix: not just pretty fibrils. *Science* 326, 1216–1219.
- Iida J**, Meijne AM, Spiro RC, Roos E, Furcht LT, et al. 1995 Spreading and focal contact formation of human melanoma cells in response to the stimulation of both melanoma-associated proteoglycan (NG2) and  $\alpha 4 \beta 1$  integrin. *Cancer Res* 55: 2177-2185.
- Jackson, D. G.** 2004 Biology of the lymphatic marker LYVE-1 and applications in research into lymphatic trafficking and lymphangiogenesis. *APMIS*112,526–538.
- Jeltsch, M.**, Tammela, T., Alitalo, K. & Wilting, J. 2003 Genesis and pathogenesis of lymphatic vessels. *Cell Tissue Res.* 314, 69–84.
- Joukov, V.**, Pajusola, K., Kaipainen, A., Chilov, D., Lahtinen, I., Kukk, E., Saksela, O., Kalkkinen, N. and Alitalo, K. 1996 A novel vascular endothelial growth factor, VEGF-C, is a ligand for the Flt4 (VEGFR-3) and KDR (VEGFR-2) receptor tyrosine kinases. *EMBO J.* 15, 290 – 298.

- Joukov, V.**, Sorsa, T., Kumar, V., Jeltsch, M., Claesson-Welsh, L., Cao, Y., Saksela, O., Kalkkinen, N. and Alitalo, K. 1997 Proteolytic processing regulates receptor specificity and activity of VEGF-C. *EMBO J.* 16, 3898 – 3911.
- Juriscic G**, Maby-El HH, Karaman S, Ochsenbein AM, Alitalo A, Siddiqui SS, Ochoa PC, Petrova TV, Detmar M. 2012 An unexpected role of semaphorin3A-neuropilin-1 signaling in lymphatic vessel maturation and valve formation. *Circ. Res.*111:426– 436.
- Kajiya K**, Hirakawa S, Ma B, Drinnenberg I, Detmar M. 2005 Hepatocyte growth factor promotes lymphatic vessel formation and function. *EMBO J.*24:2885–2895.
- Kanady JD**, Dellinger MT, Munger SJ, Witte MH, Simon AM. 2011 Connexin37 and Connexin43 deficiencies in mice disrupt lymphatic valve development and result in lymphatic disorders including lymphedema and chylothorax. *Dev. Biol.*354:253–266.
- Karkkainen, M. J.** Ferrell RE, Lawrence EC, Kimak MA, Levinson KL, McTigue MA, Alitalo K, Finegold DN. 2000 Missense mutations interfere with VEGFR-3 signaling in primary lymphoedema. *Nature Genet.*25, 153–159.
- Karkkainen, M. J.** Haiko P, Sainio K, Partanen J, Taipale J, Petrova TV, Jeltsch M, Jackson DG, Talikka M, Rauvala H, Betsholtz C, Alitalo K. 2004 Vascular endothelial growth factor C is required for sprouting of the first lymphatic vessels from embryonic veins. *Nature Immunol.* 5,74–80.
- Karpanen T**, Heckman CA, Keskitalo S, Jeltsch M, Ollila H, Neufeld G, Tamagnone L, Alitalo K 2006 Functional interaction of VEGF-C and VEGF-D with neuropilin receptors. *FASEB J* 20:1462–1472.
- Leimeister C**, Steidl C, Schumacher N, Erhard S, Gessler M. 2002 Developmental expression and biochemical characterization of Emu family members. *Dev Biol.*;249(2):204-18.
- Li, H.**, Fan, X., and Houghton, J. M. 2007 Tumor microenvironment: the role of the tumor stroma in cancer.*J. Cell. Biochem.*101, 805–815.
- Liaw L**, Birk DE, Ballas CB, Whitsitt JS, Davidson JM, Hogan BL. 1998 Altered wound healing in mice lacking a functional osteopontin gene (spp1). *J. Clin. Invest.*101:1468–1478.
- Lutter S**, Xie S, Tatin F, Makinen T 2012 Smooth muscle-endothelial cell communication activates Reelin signaling and regulate lymphatic vessel formation. *J Cell Biol.* 197(6):837-49.
- Maby-El Hajjami H, Petrova TV.** 2008 Developmental and pathological lymphangiogenesis: from models to human disease. *Histochem Cell Biol.* 130(6):1063-78.
- Majumdar M**, Tarui T, Shi B, Akakura N, Ruf W, Takada Y. 2004 Plasmin-induced migration requires signaling through protease-activated receptor 1 and integrin alpha(9)beta(1). *J. Biol. Chem.*279:37528–37534.

- Makinen**, T. Adams RH, Bailey J, Lu Q, Ziemiecki A, Alitalo K, Klein R, Wilkinson GA. 2005 PDZ interaction site in ephrinB2 is required for the remodeling of lymphatic vasculature. *Genes Dev.*19,397–410
- Makinen**, T., C. Norrme'n, and T. V. Petrova. 2007 Molecular mechanisms of lymphatic vascular development. *Cell. Mol. Life Sci.* 64:1915–1929.
- Marastoni**, S., Ligresti, G., Lorenzon, E., Colombatti, A., and Mongiat, M. 2008 Extracellular matrix: a matter of life and death. *Connect. Tissue Res.*49, 203–206.
- Mirochnik** Y, Kwiatek A, Volpert OV. 2008 Thrombospondin and apoptosis: molecular mechanisms and use for design of complementation treatments. *Curr Drug Targets* 9: 851-862.
- Mishima** K, Watabe T, Saito A, Yoshimatsu Y, Imaizumi N, Masui S, Hirashima M, Morisada T, Oike Y, Araie M, Niwa H, Kubo H, Suda T, Miyazono K. 2007 Prox1 induces lymphatic endothelial differentiation via integrin alpha9 and other signaling cascades. *Mol. Biol. Cell*18:1421–1429.
- Mongiat** M., Mungiguerra G., Bot S., Mucignat M.T., Giacomello E., Doliana R., Colombatti A. Self-assembly and supramolecular organization of EMILIN. 2000. *J Biol Chem.* 275(33): 25471-25480.
- Mongiat** M, Ligresti G, Marastoni S, Lorenzon E, Doliana R, et al. 2007 Regulation of the extrinsic apoptotic pathway by the extracellular matrix glycoprotein EMILIN2. *Mol Cell Biol* 27: 7176-7187.
- Muro** AF, Chauhan AK, Gajovic S, Iaconcig A, Porro F, Stanta G, Baralle FE. 2003. Regulated splicing of the fibronectin EDA exon is essential for proper skin wound healing and normal lifespan. *J. Cell Biol.*162: 149–160
- Navas** V, O'Morchoe PJ, O'Morchoe CC. 1991. Lymphatic valves of the rat pancreas. *Lymphology*24:146–154.
- Negrini**, D., A. Passi, G. de Luca, and G. Miserocchi. 1996. Pulmonary interstitial pressure and proteoglycans during development of pulmonary edema. *Am. J. Physiol.* 270:2000–2007.
- Norrmen** C, Ivanov KI, Cheng J, Zangger N, Delorenzi M, Jaquet M, Miura N, Puolakkainen P, Horsley V, Hu J, Augustin HG, YlaHerttuala S, Alitalo K, Petrova TV.2009. FOXC2 controls formation and maturation of lymphatic collecting vessels through cooperation with NFATc1. *J. Cell Biol.*185:439– 457.
- Ny** A, Koch M, Schneider M, Neven E, Tong RT, Maity S, Fischer C, Plaisance S, Lambrechts D, Héligon C, Terclavers S, Ciesiolka M, Kälin R, Man WY, Senn I, Wyns S, Lupu F, Brändli A, Vleminckx K, Collen D, Dewerchin M, Conway EM, Moons L, Jain RK, Carmeliet P 2005 A genetic *Xenopus laevis* tadpole model to study lymphangiogenesis. *Nat Med* 11:998–1004.
- Oliver** G. 2004 Lymphatic vasculature development. *Nat Rev Immunol.* Jan;4(1):35-45.

- Palmer EL**, Rüegg C, Ferrando R, Pytela R, Sheppard D. 1993 Sequence and tissue distribution of the integrin alpha 9 subunit, a novel partner of beta 1 that is widely distributed in epithelia and muscle. *J Cell Biol.* 123(5):1289-97.
- Pelosi, P.**, R. Rocco, D. Negrini, and A. Passi. 2007 The extracellular matrix of the lung and its role in edema formation. *An. Acad. Bras. Cienc.* 79:285–297.
- Petrova, T. V.** Mäkinen T, Mäkelä TP, Saarela J, Virtanen I, Ferrell RE, Finegold DN, Kerjaschki D, Ylä-Herttuala S, Alitalo K. 2002 Lymphatic endothelial reprogramming of vascular endothelial cells by the Prox-1 homeobox transcription factor. *EMBO J.* 21,4593–4599.
- Petrova TV**, Karpanen T, Norrmen C, Mellor R, Tamakoshi T, Finegold D, Ferrell R, Kerjaschki D, Mortimer P, Yla-Herttuala S, Miura N, Alitalo K. 2004. Defective valves and abnormal mural cell recruitment EMILIN1 Role in Lymphatic Valves November 2013 Volume 33 Number 22 mcb.asm.org 4393 underlie lymphatic vascular failure in lymphedema distichiasis. *Nat. Med.* 10:974–981.
- Pinco KA**, He W, Yang JT. 2002 Alpha4beta1 integrin regulates lamellipodia protrusion via a focal complex/focal adhesion-independent mechanism. *Mol Biol Cell* 13: 3203-3217.
- Pivetta E**, Colombatti A, Spessotto P. 2013 A Rare Bird among Major Extracellular Matrix Proteins: EMILIN1 and the Tumor Suppressor Function. *J Carcinogene Mutagene* S13:009.
- Podgrabinska S**, Braun P, Velasco P, Kloos B, Pepper MS, Skobe M. 2002 Molecular characterization of lymphatic endothelial cells. *Proc Natl Acad Sci U S A.* 10;99(25):16069-74.
- Rebhun RB**, Cheng H, Gershenwald JE, Fan D, Fidler IJ, Langley RR. 2010 Constitutive expression of the alpha4 integrin correlates with tumorigenicity and lymph node metastasis of the B16 murine melanoma. *Neoplasia*; 12:173–82
- Regenfuss B**, Onderka J, Bock F, Hos D, Maruyama K, Cursiefen C. 2010 Genetic heterogeneity of lymphangiogenesis in different mouse strains. *Am J Pathol.*;177(1):501-10.
- Rose DM**, Alon R, Ginsberg MH 2007 Integrin modulation and signaling in leukocyte adhesion and migration. *Immunol Rev* 218: 126-134.
- Sabine A**, Agalarov Y, Maby-El HH, Jaquet M, Hagerling R, Pollmann C, Bebbler D, Pfenniger A, Miura N, Dormond O, Calmes JM, Adams RH, Mäkinen T, Kiefer F, Kwak BR, Petrova TV. 2012. Mechanotransduction, PROX1, and FOXC2 cooperate to control connexin37 and calcineurin during lymphatic-valve formation. *Dev. Cell*22:430– 445.
- Sanz-Moncasi, M. P.**, Garin-Chesa, P., Stockert, E., Jaffe, E. A., Old, L. J., and Rettig, W. J. 1994 Identification of a high molecular weight endothelial cell surface glycoprotein, endoGlyx-1, in normal and tumor blood vessels. *Lab. Invest.* 71, 366–373.

- Schacht, V.** Ramirez MI, Hong YK, Hirakawa S, Feng D, Harvey N, Williams M, Dvorak AM, Dvorak HF, Oliver G, Detmar M. 2003 T1alpha/podoplanin deficiency disrupts normal lymphatic vasculature formation and causes lymphedema. *EMBO J.*22,3546–3556 .
- Schulte-Merker S,** Sabine A, Petrova TV. 2011 Lymphatic vascular morphogenesis in development, physiology, and disease. *J Cell Biol.* 16;193(4):607-18.
- Saharinen, P.** Kerkelä K, Ekman N, Marron M, Brindle N, Lee GM, Augustin H, Koh GY, Alitalo K. 2005 Multiple angiopoietin recombinant proteins activate the Tie1 receptor tyrosine kinase and promote its interaction with Tie2. *J. Cell Biol.*169,239–243.
- Seidler DG,** Goldoni S, Agnew C, Cardi C, Thakur ML, et al. 2006 Decorin protein core inhibits in vivo cancer growth and metabolism by hindering epidermal growth factor receptor function and triggering apoptosis via caspase-3 activation. *J Biol Chem* 281: 26408-26418.
- Spessotto P,** Cervi M, Mucignat MT, Mungiguerra G, Sartoretto I, Doliana R, Colombatti A. 2003 Beta 1 Integrin-dependent cell adhesion to EMILIN-1 is mediated by the gC1q domain. *J Biol Chem.*; 278(8): 6160-7.
- Spessotto P,** Bulla R, Danussi C, Radillo O, Cervi M, Monami G, Bossi F, Tedesco F, Doliana R, Colombatti A. 2006 EMILIN1 represents a major stromal element determining human trophoblast invasion of the uterine wall. *J Cell Sci.*; 119(Pt 21):4574-84.
- Spessotto P,** Lacrima K, Nicolosi PA, Pivetta E, Scapolan M, Perris R. 2009 Fluorescence-based assays for in vitro analysis of cell adhesion and migration. *Methods Mol. Biol.*522:221–250.
- Streuli CH** 2009 Integrins and cell-fate determination. *J Cell Sci* 122: 171-177.
- Tammela, T.,** T. V. Petrova, and K. Alitalo. 2005 Molecular lymphangiogenesis: new players. *Trends Cell. Biol.*15:434–441.
- Tammela T,** Alitalo K. 2010. Lymphangiogenesis: molecular mechanisms and future promise. *Cell*140:460– 476.
- Taooka Y,** Chen J, Yednock T, Sheppard D. 1999 The integrin alpha9beta1 mediates adhesion to activated endothelial cells and transendothelial neutrophil migration through interaction with vascular cell adhesion molecule-1. *J. Cell Biol.*145:413– 420.
- Todorovic V,** Chen CC, Hay N, Lau LF. 2005 The matrix protein CCN1 (CYR61) induces apoptosis in fibroblasts. *J Cell Biol* 171: 559-568.
- Vlahakis NE,** Young BA, Atakilit A, Sheppard D. 2005 The lymphangiogenic vascular endothelial growth factors VEGF-C and -D are ligands for the integrin alpha9beta1. *J. Biol. Chem.*280:4544– 4552.

- Verdone G**, Doliana R, Corazza A, Colebrooke SA, Spessotto P, Bot S, Bucciotti F, Capuano A, Silvestri A, Viglino P, Campbell ID, Colombatti A, Esposito G. 2008 The solution structure of EMILIN1 globular C1q domain reveals a disordered insertion necessary for interaction with the alpha4beta1 integrin. *J Biol Chem.*;283(27):18947-56.
- Verdone, G.**, Corazza, A., Colebrooke, S. A., Cicero, D., Eliseo, T., Boyd, J., Doliana, R., Fogolari, F., Viglino, P., Colombatti, A., Campbell, I. D., and Esposito, G. 2009 NMR-based homology model for the solution structure of the C-terminal globular domain of EMILIN1. *J. Biomol. NMR*43, 79–96.
- Vlahakis NE**, Young BA, Atakilit A, Sheppard D. The lymphangiogenic vascular endothelial growth factors VEGF-C and -D are ligands for the integrin alpha9beta1. *The Journal of biological chemistry.* 2005; 280(6):4544–4552.
- Wang JF**, Zhang X-F, Groopman JE 2001 Stimulation of beta 1 integrin induces tyrosine phosphorylation of vascular endothelial growth factor receptor-3 and modulates cell migration. *J Biol Chem* 276:41950–41957.
- Wigle JT, Oliver G.** 1999 Prox1 function is required for the development of the murine lymphatic system. *Cell*98:769–778
- Wigle JT**, Harvey N, Detmar M, Lagutina I, Grosveld G, Gunn MD, Jackson DG, Oliver G. 2002 An essential role for Prox1 in the induction of the lymphatic endothelial cell phenotype. *EMBO J.*;21(7):1505-13.
- Yaniv K**, Isogai S, Castranova D, Dye L, Hitomi J, Weinstein BM 2006 Live imaging of lymphatic development in the zebraWsh. *Nat Med* 12:711–716.
- Yokosaki Y**, Palmer EL, Prieto AL, Crossin KL, Bourdon MA, Pytela R, Sheppard D. 1994 The integrin alpha 9 beta 1 mediates cell attachment to a non-RGD site in the third fibronectin type III repeat of tenascin. *J. Biol.Chem.*269:26691–26696.
- Yokosaki Y**, Matsuura N, Sasaki T, Murakami I, Schneider H, Higashiyama S, Saitoh Y, Yamakido M, Taooka Y, Sheppard D.1999. The integrin alpha(9)beta(1) binds to a novel recognition sequence (SVVYGLR) in the thrombin-cleaved amino-terminal fragment of osteopontin. *J. Biol. Chem.*274:36328–36334.
- Yuan, L.** Moyon D, Pardanaud L, Bréant C, Karkkainen MJ, Alitalo K, Eichmann A. 2002 Abnormal lymphatic vessel development in neuropilin 2 mutant mice. *Development* 129,4797–4806.
- Zacchigna L**, Vecchione C, Notte A, Cordenonsi M, Dupont S, Maretto S, Cifelli G, Ferrari A, Maffei A, Fabbro C, Braghetta P, Marino G, Selvetella G, Aretini A, Colonnese C, Bettarini U, Russo G, Soligo S, Adorno M, Bonaldo P, Volpin D, Piccolo S, Lembo G, Bressan GM. 2006 Emilin1 links TGF-beta maturation to blood pressure homeostasis. *Cell.* 124(5): 929-42.

**Zanetti M**, Braghetta P, Sabatelli P, Mura I, Doliana R, Colombatti A, Volpin D, Bonaldo P, Bressan GM. 2004 EMILIN-1 deficiency induces elastogenesis and vascular cell defects. *Mol Cell Biol.* 24(2): 638-50.

**Zhang, W.**, and Huang, P. 2011 Cancer-stromal interactions: role in cell survival, metabolism and drug sensitivity. *Cancer Biol. Ther.* 11, 150–156.

# **APPENDIX**

The present thesis is based mainly on the following work:

- Danussi C and **Del Bel Belluz L**, Pivetta E, Modica TM, Muro A, Wassermann B, Doliana R, Sabatelli P, Colombatti A, Spessotto P. (2013) EMILIN1/ $\alpha$ 9 $\beta$ 1 integrin interaction is crucial in lymphatic valve formation and maintenance. *Mol Cell Biol.*; 33(22):4381-94. doi: 10.1128/MCB.00872-13.

Molecular and Cellular Biology has chosen our image (Fig. 10, the central photo in the top line) for their cover of MCB volume 33, issue 22.

I mentioned also the other two works published by our group during my Ph.D. course:

- Danussi C, Petrucco A, Wassermann B, Modica TM, Pivetta E, **Del Bel Belluz L**, Colombatti A, Spessotto P. (2012) An EMILIN1-negative microenvironment promotes tumor cell proliferation and lymph node invasion. *Cancer Prev. Res.*5:1131–1143.
- Danussi C, Petrucco A, Wassermann B, Pivetta E, Modica TM, **Del Bel Belluz L**, Colombatti A, Spessotto P. (2011) EMILIN1- $\alpha$ 4/ $\alpha$ 9 integrin interaction inhibits dermal fibroblast and keratinocyte proliferation. *J. Cell Biol.*195:131–145.

